

**Structural characterisation of the interaction between RBBP6 and the
multifunctional protein YB-1**

by

Victor Muleya



A thesis submitted in partial fulfilment of the requirements of the M.Sc. Degree in
Biotechnology at the Department of Biotechnology, Faculty of Science, University of the
Western Cape.

Supervisor: Dr. David J.R. Pugh

October 2010

Keywords:

RBBP6

YB-1

Interaction

RING

¹⁵N-HSQC

NMR

Yeast 2-hybrid

Co-immunoprecipitation

Homodimerisation

Ubiquitination



Abstract

Structural characterisation of the interaction between RBBP6 and the multifunctional protein YB-1

Victor Muleya

M.Sc. (Biotechnology) thesis, Department of Biotechnology, Faculty of Natural Sciences, University of the Western Cape.

Retinoblastoma binding protein 6 (RBBP6) is a 250 kDa RING finger-containing protein whose function is known to be mediated through interaction with other proteins. RBBP6 plays a role in the regulation of the tumour suppressor protein p53 and is also thought to be involved in mRNA splicing although its role has yet to be characterised. A recent study utilising a yeast 2-hybrid screen identified the cancer-associated protein known as YB-1 as an interacting partner of RBBP6, and showed that RBBP6 ubiquitinates YB-1, leading to its degradation in the proteasome.

Human Y-box binding protein 1 (YB-1) is member of the cold-shock domain family of proteins, which regulates a number of growth related genes through both transcriptional and translational mechanisms. YB-1 is a cell-survival factor whose expression is increased in proliferating normal and cancer cells. It also protects cells against p53-mediated apoptosis by repressing the p53-promoter and down-regulating endogenous p53. The interaction between RBBP6 and YB-1 involves the RING finger-like domain of RBBP6 and the C-terminal 62 amino acids of YB-1.

As a means of further localising the interaction, truncated fragments derived from the C-terminal region of YB-1, were tested for their interaction with the RING finger domain of RBBP6 using three different assays: a directed yeast 2-hybrid assay, co-immunoprecipitation and NMR chemical shift perturbation analysis. Our results suggest that the entire 62 amino acid region at the C-terminal domain of YB-1 may be involved in the interaction with RBBP6. Using chemical shift perturbation analysis, this study provides an indication of where YB-1 binds to the RING finger. This represents the first step towards the design of therapeutics aimed at modulating the interaction between RBBP6 and YB-1 as a means of targeting the oncogenic effects of YB-1.

In order to identify E2 enzymes involved in the ubiquitination of YB-1, we examined the efficiencies of selected E2s in an *in vitro* ubiquitination assay. UbcH5c and UbcH7 were both found to catalyse the ubiquitination of YB-1 in conjunction with RBBP6, whereas Ubc13 was not. Finally, we show using NMR that two single-point mutations of the RING finger-like domain are sufficient to abolish homodimerisation of the domain. These will be used in future studies to investigate the requirement for homodimerisation on the ubiquitination activity of RBBP6.

Declaration

I declare that “**Structural characterization of the interaction between RBBP6 and the multifunctional protein YB-1**” to be my own work, which has not been submitted for any degree or examination in any other institution, and that all the sources I have used or quoted have been indicated and acknowledged by complete references.

Victor Muleya

October 2010



Signed

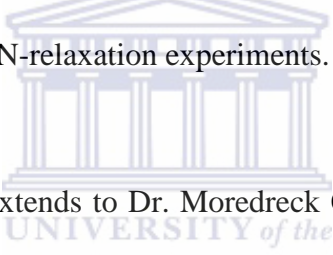
Dedication

With love and affection to my late parents Aram and Pauline and to God be the glory.



Acknowledgements

I am exceedingly indebted to my supervisor Dr. David J. R. Pugh for his scientific expertise and guidance throughout the entire project, without which the completion of this study would have been **absolutely** impossible. My most sincere gratitude is also due to Professor Jasper Rees who permitted most of the work done in this study to be carried out in his laboratory. I am also eternally grateful to Professor Johanna Moolman-Smook from the MRC unit in Stellenbosch University, who, out of her benevolence, permitted me to use her laboratory for the yeast 2-hybrid experiments and for the generation of ^{35}S -labelled proteins. I would also like to convey my gratitude to Dr. Andrew Artkinson (University College of London) for confirming our homodimerisation findings using ^{15}N -relaxation experiments.



My most profound gratitude also extends to Dr. Moredreck Chibi (CNRS, University of Paris), whose doctoral study generated an impetus for this study. I would also like to convey my eternal gratitude to the members of the protein-protein interaction analysis and NMR group at UWC. To Dr. Abidemi Kappo, the RING finger expert (also known as the Lord of the RING), for his input on the optimization of the production of ^{15}N -labelled protein. To the cloning expert, Andrew Faro, for transferring his scientific expertise to me and for displaying his prowess in the exquisite art of protein purification, much to my delight. I would also like to thank Takalani Mulaudzi, who saw this study from its infancy, for encouraging me to strive to be a better scientist. I would also like to thank Dr. John Poole for assisting me in processing NMR data, may God truly bless him beyond all measure. To Melvine Pretorius, thanks for acquiring our orders on time and making sure that we never run short of reagents. To the members of the Biochemistry lab, I

would like to thank them for the spirit of camaraderie that we all enjoyed in the Biotechnology department.

Many thanks are also due to William Mavengere, from the Institute of Microbial Biotechnology and Metagenomics (IMBM), for assisting me with the FPLC machine in his lab. I would also like to convey my most sincere gratitude to my colleagues and friends Clive Mketsu, Thulani Makhalanyane, Pascoe Bilibana Mawethu, Siyamcela Genu, Thabiso Mothibedi and Kgomotso Taukobong, Tshifhiwa Mamphogoro, Edukondalu Mullapudi, Nagadevi Mullapudi, Lilia Polle, Nils Kuklik, Godfrey Madzivire, Walter Mudzimbabwe, and Nyika Mtemeri. Without these guys my life at UWC would have been painstakingly boring. To my family, I love you guys, thank you for believing in me. We come a long way and I believe we are destined for greater heights.

My most profound gratitude also extends to my spiritual family at Hillsong Church, Cape Town for being so dependable. Finally, I would also like to thank the National Research Foundation of South Africa for funding this work, but more so, to Dr. David J. R. Pugh for securing this financial support.

Gratitude shown in moderation is a sign of mediocrity.

List of tables and figures

Tables

Chapter 2

Table 2.1: PCR reaction set up for the amplification of DNA fragments.

Table 2.2: Components used to make 4% stacking gels and 16% separating gels for SDS-PAGE.

Table 2.3: Components of the ubiquitination assay.

Chapter 3

Table 3.1: Primers used for the amplification of YB-1 derived fragments.

Table 3.2: Primers for the PCR amplification of bait and prey inserts.

Table 3.3: Synthetic peptides and their amino acid composition.

Table 3.4: Absorbance values for the gamma globulin standards and RING.

Table 3.5: K_D values and total chemical shifts.

Figures

Chapter 1

Fig. 1.1: Y-box proteins from different organisms.

Fig. 1.2: Domain organisation in YB-1.

Fig. 1.3: Illustration of the domain organisation in human RBBP6.

Fig. 1.4: A cartoon representation of the 3D structure of the RING finger domain of human RBBP6.

Fig. 1.5: A schematic illustration of the ubiquitin-proteasome pathway.

Fig. 1.6: An illustration of the classical yeast two-hybrid system.

Chapter 2

Fig. 2.1: The restriction map of pACT2 AD vector (Clontech) for cloning cDNA of prey proteins used in the yeast two-hybrid.

Fig. 2.2: Restriction map and main features of pGBKT7 vector (Clontech).

Fig. 2.3: Reading frame and main features of pGEX-6P-2.

Chapter 3

Fig. 3.1: An illustration of the designed fragment peptides tested for interaction with the RING finger domain of RBBP6.

Fig. 3.2: A 1 % agarose gel image showing PCR amplification of YB-1₂₇₇₋₃₀₆ and YB-1₂₉₂₋₃₂₄.

Fig. 3.3: A yeast 2-hybrid assay showing that YB-1₂₇₇₋₃₀₆ and YB-1₂₉₂₋₃₂₄ interact with RING *in vivo*.

Fig. 3.4: A 1% agarose gel showing the amplification of cDNA of test proteins to be subjected for co-IP analysis.

Fig. 3.5: An autoradiograph showing the immunoprecipitation of *in vitro* generated ³⁵S-labelled proteins.

Fig. 3.6: An illustration of the synthetic peptides tested for interaction with the RING finger domain of RBBP6 using ¹H-¹⁵N-HSQC NMR.

- Fig. 3.7: SDS-PAGE analysis of the small-scale expression of GST-RING in a 16 % acrylamide gel.
- Fig. 3.8: Large-scale expression, affinity purification and cleavage of GST-RING using PreScission™ 3C Protease.
- Fig. 3.9: Purification of RING finger domain by size exclusion chromatography.
- Fig. 3.10: Gamma globulin standard curve for the determination of the protein concentration of the RING finger domain.
- Fig. 3.11: Overlay of ^1H - ^{15}N -HSQC spectra of ^{15}N -labeled RING with increasing concentration of unlabelled CTD-1 peptide.
- Fig. 3.12: Composite chemical shifts of residues that displayed significant perturbations on titration with CTD-1.
- Fig. 3.13: Overlay of ^1H - ^{15}N -HSQC spectra of ^{15}N -labeled RING with increasing concentration of unlabelled CTD-2 peptide.
- Fig. 3.14: Surface representation of the homodimer of the RING finger-like domain of RBBP6 showing the YB-1 binding site.

Chapter 4

- Fig. 4.1: An autoradiograph showing the ubiquitination of YB-1 in the presence of different E2s.
- Fig. 4.2: Schematic illustration of the effect of concentration resonances from the ^1H - ^{15}N -HSQC spectrum of the RING finger domain of RBBP6.
- Fig. 4.3: NMR analysis of the residue resonances of the RING^{K313E} mutant on an ^1H - ^{15}N -HSQC spectra.

Chapter 5

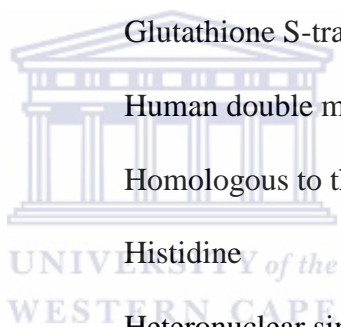
Fig. 5.1: An illustration of some of the proteins that interact with YB-1.



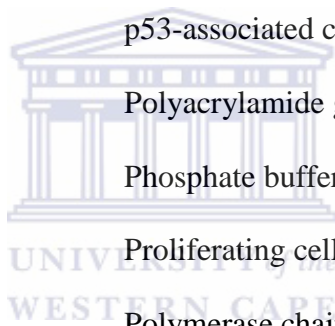
Abbreviations

AP	Alanine/proline - rich
APS	Ammonium persulphate
Asp	Aspartic acid
ATP	Adenosine tri-phosphate
BIR	Baculoviral IAP repeat
bp	Base pair
BSA	Bovine serum albumin
C-terminus	Carboxy terminus
CHIP	Carboxyl terminus of Hsp70-interacting protein
Co-IP	Co-immunoprecipitation
CPF	Cleavage and polyadenylation factor
CRS	Cytoplasmic retention signal
CSD	Cold shock domain
CSP	Cold shock protein
CSPs	Chemical shift perturbations
CV	Column volume
DNA	Deoxyribonucleic acid
dNTP	2'-deoxynucleoside 5'-triphosphate
DPA	DNA polymerase α
DTT	1,4-dithio-DL-threitol
DWNN	Domain with no name

EDTA	Ethylenediaminetetra acetic acid
EGFR	Epidermal growth factor receptor
eIF4E	Eukaryotic translation initiation factor 4E
EMT	Epithelial-to-mesenchymal transition
ERS	Energy regeneration solution
Fig	Figure
Gln,Q	Glutamine
Glu,E	Glutamic acid
Gly,G	Glycine
GST	Glutathione S-transferase
Hdm2	Human double minute 2
HECT	Homologous to the E6-AP C-terminus
His, H	Histidine
HSQC	Heteronuclear single quantum coherence
Ile, I	Isoleucine
IPTG	Isopropyl-1-thio-D-galactopyranoside
kDa	Kilodaltons
Leu, L	Leucine
LB	Luria Bertani
Lys,K	Lysine
MDR1	Multidrug resistance 1
min	Minute
mRNA	Messenger RNA



mRNPs	Messenger ribonucleoprotein particles
MDM2	Murine double minute 2
MWCO	Molecular weight cut-off
NEIL2	Nei-like-2
NMR	Nuclear magnetic resonance
N-terminus	Amino terminal
NLS	Nuclear localisation signals
NPC	Nuclear pore complex
P2P-R	Proliferation potential protein-related
PACT	p53-associated cellular protein-testis derived
PAGE	Polyacrylamide gel electrophoresis
PBS	Phosphate buffered saline
PCNA	Proliferating cell nuclear antigen
PCR	Polymerase chain reaction
PDB	Protein data bank
Phe, F	Phenylalanine
PPi	Inorganic pyrophosphate
ppm	Parts per million
pRb	Retinoblastoma gene product
PREs	Paramagnetic relaxation enhancements
RBBP6	Retinoblastoma binding protein 6
RING	Really interesting new gene
RNA	Ribonucleic acid



s	Seconds
Ser, S	Serine
SDS	Sodium dodecyl sulphate
SnRNPG	small nuclear ribonucleoprotein G
SR	Serine-rich
TAE	Tris acetate EDTA
Thr, T	Threonine
Trp, W	Tryptophan
Ubc	Ubiquitin-conjugating enzyme
UV	Ultra violet
YB-1	Y-box binding protein-1
Y2H	Yeast 2-hybrid technique.
XIAP	X-linked inhibitor of apoptosis protein
zBTB38	Zinc finger and BTB domain containing 38
Zn ²⁺	Zinc ions

Symbols

®	registered trademark
™	unregistered trademark

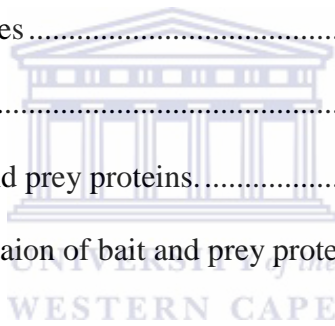
Table of Contents

Keywords:.....	i
Abstract.....	ii
Declaration.....	iv
Dedication.....	v
Acknowledgements.....	vi
List of tables and figures.....	viii
Abbreviations.....	xii
Symbols.....	xv
Table of Contents.....	xvi
Chapter 1: General introduction.....	1
1.1 Introduction.....	1
1.2 Y-Box Binding Protein Family.....	4
1.3 Human Y-box binding protein-1 (YB-1).....	6
1.4 Functions of YB-1.....	8
1.4.1 Transcriptional regulation.....	10
1.4.2 Translational control and mRNA metabolism.....	11
1.4.3. Stress response.....	12
1.4.4 DNA repair.....	13
1.4.5 Other functions of YB-1.....	14
1.4.6 Clinical significance of YB-1.....	15
1.4.7 YB-1 in protein-protein interactions.....	17
1.5 Retinoblastoma binding protein 6 (RBBP6).....	17



1.5.1 RBBP6 in cell development and tumorigenesis.....	19
1.5.2 RBBP6 in mRNA processing.....	22
1.5.3 Turnover of proteins	23
1.6 Ubiquitination	24
1.6.1 Ubiquitin-conjugating enzymes (E2s)	26
1.6.2 Ubiquitin-protein ligases (E3s)	27
1.7 Methods for identifying and investigating protein-protein interactions	30
1.7.1 Protein-protein interactions as probed by NMR	30
1.7.2 Yeast two-hybrid (Y2H)	31
1.7.3 Co-immunoprecipitation (Co-IP) assays.....	35
1.8 Justification and aims of the study.....	35
Chapter 2: Materials and methods.....	38
2.1 General chemicals and enzymes	38
2.2 Synthetic peptides	40
2.3 Stock solutions, buffers and media	40
2.4 Commercial antibodies	44
2.3 Plasmid vectors	45
2.3.1 pACT2 AD vector.....	45
2.3.2 pGBKT7-R.....	45
2.3.3 pGEX-6P-2	48
2.4 Bacterial cultures	48
2.4.1 Bacterial strain chromosomal genotype.....	48
2.4.2 Preparation of competent cells for transformation.....	50

2.4.3 Bacterial transformation with plasmid DNA	50
2.4.4 Extraction of plasmid DNA	51
2.5 Manipulation of plasmid DNA	51
2.5.1 Primer design	51
2.5.2 Amplification of DNA by PCR.....	52
2.5.3 Analysis of DNA.....	52
2.5.4 Purification of DNA.....	52
2.5.5 Restriction enzyme digestion.....	53
2.5.6 Ligation of DNA	54
2.5.7 Screening for positive clones	54
2.6 Co-immunoprecipitation	55
2.6.1 <i>In vitro</i> synthesis of bait and prey proteins.....	55
2.6.2 <i>In vitro</i> co-immunoprecipitation of bait and prey proteins	56
2.7 Yeast 2-hybrid methods	56
2.7.1 Yeast strains used.....	56
2.7.2 Transformation of yeast	57
2.7.3 Yeast mating	58
2.8 Recombinant protein expression.....	58
2.8.1 Small scale protein expression.....	58
2.8.2 Large scale protein expression.....	59
2.8.3 Expression in ¹⁵ N-labelled minimal media	59
2.9 Glutathione affinity chromatography.....	60
2.9.1 Preparation of glutathione affinity column	60



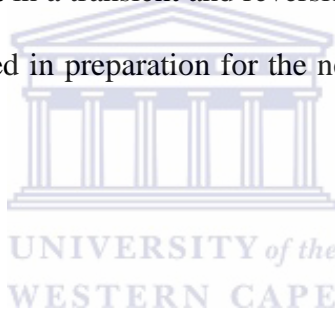
2.9.2 Purification of the crude lysate	60
2.9.3 Cleavage of recombinant protein	61
2.9.4 Size exclusion chromatography	61
2.10 SDS-PAGE	62
2.11 Determination of protein concentration	63
2.12 Methods in biomolecular NMR	64
2.12.1 Sample preparation	64
2.12.2 NMR titration experiments	64
2.13 <i>In vitro</i> ubiquitination assays	65
2.14 Generation of RING mutants	66
Chapter 3: Investigation of the interaction between the RING finger of RBBP6 and YB-1	67
3.1 Introduction	67
3.2 Analysis of the interaction between YB-1 and the RING finger domain of RBBP6 using a Yeast 2-hybrid assay	67
3.2.1 Generation of YB-1 derived fragments	68
3.2.2 Direct yeast 2-hybrid assay	68
3.3 Analysis of the interaction between YB-1 and the RING finger domain of RBBP6 using co- immunoprecipitation assays	72
3.3.1 Expression of proteins for use in the co-IP assay	72
3.3.2 RING finger co-immunoprecipitates YB-1 ₂₉₂₋₃₂₄ <i>in vitro</i>	74
3.4 Analysis of the interaction between YB-1 and the RING finger domain of RBBP6 using NMR spectroscopy	77
3.4.1 Expression and purification of the RING finger domain of RBBP6 for use in NMR	79

3.4.2 Determination of protein concentration	83
3.4.4 RING interacts with YB-1 through part of its C-terminal helix.	85
Chapter 4: Functional investigations	90
4.1 Identification of cognate RBBP6 E2s using an <i>in vitro</i> ubiquitination assay	90
4.1.1 UbcH5c and UbcH7 facilitate YB-1 ubiquitination <i>in vitro</i>	91
4.2 Investigation of the effect of mutagenesis on the homodimeric state of the RING finger	91
Chapter 5: Discussion and Conclusions.....	96
5.1 <i>In vitro</i> investigation of the RBBP6/YB-1 interaction	96
5.2 Ubiquitination of YB-1	97
5.3 Implications of the RBBP6/YB-1 interaction for human health.....	98
5.4 Prospective studies.....	100
References	101
Appendix II: Sequence analysis of YB-1 ²⁷⁷⁻³⁰⁶ cloned into pACT2 AD vector.	118
Appendix III: Sequence analysis of YB-1 ²⁹²⁻³²⁴ cloned into pACT2 AD vector.....	118
Appendix IV: Sequence analysis of RING ^{N312D} cloned into pGEX-6P-2 vector.	119
Appendix V: Sequence analysis of RING ^{K313E} cloned into pGEX-6P-2 vector.....	120

Chapter 1: General introduction

1.1 Introduction

Proteins have a propensity to specifically bind to other proteins as a means of mediating cellular function. These protein associations are of central importance for virtually every process in a living cell, including DNA replication, transcription, mRNA translation, protein degradation and signal transduction, to mention only a few. Many of these cellular processes are enacted by networks of interacting multi-protein complexes. The protein components that constitute these functional assemblies often interact in a transient and reversible manner and their arrangement is rapidly assembled and disassembled in preparation for the next required activity (Hanlon *et al.*, 2010).



A good example of a protein which exerts its function through protein-protein interaction is that of X-linked Inhibitor of Apoptosis Protein (XIAP). Through its Baculoviral IAP Repeat (BIR) domain, XIAP interacts with executioner caspases thereby inhibiting their function and preventing apoptosis (Abhari *et al.*, 2010). Protein-protein associations are also important in receptor-ligand interactions on cell surfaces, converting an extracellular signal into a response through a relay of protein-protein interactions. For example, extracellular Notch-3 receptor domains on the surface of mesangial and immune cells interact with a protein known as Y-box binding protein 1 (YB-1) upon cytokine challenge. This interaction activates Notch-3 signalling, resulting in nuclear translocation of the Notch-3 intracellular domain and subsequent up-regulation of Notch target genes (Rauen *et al.*, 2009). Aberrations in such intricate protein

associations often lead to disease states such as cancer. Deciphering these protein-protein interactions is crucial in the understanding of cellular processes and pharmaceutical development.

Retinoblastoma binding protein 6 (RBBP6) is a 250 kDa multi-functional human protein whose functions appear to be mediated predominantly through protein-protein interactions. RBBP6 plays an as-yet uncharacterised role in the splicing and 3'-end processing of messenger RNA (mRNA): its yeast homologue, Mpe1, forms part of the Cleavage and Polyadenylation Factor (CPF) and this human protein forms part of the 3'-end processing complex (Shi *et al.*, 2009). It has been shown to interact with mRNA splicing-associated protein SmG (Pugh and Chibi, unpublished data). RBBP6 interacts directly with the tumour suppressor p53 and facilitates its ubiquitination by Murine Double Minute 2 (MDM-2) (Li *et al.*, 2007). In addition, RBBP6 also interacts with another prototypical tumour suppressor protein, the Retinoblastoma gene product (pRB), underscoring its significance in tumourigenesis (Simons *et al.*, 1997). A recent study has employed a novel systems genetics approach, to implicate RBBP6 in the regulation of transcription, in particular estrogen-dependant transcription (Peidis *et al.*, 2010).

RBBP6 is also involved in the ubiquitination of certain protein substrates due to the presence of a RING finger domain that confers E3 ubiquitin-ligase activity. In a recent study employing the yeast 2-hybrid technique, RBBP6 was identified as an interaction partner of the multifunctional protein Y-box binding protein 1 (YB-1) (Chibi *et al.*, 2008). This interaction was mapped to a 62 amino acid region at the C-terminus of YB-1. The RBBP6/YB-1 interaction was shown to lead to

the ubiquitination of YB-1, consequently resulting in the proteolytic degradation of YB-1 in a proteasome-dependant manner (Chibi *et al.*, 2008).

YB-1 is a prototypical member of the cold shock domain family of proteins that are known to be involved in both translational and transcriptional gene regulation (Lu *et al.*, 2005). By and large, YB-1 can be broadly characterised as a cell survival factor that up-regulates a number of growth-promoting genes and its expression is closely correlated with cell proliferation. YB-1 expression has been shown to be up-regulated in proliferating human adult tissues and in a number of human carcinomas (Matsumoto *et al.*, 2005). Consistent with this observation, YB-1 over-expression has been linked to adverse clinicopathological effects in most human cancers. YB-1 has also been demonstrated to be anti-apoptotic through its ability to repress the transcription of the tumour suppressor protein p53, thereby enabling tumourigenic cells to survive (Lasham *et al.*, 2003; Homer *et al.*, 2005). As a result of its overwhelming significance in tumourigenicity, YB-1 is increasingly being identified as an important marker of prognosis in clinical oncology (Dahl *et al.*, 2009; Huang *et al.*, 2005; Kashihara *et al.*, 2009).

The principal aim of this study is to understand the structural basis of the RBBP6/YB-1 interaction and to gain more insight into the mechanism involved in YB-1 ubiquitination. This chapter reviews the structural organisation and the pleiotropic functions of both RBBP6 and YB-1. Since the functions of these proteins appear to be mediated by protein-protein interactions, this chapter also reviews the techniques available for studying protein-protein interactions, with the main focus on biomolecular NMR, complex immunoprecipitation (Co-IP) and the yeast 2-hybrid (Y2H) technique.

1.2 Y-Box Binding Protein Family

Y-Box binding proteins are multifunctional proteins belonging to the cold shock domain family, a highly conserved protein family found in plants, bacteria and animals (Kohno *et al.*, 2003). They were originally identified as DNA-binding proteins that are capable of interacting with the *cis*-acting DNA regulatory element known as the Y-box element (inverted CCAAT-box or GGTTA)(Didier *et al.*, 1988). Due to their DNA-binding properties, Y-box proteins control the transcription and translation of a number of genes.

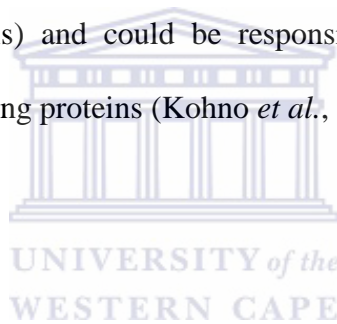
Apart from their inherent ability to interact with DNA, Y-box proteins have also been shown to interact with a myriad of cellular and viral proteins that are involved in a number of cellular processes. Y-box proteins exhibit functional pluripotency as they are involved in a diverse range of biological functions including transcriptional modulation of a wide array of genes, chromatin modification, translational masking of mRNA, participation in eukaryotic redox signalling pathways, RNA chaperoning, cell cycle control and stress response (Ruzanov *et al.*, 1999; Uchiumi *et al.*, 2006; Khandelwal *et al.*, 2009).

Y-box proteins share a common domain arrangement across a wide range of taxa, consisting of an N-terminal domain, the evolutionarily conserved Cold Shock Domain (CSD) and a C-terminal tail domain. The N-terminal domain of most Y-box proteins is an alanine/proline-rich domain which has been shown to confer Y-box proteins in *Caenorhabditis tentans*, human and rabbit an ability to bind to actin filaments (Soop *et al.*, 2003; Khandelwal *et al.*, 2009). However, current understanding of the functional role of the N-terminal domain in non-human Y-box proteins is limited.

The CSD is a highly stable domain which confers nucleic acid-binding properties to the Y-box proteins. It is noteworthy that prokaryotes lack the CSD, but they contain a domain similar to the CSD in the form of Cold Shock Proteins (CSPs). Well documented CSPs are those from the mesophilic bacterium *Escherichia coli*, which have been implicated to play a role in the cold shock response during the cold acclimation phase (Phadtare, 2004); for example CspA functions as an RNA chaperone that facilitates translation at low temperature by blocking the formation of secondary RNA structures in mRNA (Inouye *et al.*, 2004). The CSD-containing proteins were initially characterised for prokaryotes and higher animals but are increasingly being characterised in both lower animals and plants as well. CSD proteins have been well-documented in *Arabidopsis Thaliana*, tobacco, *Chlamydomonas reinhardtii*, *Ceratopteris richardii* and wheat (Karlson *et al.*, 2002; Karlson *et al.*, 2003; Kim *et al.*, 2007). As with prokaryotic CSPs, CSD proteins in higher plants have been shown to function as RNA chaperones capable of destabilising RNA secondary structure and have also been demonstrated to regulate translation under low temperatures (Nakaminami *et al.*, 2006).

The structure of the C-terminal domain of Y-box proteins varies significantly across taxa. These structural differences are shown in Fig 1.1. In vertebrate Y-box binding proteins, the C-terminal domain consists of alternating clusters of basic and acidic amino acids (B/A repeats), each about 30 amino acids in length. This feature is also found in proteins that bind to ribonucleoprotein complexes for shuttling between the nucleus and the cytoplasm (Wu *et al.*, 2007; Shu-Nu *et al.*, 2000). Within invertebrate Y-box proteins there is significant variation in their C-terminal domains. In *Drosophila melanogaster* and in the marine invertebrate *Aplysia californica* the tail domain lacks acidic amino acids and contains multiple RNA-binding RGG repeats (Takiya *et al.*,

2004). In *Caenorhabditis elegans* the C-terminal domain contains zinc fingers (Worringer *et al.*, 2007) and in *Schistosoma mansoni* it contains a fibroin-like β -sandwich structure due to the presence of tandem repeats of arginine and glycine residues (Valadao *et al.*, 2002). These tandem repeats of arginine and glycine residues are predicted to project towards a common surface, providing a second site for nucleic acid binding. The presence of distinct nucleic acid binding sites within a protein is often associated with regulatory functions, as it allows the protein to regulate a number of different genes. These structural alterations in the C-terminal domain may have been necessary for the evolution from poikilotherms (organisms whose internal temperature varies along with that of the ambient environmental temperature) to homiotherms (organisms that maintain thermal homeostasis) and could be responsible for conferring the pleiotropic functions exhibited by Y-box binding proteins (Kohno *et al.*, 2003).



1.3 Human Y-box binding protein-1 (YB-1)

Human Y-box binding protein-1, also known as dbpB or p50, is the most extensively studied of the Y-box proteins. It is a 43 kDa protein which was initially identified as a transcription factor that specifically recognises the Y-box promoter element (inverted CCAAT or GGTTA) in a variety of different genes (Didier *et al.*, 1988). The YB-1 gene comprises 8 exons spanning 19 kb of genomic DNA, located on chromosome 1p34 (Kuwano *et al.*, 2004). The mRNA is approximately 1.5 kb long and encodes a 324 amino acid protein.

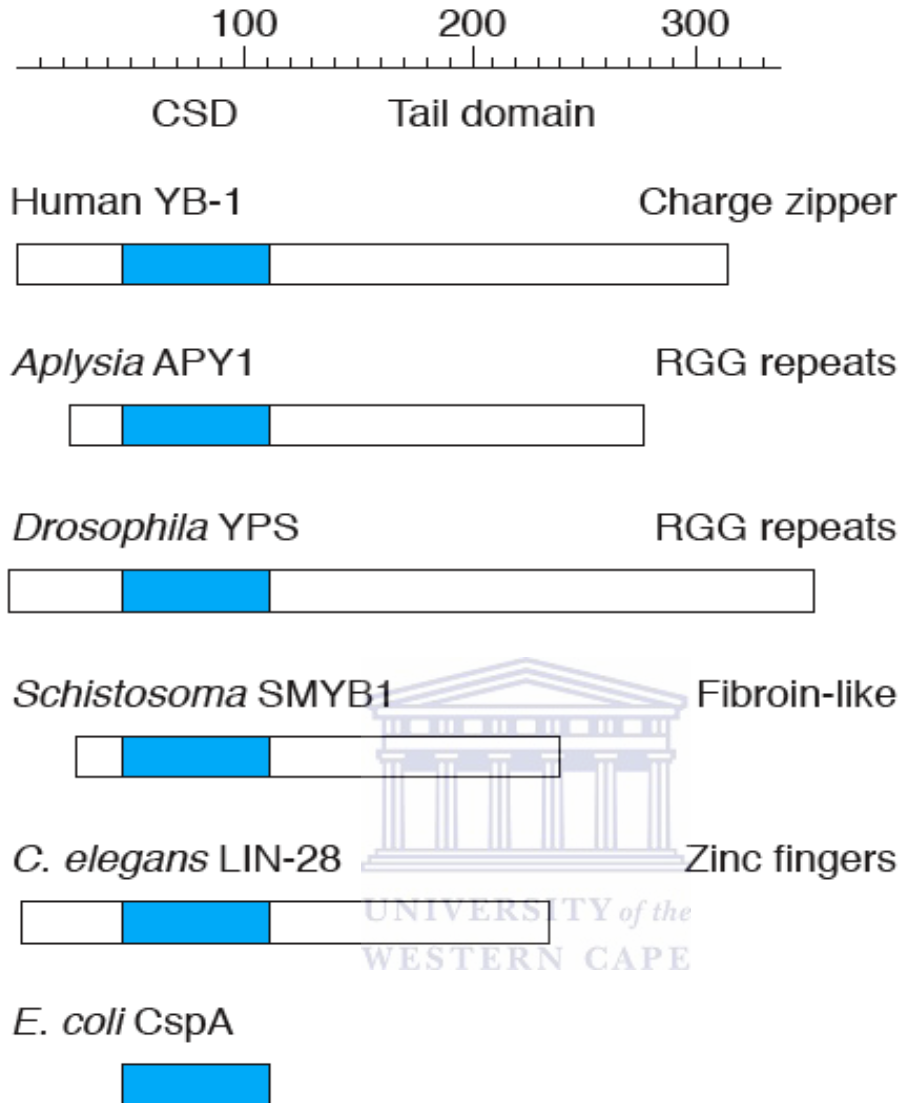


Fig. 1.1 Y-box proteins from different organisms. The Y-box proteins are aligned at their CSDs (the blue region) and the different features on the C-terminal tail domains are indicated. The C-terminal tail domains differ significantly in their sequence organisation. Adapted from(Matsumoto *et al.*, 1998).

The structure of YB-1 is characteristic of Y-box proteins, consisting an N-terminal alanine/proline-rich domain (AP), cold-shock domain (CSD) in its central part and a C-terminal tail domain (Fig. 1.2). The C-terminal tail domain is composed of four alternating clusters of negatively and positively charged amino acids and is the major domain that mediates protein-protein interactions involving YB-1 (Selivanova *et al.*, 2010). The N-terminal AP domain of YB-1 is known to associate with actin microfilaments, presumably contributing to mRNA localization (Chernov *et al.*, 2008). YB-1 also contains an ATP-binding motif at its N-terminus between residues 28-58 which is thought to play a major role in the strand separation activities involving YB-1 (Guay *et al.*, 2008; Gaudreault *et al.*, 2004). The N-terminal domain also mediates YB-1's cell proliferation- promoting function by sequestering cyclin D1 in the cytoplasm (Khandelwal *et al.*, 2009).



1.4 Functions of YB-1

YB-1 shuttles between the nucleus and the cytoplasm, exhibiting different functions depending on its cellular localization. The mechanism of YB-1 translocation to the nucleus is a poorly understood phenomenon and there are several conflicting hypotheses (Sorokin *et al.*, 2007; Cohen *et al.*, 2010; Basaki *et al.*, 2007). When in the nucleus, YB-1 controls the transcription of a number of genes involved in cell proliferation and differentiation (En-Nia *et al.*, 2005; Jurchott *et al.*, 2003) whereas in the cytoplasm it plays crucial functions in RNA metabolism and interacts with tubulin and microtubules, promoting microtubule assembly (Chernov *et al.*, 2008).

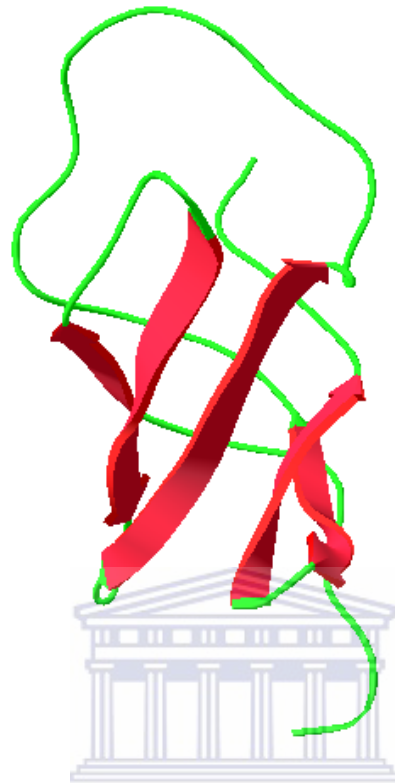
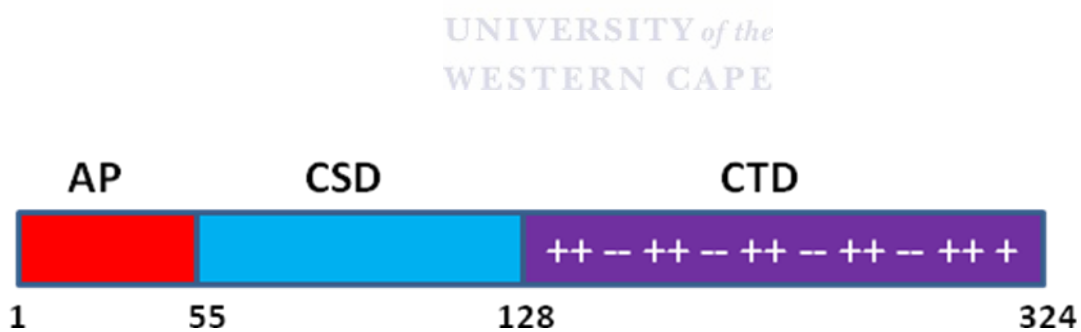
A**B**

Fig. 1.2 Domain organisation in YB-1. (A) Cartoon representation of the 3D structure of the CSD from human YB-1 (PDB: 1H95). The CSD is a stable domain containing a 5-stranded anti-parallel β -sheet. The β -strands are shown in red arrows, while the connecting loops are shown in green. Figure created using Swiss PDB viewer. Adapted from (Kloks *et al.*, 2002). (B) Schematic representation of the structure of YB-1 showing the three constitutive domains and their amino acid boundaries: the alanine/proline-rich (AP) N-terminal domain spanning from 1 to 55, the cold-shock domain (CSD) from 55 to 128 and the C-terminal tail domain (CTD) from 128 to 324. ++ and -- indicate alternating clusters of basic and acidic amino acids, respectively. Adapted from (Sorokin *et al.*, 2007).

1.4.1 Transcriptional regulation

The number of genes in the cell regulated by YB-1 is very large. Among others, these genes include histones, dihydrofolate reductase, thymidine kinase and thymidine synthase, Proliferating Cell Nuclear Antigen (PCNA), topoisomerase II α , and DNA Polymerase α (DPA) (En-Nia *et al.*, 2005). Most YB-1 responsive genes are growth-promoting and many of them are involved in DNA replication, including Epidermal Growth Factor Receptor (EGFR), PCNA, human growth factor receptor (HER)-2, cyclin A, cyclin B1 and DPA, all of which are regulated by YB-1 in a Y-box dependent manner (Evdokimova *et al.*, 2006a; Kloks *et al.*, 2002). The promoter regions of most YB-1 responsive genes contain a Y-box sequence motif along their sequences (CTGATTGG), also known as the inverted CCAAT box. YB-1 recognizes and binds to this Y-box element, thereby activating or repressing expression of these genes.

For example, the Y-box is present in the promoter region of the Multidrug Resistance 1 (*MDR1*) gene which codes for P-glycoprotein, an adenosine triphosphate-dependent (ATP-dependent) efflux pump that reduces drug accumulation in chemo-resistant cells (Choi, 2005; Wang *et al.*, 2006). YB-1 activates the *MDR1* gene, leading to the overexpression of the P-glycoprotein gene (Saji *et al.*, 2003; Vaiman *et al.*, 2006). It has also been reported that nuclear expression of YB-1 protein correlates with P-glycoprotein expression in human breast carcinomas (Huang *et al.*, 2004; Wang *et al.*, 2006).

The expression of two genes, *EGFR* and *HER-2*, both of which promote tumour growth, has also been shown to be regulated by YB-1 (Stratford *et al.*, 2007; Wu *et al.*, 2006). Wu and co-workers demonstrated that the disruption of YB-1 resulted in the suppression of levels of EGFR and

HER-2, the products of the *EGFR* and *HER-2* genes respectively (Wu *et al.*, 2006). *Cyclin A* and *cyclin B1* genes, both of which are crucial for cell cycle progression, have also been demonstrated to be transcriptionally activated by the nuclear accumulation of YB-1 (Jurchott *et al.*, 2003). Both contain a CCAAT-box within their promoters, to which YB-1 has been shown to bind (En-Nia *et al.*, 2005; Saji *et al.*, 2003). Cyclin A is required for the onset of DNA replication in the G₂-S phase transition of the cell cycle and independently induces DNA replication, but executes this role synergistically with cyclin E (Tsang *et al.*, 2007). Overexpression of cyclin A affects cell cycle progression and leads to accelerated entry into the S phase which supports the multiplication of tumorigenic cells.

1.4.2 Translational control and mRNA metabolism

YB-1 is a non-specific RNA-binding protein that is involved in the regulation of a broad range of mRNA metabolic processes including transcription, splicing, and translation and even mRNA stability. The RNA-binding ability of YB-1 is conferred by the RNA-binding motifs present in the CSD of YB-1. YB-1 has been shown to inhibit mRNA translation in both cap-dependent and cap-independent mechanisms. Consistent with its inhibitory role in translation, YB-1 is a major constituent of Messenger Ribonucleoprotein Particles (mRNPs), cytoplasmic complexes which are responsible for the storage of mRNA in a translationally inactive (silent) state (Skabkin *et al.*, 2004). While in this complex, YB-1 binds in close proximity to the mRNA cap structure and is able to displace the initiation factors, Eukaryotic translation Initiation Factor 4E (eIF4E) and eIF4G from the transcript, thereby causing mRNA translational silencing (Nekrasov *et al.*, 2003).

The cap-dependent mechanism of translational silencing by YB-1 has been well documented. The association of YB-1 with the capped 5'-terminus of the mRNA is regulated via phosphorylation by the serine/threonine protein kinase Akt (Evdokimova *et al.*, 2006b). Evdokimova and co-workers showed that Akt-phosphorylated YB-1 failed to inhibit cap-dependent translation of a reporter mRNA. YB-1 has recently been implicated in the regulation of mRNA translation using a novel cap-independent mechanism (Mouneimne *et al.*, 2009). This has been reported to occur when epithelial cancer cells transform to mesenchymal cells during the invasive phase of metastasis in a process known as Epithelial-to-Mesenchymal Transition (EMT). YB-1 regulates transcription of many EMT-related proteins in a cap-independent manner (Evdokimova *et al.*, 2009).



1.4.3. Stress response

Several studies have demonstrated that YB1 is directly involved in the cellular response to genotoxic stress. YB-1 contains a non-canonical Nuclear Localisation Signal (NLS) at its C-terminus as well as a Cytoplasmic Retention Signal (CRS) (Bader *et al.*, 2005; Sorokin *et al.*, 2005). Until very recently, the nuclear export of YB-1 was believed to be dependent on proteolytic cleavage of the C-terminal 105-amino-acids of YB-1 which contain the cytoplasmic retention signal (Sorokin *et al.*, 2005). This proteolytic cleavage was thought to be induced by genotoxic stimuli. However a recent study has shown that the nuclear export of YB-1 is independent of proteolytic cleavage by the 20S proteasome and that the full length YB-1 protein is present in the nucleus (Cohen *et al.*, 2010). The relationship between these sets of observations is not clear but there is a consensus among researchers that import of YB-1 into the nucleus can

be induced by stress and genotoxic stimuli such as UV radiation, hyperthermia, and anticancer agents.

The nucleocytoplasmic transport of YB-1 is thought to occur through the Nuclear Pore Complex (NPC) – a large protein complex spanning the nuclear envelope (Serokin *et al.*, 2007). The nuclear transport of YB-1 is mediated by a family of transport receptors known as karyopherins, which, bind their cargoes via recognition of an NLS. Once in the nucleus, nuclear YB-1 protects cells from genotoxic insults associated with exposure to DNA-damaging agents like UV radiation and anticancer drugs. It preferentially binds to the cross-linked regions of structurally altered DNA promoting the re-annealing of damaged DNA (Skabkin *et al.*, 2001; Sorokin *et al.*, 2005).



1.4.4 DNA repair

YB-1 plays a role in maintaining genome stability through its interaction with DNA repair proteins. *In vitro* binding studies have demonstrated that YB-1 binds to several DNA repair proteins including MutS Homolog 2 (MSH2), DNA polymerase α , ku80 and the Werner syndrome protein WRN (Gaudreault *et al.*, 2004). Apart from its ability to repair nuclear DNA, YB-1 has recently been implicated in the repair of mitochondrial DNA (de Souza-Pinto *et al.*, 2009). de Souza-Pinto and co-workers demonstrated that YB-1 participates in the mitochondrial mismatch repair mechanism and they were able to show that depletion of YB-1 resulted in an increased rate of mitochondrial DNA mutagenesis.

YB-1 exhibits both intrinsic endonuclease and 3'-5' exonuclease activity on double stranded DNA but has been shown to bind preferentially to single-stranded nucleic acids (Gaudreault *et al.*, 2004). In addition, YB-1 is a potent enhancer of the nucleotide excision activity of the base-specific DNA glycosylase known as NEIL2 (Nei-Like-2), stimulating its activity 7-fold (Das *et al.*, 2007). NEIL2-initiated base excision activity is significantly reduced in YB-1-depleted cells, suggesting that YB-1 performs a regulatory role in NEIL2-mediated repair under oxidative stress. This substantial body of evidence espouses the participation of YB-1 in the cell's robust base excision repair mechanism.

1.4.5 Other functions of YB-1

Apart from regulating cellular functions such as transcription, RNA metabolism and DNA repair, YB-1 has been reported to be involved in numerous other cellular processes. Pathogenic viruses use host derived YB-1 protein to *trans-activate* transcription from viral promoters in infected cells. YB-1 facilitates adenoviral replication and the release of viral particles from infected cells (Glockzin *et al.*, 2006). Furthermore, YB-1 has been shown to inhibit the ability of p53 to cause cell death by preventing transactivation of pro-apoptotic genes (Homer *et al.*, 2005).

Intercellular functions of YB-1 have been well-studied, and it is only recently that extracellular functions of YB-1 have come to light. Upon cytokine challenge, which usually occurs under inflammatory conditions, mesangial and immune cells both secrete YB-1 (Frye *et al.*, 2009). Extracellular YB-1 has been shown to increase DNA synthesis, proliferation and migration suggesting that it exerts mitogenic as well as promigratory effects in inflammation. In another elegant study, extracellular YB-1 was shown to associate with outer cell membrane components

and interact with extracellular Notch-3 receptor domains on the cell surface of mesangial and immune cells (Rauen *et al.*, 2009). The interaction of YB-1 with Notch-3 receptors activates intercellular Notch-3 signalling and the transcription of Notch responsive genes.

1.4.6 Clinical significance of YB-1

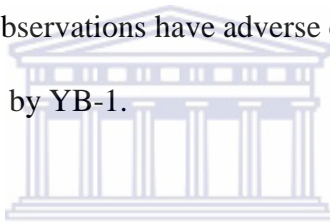
YB-1 plays a crucial role in cellular resistance to cancer therapeutic agents, whose mechanism of action is largely dependent on destabilisation of cellular DNA. Since YB-1 is involved in DNA repair systems, it poses a threat to the success of DNA-damaging anticancer agents like chemotherapeutic drugs and UV irradiation (Fujita *et al.*, 2005).

YB-1 also promotes resistance by upregulating the removal of chemotherapeutic agents from the cell (Vaiman *et al.*, 2006). YB-1 activates the *MDR1* gene which encodes P-glycoprotein which is overexpressed in various human tumors after chemotherapy. P-glycoprotein is an ATP-dependant efflux pump that flushes out xenobiotic drugs from cells. Most of these xenobiotic compounds are anti cancer drugs which, when flushed out of the cell, fail to exert their therapeutic efficacy. As a result, drug resistance is conferred to cancerous cells.

It has been demonstrated that YB-1 overexpression is closely associated with unfavourable clinical outcomes in most human carcinomas (Kuwano *et al.*, 2004). The level of nuclear expression of YB-1 is predictive of drug resistance and patient survival in a variety of human cancers. In predictive oncology, YB-1 has of late replaced conventional prognostic markers of breast cancer like the EGFR and HER-2 (Dahl *et al.*, 2009; Huang *et al.*, 2004; Kashihara *et al.*,

2009). In molecular diagnosis of breast cancer, YB-1 is used as a predictor of tumour aggressiveness, virulence and resistance to chemotherapeutic drugs (Habibi *et al.*, 2008).

For cancerous cells to metastasise, they first need to undergo the Epithelial-to-Mesenchymal Transition (EMT). YB-1 promotes the transcription of various EMT promoting factors, including Snail 1 and Twist (Evdokimova *et al.*, 2009; Mouneimne *et al.*, 2009). Furthermore, YB-1 is believed to promote metastasis of tumours by enhancing the transcription of gelatinase A, a matrix metalloproteinase that facilitates cell migration (Mertens *et al.*, 2002). More recent studies have also shown that extracellular YB-1 may be capable of exerting promigratory effects on cells (Frye *et al.*, 2009). These observations have adverse clinical implications as they point to the promotion of tumour metastasis by YB-1.



Since YB-1 activates growth-promoting genes and encourages tumour metastasis, it is hardly surprising that YB-1 expression is significantly correlated with tumour size, degree of invasion, lymph node metastasis and poor prognosis in lung cancer and synovial sarcoma (reviewed in (Fujii *et al.*, 2008). YB-1 also contributes to breast tumour aggressiveness, especially in invasive ductal breast cancer, as a result of the induction of the epidermal growth factor EGF receptor pathway (Berquin *et al.*, 2005). YB-1 levels have also been found to be up-regulated during prostate cancer progression (Gimenez-Bonafe *et al.*, 2004).

Taken together these observations have shown YB-1 to be highly correlated with adverse clinicopathological effects in many human carcinomas. Many studies have proposed targeting of YB-1 as a means of containing cancer. However it has also been pointed out that direct targeting

of YB-1 might prove to be futile or even counterproductive since YB-1 has been shown to be an important factor in keeping cells dormant after they metastasize (Mouneimne *et al.*, 2009).

1.4.7 YB-1 in protein-protein interactions

YB-1 performs most of its physiological functions through protein-protein interactions and it interacts with a number of cellular and viral proteins that are involved in various cellular processes. YB-1 exerts its pro-tumourigenic effects by suppressing the transcription of pro-apoptotic genes through its interaction with the tumour suppressor protein p53 (Homer *et al.*, 2005). Recently, another modular protein known as Retinoblastoma Binding Protein 6 (RBBP6) has been shown to interact with YB-1 (Chibi *et al.*, 2008). The interaction is believed to occur through the RING finger domain of RBBP6 and the C-terminal domain of YB-1. *In vivo* studies by Chibi and co-workers have demonstrated that this interaction is crucial for the ubiquitination and subsequent degradation of YB-1 by the 26S proteasome (Chibi *et al.*, 2008).

1.5 Retinoblastoma binding protein 6 (RBBP6)

Retinoblastoma binding protein 6 is a 250 kDa human protein that was initially shown to bind to the retinoblastoma gene product, pRB, and accordingly designated as RBBP6 (Sakai *et al.*, 1995). Its significance in cancer is highlighted by its interaction with both of the prototypical tumour suppressor proteins, p53 and pRB (Li *et al.*, 2007; Simons *et al.*, 1997). While the physiological relevance of the RBBP6/pRB interaction remains unclear, RBBP6 has been shown to negatively regulate p53, interfering with p53's binding to DNA. RBBP6 has been reported to

play a crucial role in the ubiquitination of p53 by MDM-2. Recent studies have shown human RBBP6 to play significant roles in transcription and mRNA editing (Peidis *et al.*, 2010; Pugh *et al.*, 2006; Shi *et al.*, 2009).

The domain structure of human RBBP6 is shown schematically in Fig. 1.3. RBBP6-like proteins are present in all eukaryotic genomes for which sequence data is available, but have not been found in prokaryotes. The first 3 domains - DWNN, Zinc knuckle and RING finger - are well conserved across all eukaryotes. However the C-terminal region is poorly conserved with few conserved domains being identified so far. At the N-terminus of all RBBP6 orthologues is the DWNN domain which adopts a ubiquitin-like fold (Pugh *et al.*, 2006). Analysis of cDNA data shows that the DWNN domain is only expressed as an independent splicing isoform in vertebrates. There is a di-glycine peptide in the DWNN domain, which resembles the conserved di-glycine motif found at position 75 and 76 of ubiquitin which is essential for conjugation of ubiquitin to other proteins. The presence of the di-glycine motif in the DWNN domain has led to the suggestion that the DWNN domain may be covalently linked to proteins in the same manner as ubiquitin (Pugh *et al.*, 2006).

Another functionally relevant domain in human RBBP6 is the RING (Really Interesting New Gene) finger domain (Fig.1.4). The RING motif consists of a series of eight conserved cysteines and/or histidines, which bind two Zn^{2+} ions in a cross-braced configuration. However, sequence alignments indicate that the RBBP6 RING finger may also be classified as a member of the U-box family of domains which adopt the same structure as RING fingers but do not require Zn^{2+} ions to fold. The presence of the RING finger domain in RBBP6 confers E3-ubiquitin ligase

activity to RBBP6, implicating this protein in the ubiquitination and subsequent degradation of substrate proteins in a proteasome-dependent manner (Chibi *et al.*, 2008). The structure of the RING finger like-domain has recently been determined using NMR spectroscopy and shown to adopt a homodimeric configuration very similar to that found in U-boxes (Pugh and Kappo, unpublished data).

In addition to the DWNN domain and the RING finger domain, human RBBP6 contains a zinc knuckle domain that is thought to confer mRNA-binding activity to proteins ((Vo *et al.*, 2001) and a serine/arginine rich domain (SR domain) that is commonly found in splicing factors. Both of these are likely to play roles in the mRNA-processing functions of RBBP6, although the precise mechanisms remain to be discovered. Finally, human RBBP6 contains regions identified as interacting with p53 and pRb. These extra protein modules in human RBBP6 are thought to have been acquired later during evolution and are believed to confer new functionalities not required in lower eukaryotes, such as tumour suppression and apoptosis.

1.5.1 RBBP6 in cell development and tumourigenesis

The RBBP6 homologue in mice, known as p53-associated cellular protein-testes derived (PACT), interacts with the tumor suppressor protein p53 (Li *et al.*, 2007). Li and co-workers have demonstrated that the PACT/p53 interaction negatively regulates p53 by increasing the ubiquitination and resultant proteasomal degradation of p53 by MDM-2. Since p53 plays a pivotal role in driving the process of programmed cell death, down regulation of p53 as a result of the PACT/p53 interaction has considerable implications in tumourigenesis. Studies on the functions of PACT using PACT knock-out mice revealed that disruption of PACT leads to early

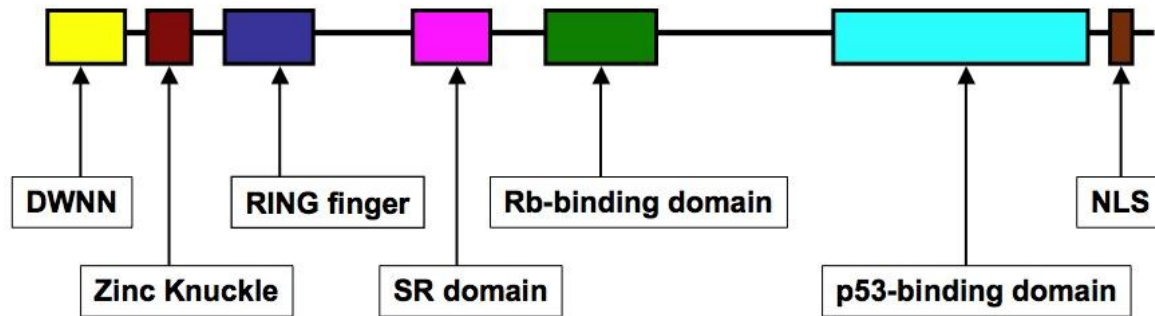
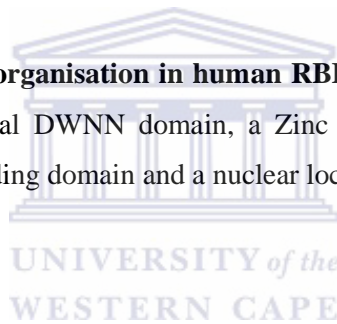


Fig. 1.3 Illustration of the domain organisation in human RBBP6. The RBBP6 protein is a modular protein that consists of an N-terminal DWNN domain, a Zinc knuckle, a RING finger domain, SR domain, Rb-binding domain, p53-binding domain and a nuclear localisation signal at its C-terminal end.



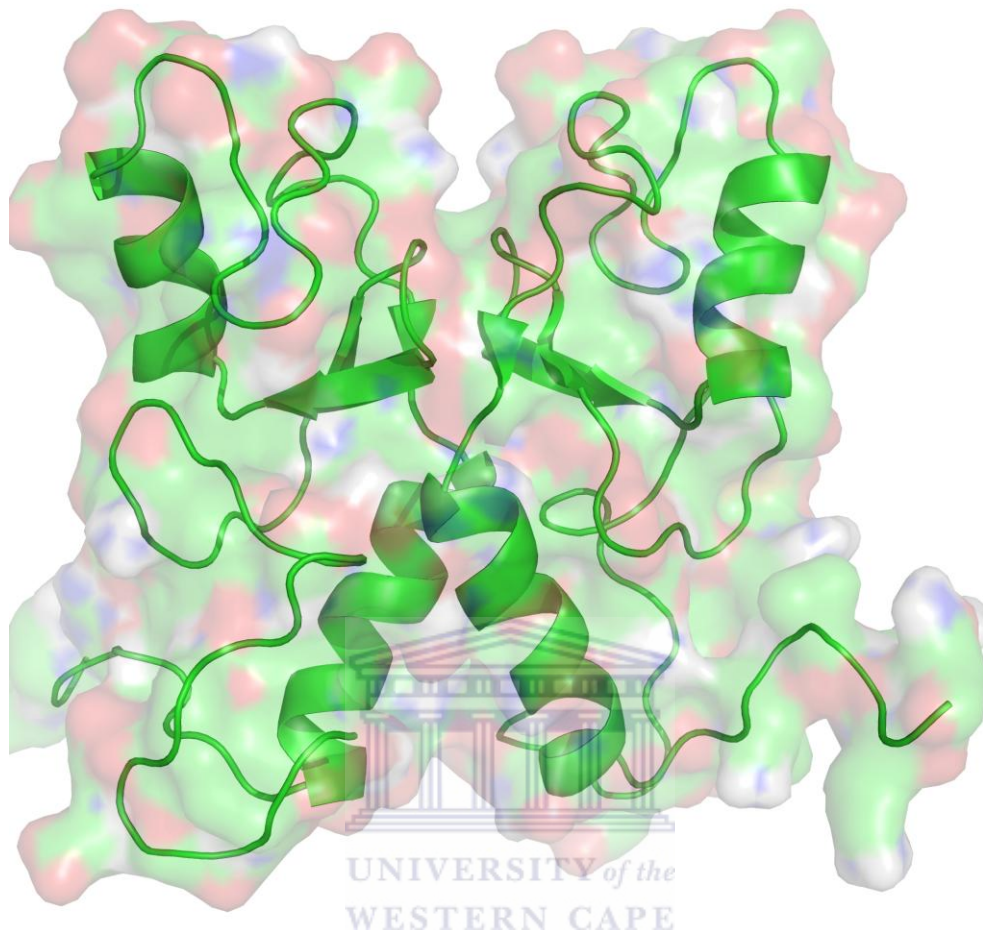


Fig. 1.4 A cartoon representation of the homodimeric structure of the RING finger-like domain of human RBBP6. The picture shows the superimposed ribbon and space-filling models of the homodimeric RING finger domain. Each monomer is stabilised by two zinc ions (not shown in the above picture), and consists of a three-stranded anti-parallel B-sheet (shown as green arrows) and two alpha helices (green coils), linked by loops. Adapted from Pugh *et al.*, unpublished data.

embryonic death accompanied by widespread apoptosis (Li *et al.*, 2007). Taken together, these findings suggest that PACT is anti-apoptotic in mice and that it is essential for development. On the other hand, studies done on human MCF breast cancer cells suggest that RBBP6 promotes apoptosis (Gao *et al.*, 2003; Gao *et al.*, 2002).

RBBP6 expression has been shown to be up regulated in oesophageal cancer (Yoshitake *et al.*, 2004). Yoshitake and co-workers demonstrated that RBBP6 promotes the proliferation of oesophageal cancer cells and that antibodies against RBBP6 can be successfully used in immunotherapy against oesophageal cancer, leading to decreases in tumour size.

1.5.2 RBBP6 in mRNA processing

Until recently the evidence for the involvement of RBBP6 in mRNA 3'-end processing and splicing was based on the presence of an SR domain, commonly found in splicing proteins, and the involvement of the yeast orthologue in the cleavage and polyadenylation factor (CPF) (Vo *et al.*, 2001; Shi *et al.*, 2009). Recently, RBBP6 has been shown to be a member of the human 3'-end processing complex (Shi *et al.*, 2009). The human pre-mRNA 3'-end processing complex contains approximately 85 proteins which are intricately linked to other cellular events. Shi and co-workers were the first to successfully isolate and purify a functional human pre-mRNA processing complex which they then subjected to mass spectrometry to identify the component proteins. Analysis of the protein composition of the human pre-mRNA processing revealed that RBBP6 is a component of the polyadenylation machinery.

Although it has yet to be directly tested for its role in pre-mRNA processing, it is likely that RBBP6, just like its yeast homologue Mpe1, functions in pre-mRNA processing (Vo *et al.*, 2001). Using the tandem affinity purification, Mpe1 was shown to be an integral component of the cleavage and polyadenylation factor (CPF) complex. The CPF complex functionally cooperates with the poly(A) binding protein, Pab1p, and cleavage factor I in mRNA cleavage and polyadenylation (Vo *et al.*, 2001). Stable CPF devoid of Mpe1 failed to specifically cleave and polyadenylate mRNA, suggesting that Mpe1 is strictly required for CPF-mediated RNA processing.

Since RBBP6 interacts with p53 and pRb, it has been speculated that RBBP6 may link mRNA 3'-end formation to pRb/p53 pathways and tumorigenesis (Shi *et al.*, 2009). Furthermore, using the yeast 2-hybrid technique, RBBP6 has recently been shown to interact with Small Nuclear Ribonucleoprotein G (snRPG) through its DWNN domain (Pugh, *et al.*, unpublished data), which is a crucial component of the RNA processing machinery in the cell. Taken together, these observations substantiate the involvement of RBBP6 in pathways involved in mRNA processing.

1.5.3 Turnover of proteins

Human RBBP6 has intrinsic E3 ubiquitin ligase activity due to the presence of the RING finger domain in its structure (Chibi *et al.*, 2008). RBBP6 has been shown to ubiquitinate YB-1 both *in vitro* and *in vivo*, leading to the suppression of YB-1 levels in a proteasome-dependant manner. RBBP6 has also been shown to ubiquitinate the methyl-binding transcriptional repressor zBTB38 (Zinc finger and BTB domain containing 38) (Chibi and Pugh, unpublished data) and it is possible that other substrates remain to be identified

In addition to E3 ligase activity, a report from Li and co-workers suggests that RBBP6 also has E4 ligase activity (Li *et al.*, 2007). Li and co-workers showed that although RBBP6 was not itself responsible for ubiquitination of p53, it was nevertheless required for ubiquitination of p53 by MDM-2. They suggested that RBBP6 may play the role of a molecular scaffold, recruiting p53 and MDM-2 and thereby facilitating their interaction.

1.6 Ubiquitination

Ubiquitination is a highly specific, energy-dependant degradation process that is achieved through the attachment of one or more ubiquitin moieties to a target protein (Fig.1.5). Once tagged with ubiquitin, the target molecules are then degraded in the proteasome, a barrel-shaped protein complex, where proteins are disassembled by proteases. Ubiquitination is a concerted action of three different enzymes: ubiquitin-activating enzyme E1, ubiquitin-conjugating enzyme E2, and substrate-specific ubiquitin-protein ligase E3 (Kerscher *et al.*, 2006). It is thought that additional conjugation factors known as E4 ligases may also be required for polyubiquitination of protein substrates. However, although E4 ligases have been described in the ubiquitination mechanisms of a few yeast and human proteins (Grossman *et al.*, 2003; Haenzelmann *et al.*, 2010), their role is still in dispute.

Ubiquitin is activated by the E1 enzyme, which cleaves it after the di-glycine motif and attaches it to its active site cysteine by a thioester linkage. This transfer consumes ATP, making it an energy-dependent process. The ubiquitin moiety is then transferred to a cysteine on the E2 enzyme, also involving a thioester linkage before being transferred to a lysine residue on the

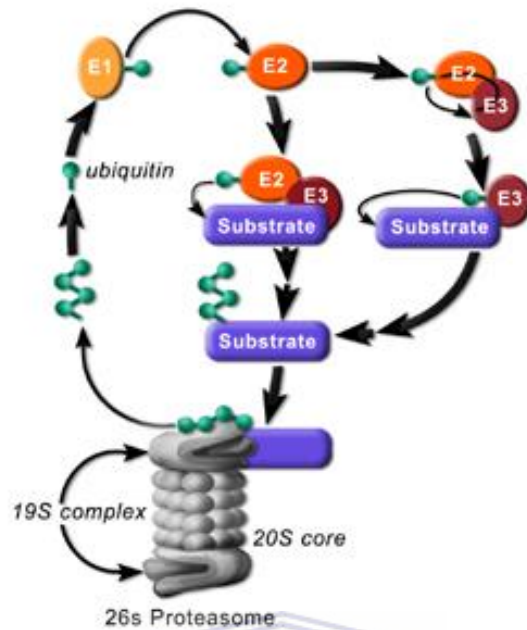
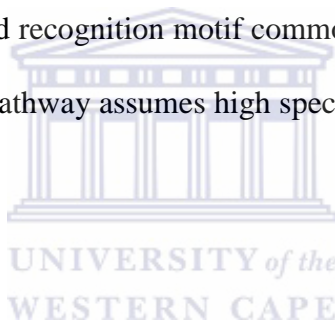


Fig. 1.5 A schematic illustration of the ubiquitin-proteasome pathway. Ubiquitination of proteasomal substrate proteins is performed by a complex system consisting of ubiquitin activating (E1) enzymes, ubiquitin-conjugating (E2) enzymes and substrate recognition proteins (E3 enzymes). In the final step ubiquitin is either directly transferred from E2 to the protein substrate or via an E3 with the formation of a thiol ester bond between E2 and E3. The ubiquitin moiety is recycled when the cycle is complete.

substrate by an isopeptide linkage. In RING finger-containing E3s the role of the RING is to bind the ubiquitin-bound E2, bringing it into contact with the substrate which is bound by a separate substrate binding domain of the E3. In HECT-containing E3s the HECT domain interacts first with the E2, causing ubiquitin to be covalently linked to the HECT domain itself, and then with the substrate-binding domain, which is typically a separate protein associating with the HECT domain through non-covalent interactions.

Substrate specificity increases as the three-step process advances. E1 interacts with all E2s, which interact with a more limited subset of cognate E3s. E3s in turn target a limited array of substrate proteins based on a shared recognition motif common to proteins being labelled. In this manner the ubiquitin-proteasome pathway assumes high specificity in the selection of proteins to be labelled (Markson *et al.*, 2009).



1.6.1 Ubiquitin-conjugating enzymes (E2s)

A number of ubiquitin-conjugating enzymes (UBC), also known as E2s, varies widely across different organisms. In the relatively small genome of *Saccharomyces cerevisiae* 16 genes code for E2-like proteins (van Wijk *et al.*, 2010), whereas over 30 E2s have been identified in human, all of which share a conserved UBC domain of approximately 150 amino acid residues (Arai *et al.*, 2006). Functions of these enzymes include roles in DNA repair, cell cycle progression, organelle biogenesis, secretion and stress response. Some of these E2s have more specific roles whereas others have overlapping functions. Specific functions of some E2s may be the result of their association with specific E3s, which in turn binds to their specific protein substrates.

E2s can bind directly to protein substrates or in combination with an E3. The stringency of E2-E3 interactions depend on the identity of the E2 or E3 involved. Some E2s can interact with more than one E3 enzyme and some E3s can interact with several E2s. For example, using a structure-based yeast 2-hybrid approach, Klevit and co-workers demonstrated that the human RING E3 BRCA1 interacts with ten E2s (Christensen *et al.*, 2009). Based on their observations, Klevit and co-workers postulated that the ability of BRCA1 to interact with more than one E2 could be a common feature among other RING and U-box E3s. The fact that many E2s are capable of interacting with the same E3 demonstrates a form of functional redundancy especially within the E2 enzyme family which has undergone evolutionary expansion.

1.6.2 Ubiquitin-protein ligases (E3s)

Ubiquitin-protein ligases are classified into four types: namely the HECT (homologous to E6-associated protein C-terminus), RING (really interesting new gene) or U-box (a modified RING motif without the full complement of Zn²⁺-binding ligands) and N-end rule E3 ligases. The first to be identified were the N-end rule E3 ligases which bind N-end rule protein substrates that have basic (Type I) or bulky hydrophobic (Type II) N-terminal amino acid residues (Baboshina *et al.*, 2001). The N-end rule E3s bind proteins bearing N-termini type I and type II residues with higher affinities compared with proteins bearing other residues (Type III). Paradoxically, a significant fraction of eukaryotic protein degradation occurs through the N-end rule pathway, although the majority of cellular proteins are type III substrates. Many human N-end rule E3s have been characterised thus far (Kume *et al.*, 2010; Zenker *et al.*, 2005; Tasaki *et al.*, 2005). The N-end rule recognition mechanism is strongly conserved in eukaryotic evolution (Mogk *et al.*, 2007). Surprisingly, the N-end rule pathway of protein degradation has recently been

reported in bacteria although prokaryotes are known to be devoid of a ubiquitin system (Varshavsky, 2008).

A second major family of E3 enzymes was originally identified by its sequence similarity to the C-terminal region of the E6-associated protein (E6-AP), an E3 ubiquitin-protein ligase. This homologous C-terminal region is a 350 amino acid-long region known as the homologous to E6-AP C-terminus (HECT) domain. The HECT domain binds to specific E2s, accepts ubiquitin from the E2 to form a ubiquitin-thioester intermediate with its HECT active cysteine, and then transfers ubiquitin to the ϵ -amino group of a lysine side chain either directly on a substrate or to a ubiquitin moiety already conjugated to a substrate, producing a polyubiquitin chain. The formation of a thioester intermediate with Ub is unique to HECT E3s and has not been observed with other classes of E3s. Most HECT-domain proteins are either E3 enzymes themselves or form part of multi-protein complexes with E3-like activities. Examples of HECT domain proteins include E6AP, Nedd4 (which ubiquitinates epithelial Na⁺ channel subunits), HectH7, HectH6 (p532), Smurf-1, and Wwp2 (Edwin *et al.*, 2010; Beaudenon *et al.*, 2008; Yamashita *et al.*, 2005).

The third type of E3s are the RING finger motif-containing E3s. Several of these proteins have been shown to have E3 ubiquitin ligase activity (Deshaies *et al.*, 2009). RING E3s interact simultaneously with E2 and with substrate suggesting that facilitate the recruitment of E2s to the vicinity of proteins to be ubiquitinated (Joazeiro *et al.*, 2000). Interestingly, some RING finger-containing E3s bind their cognate E2s predominantly via regions outside the RING, since mutations in this region are known reduce the E3 ligase activity. An example is, Ubr1p, a RING

finger-containing E3, which interacts with its cognate E2, Rad6p, via a region outside the RING finger. Mutations in the RING finger region abrogate the ubiquitination function of Ubr1p and yet have no effect on the binding to Rad6p and the protein substrate (Joazeiro *et al.*, 1999). In light of this observation, it is thought that such RING finger domains could play an allosteric regulatory role with respect to the E2.

The last class of E3 ligases to be classified was the U box-containing E3s. These were originally identified as being able to extend existing ubiquitin chain but not to initiate them (Hatakeyama *et al.*, 2001), but many of them have subsequently been shown to be able to initiate them as well, making them additional members of the E3 family. E3s classified under this type contain a U-box domain, an approximately 70 amino acid-long domain present in proteins from yeast to humans, which adopts a structure identical to the RING fingers although it does not require zinc in order to fold. Deletion of the U-box or mutation of conserved amino acids within it abolishes ubiquitination activity of most U-box-containing E3s. They differ from other types of E3 ligases in the sense that some U-box proteins catalyze polyubiquitination by targeting lysine residues of ubiquitin other than lysine-48, which is utilized by HECT and RING-finger E3 enzymes for polyubiquitination. A well-characterized U-box containing protein is the carboxyl terminus of Hsc70-interacting protein, (CHIP) which was one of the first U-box containing E3s to have been demonstrated to possess intrinsic ubiquitin-ligase activity (Hatakeyama *et al.*, 2001).

1.7 Methods for identifying and investigating protein-protein interactions

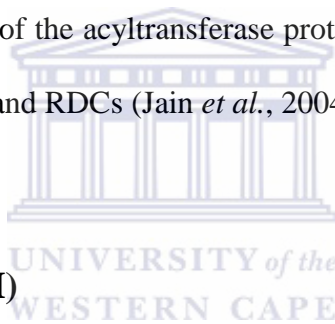
Many techniques are available for investigating the interactions between proteins. These include genetic techniques such as yeast 2-hybrid analysis, cell biology techniques such as co-immunoprecipitation assays and biophysical methods such as BIACore, Circular Dichroism, fluorescence, NMR and X-ray crystallography.

1.7.1 Protein-protein interactions as probed by NMR

Biomolecular NMR spectroscopy has proven to be a powerful tool in characterising biomolecular interactions, including transient and weak ones that usually escape other characterisation approaches (Vaynberg *et al.*, 2006). One of the most attractive advantages of biomolecular NMR is that the information obtained is resolved down to the level of individual amino acids. NMR can therefore be used to map protein-protein interfaces as well as to determine the structures of dynamic protein complexes that are difficult to crystallise and those which may crystallise in a non-biological conformation.

A number of parameters can be employed in biomolecular NMR for the investigation of protein-protein interactions and solution of structures of protein complexes. These include nuclear overhauser effects (NOEs), residual dipolar couplings (RDCs), chemical shift perturbations (CSPs) and paramagnetic relaxation enhancements (PREs). Of these, CSPs are the most widely used for protein-protein interactions (McCoy *et al.*, 2002). This involves the acquisition of NMR spectra of an isotope-labelled protein alone and when bound to an unlabelled ligand. The ligand

can be a short synthetic peptide or a heterologously expressed recombinant protein. The CSPs provide a per residue characterisation of the protein-protein interface and enable the local effects and conformational dynamics associated with ligand binding to be closely studied. In addition, CSPs allow for the binding affinities between interacting proteins to be quantified. The CSP data obtained from NMR can also be used in conjunction with data-driven docking procedures to solve the structures of protein complexes. In one approach, known as HADDOCK, CSP data are translated into ambiguous interaction restraints to drive the docking process (van *et al.*, 2006). The CSP interaction restraints can be combined with residual dipolar coupling (RDC) data, allowing a better definition of the relative orientation of the components (van Dijk *et al.*, 2005). For example, the 95 kDa complex of the acyltransferase protein with the acyl carrier protein has been modelled based on CSP data and RDCs (Jain *et al.*, 2004).



1.7.2 Yeast two-hybrid (Y2H)

The yeast two-hybrid (Y2H) system is a molecular genetic test which utilises the reconstitution of an active transcription factor to assay for protein-protein interactions (Causier, 2004). The Y2H system is based on the finding that some eukaryotic transcription factors have separable DNA-binding (BD) and transcription activation domains (AD) which can be physically separated and reconstituted, fused to exogenous proteins known as bait and prey respectively. Interaction between the bait and prey proteins reconstitutes the active transcription factor, producing a positive read-out of down-stream reporter genes (Fig. 1.6).

Fields and co-workers were the first to develop the Y2H technique in the study of protein-protein interactions (Fields *et al.*, 1989). They utilised a product of the yeast gene *GAL4*, a protein with

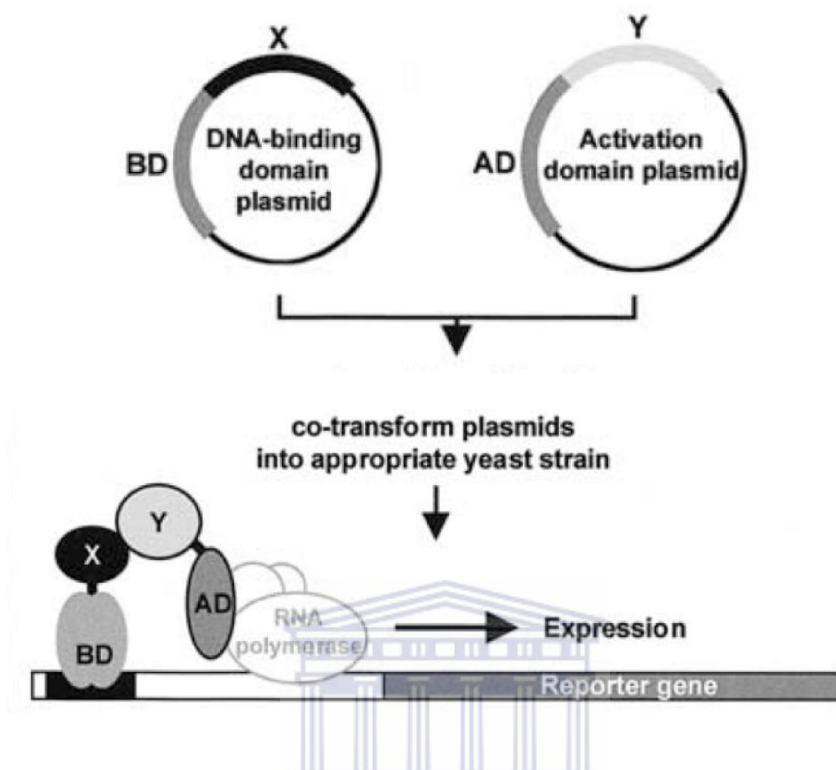
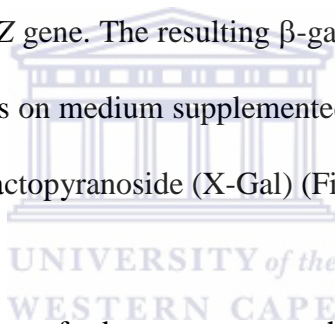


Fig. 1.6 An illustration of the classical yeast two-hybrid system. Two plasmids are constructed, one encoding the test protein X fused in-frame with the DNA-binding domain (BD) of a transcription factor such as GAL4, the second plasmid encoding test protein Y fused in-frame with the transcription activation domain (AD). The plasmids are co-transformed into a suitable yeast strain where the fusion proteins are expressed. Interaction between X and Y reconstitutes an active transcription factor which specifically binds to elements upstream of the reporter genes and activates their expression. Adapted from (Causier *et al.*, 2002).

two functional domains that activate transcription of genes involved in galactose metabolism. The BD of the GAL4 protein binds to DNA sequences within the promoter region of *GAL1* and the AD of the GAL4 protein stimulates transcription. Fields and Song constructed two separate plasmids, containing the cDNA sequence coding for the DNA-binding domain of *GAL4* (*GAL4_{BD}*) fused in-frame to DNA sequences coding for the yeast protein SNF1. The other plasmid containing the sequence coding for the transcriptional activating domain of *GAL4* (*GAL4_{AD}*) fused in-frame to DNA sequences coding for the yeast protein SNF4. They introduced these two plasmids into a yeast strain containing the *lacZ* reporter gene from *E. coli* fused to the *GAL1* promoter. Interaction between SNF1p and SNF4p allowed the GAL4 activating domain to activate the transcription of the *lacZ* gene. The resulting β -galactosidase activity was detected by the formation of blue yeast colonies on medium supplemented with the chromogenic substrate 5-bromo-4-chloro-3-indolyl- β -D-galactopyranoside (X-Gal) (Fields *et al.*, 1989).



The Y2H technique offers a number of advantages over other biochemical procedures used to analyse protein-protein interactions. It is relatively inexpensive, since it avoids costly procedures such as antibody production and protein purification. The sensitivity of Y2H is better than that of many *in vitro* techniques and hence it is more suited for the detection of weak and transient interactions, which are commonly found in signalling cascades (Piehler, 2005). Importantly, proteins expressed using *in vitro* techniques or in bacteria often lack key post-translational modifications that may be important for certain protein-protein interactions and these proteins may not fold correctly or may not be stable in the buffer conditions used in *in vitro* techniques. Since the yeast is a eukaryote and the screen takes place *in vivo*, many of these limitations do not apply.

One of the most appealing features of the Y2H is that the interacting protein does not have to be cloned following identification, but is already available in a convenient plasmid. Y2H plasmids typically contain flanking regions coding for immune-affinity tags and promoters for *in vitro* expression of proteins.

The technique is not without limitations, however, since transcription events only happen within the nucleus, it is necessary that both the bait and prey are capable of localising to the nucleus. Consequently the technique may not be suitable for interactions involving membrane proteins, which are unlikely to be soluble in the nucleus. Also, the incidence of false positives in Y2H is common since some proteins are promiscuous interactors and also because some proteins have intrinsic transcriptional activation activity. Mechanisms for eliminating or controlling for these false positives are therefore necessary. In addition, the yeast cell environment may not fully mimic mammalian cells; for example, post-translational modifications may not be replicated in yeast. Therefore, as with most scientific tools, it is imperative for results derived using the Y2H technique to be confirmed by independent methods.

In a yeast 2-hybrid screen, cDNA libraries are cloned into pACT2 vector and a screen is carried out to identify prey proteins interacting with the bait protein. In a direct yeast 2-hybrid assay a smaller number of proteins or mutants are directly tested for their ability to interact with the bait protein. This format is especially useful for investigating the effects of mutations on a known interaction. In this case the presence of a positive control (the previously identified wild type interaction) makes many of the disadvantages described above irrelevant.

1.7.3 Co-immunoprecipitation (Co-IP) assays

Co-immunoprecipitation is one of the oldest and most widely used technique for studying protein-protein interactions. It uses the specificity of antibodies to isolate target proteins out of complex sample mixtures with the antibodies therefore being isolated using protein A or protein G coupled to agarose or sepharose beads (Berggard *et al.*, 2007). Complexes containing the target protein, antibody, protein A or G and beads are then isolated by centrifugation. Protein components in the complexes are visualized by Western Blotting or autoradiography in the case of radio-labelled proteins. If an antibody against the protein of interest is not available, recombinant DNA technology can be used to incorporate immunoaffinity tags of 10-20 amino acids in length into the protein (Angers *et al.*, 2002). Common peptide tags include hemagglutinin (HA) or Myc epitopes for which antibodies are commercially available. A typical co-IP assay involves subjecting a mixture of the two putatively interacting proteins to immunoprecipitation using an antibody against one of the proteins and western blotting using an antibody against the second protein. If the second protein is observed when the first protein is present, but not when it is absent, the interaction is confirmed.

1.8 Justification and aims of the study

YB-1 has recently assumed great significance in cancer, mainly through its role in directing the transcription of a large number of genes that facilitate the development of tumours. High levels of YB-1 are a recognised marker of poor prognosis for the patient, suggesting that therapies aimed at targeting YB-1 may be a promising approach for combating cancer. Through its

interaction with the C-terminus of YB-1, RBBP6 mediates the ubiquitination and degradation of YB-1, thereby making RBBP6 a potential effector of such an approach. As a means of initiating such a strategy, a number of questions first need to be answered, including: how strong is the interaction, how does the interaction contribute to ubiquitination of YB-1, which residues from each protein are involved in the interaction, and what is the effect of mutating them on the interaction itself and on the cell as a whole. This thesis aims to answer two of these questions: 1. Can the interaction be validated and the strength of the interaction measured using NMR, and 2. Which residues are involved.

A previous Y2H screen identified the interaction between RBBP6 and YB-1 and demonstrated that it is localized to a 62 amino acid region at the C-terminus of YB-1. This study will firstly use Y2H, co-IP and NMR to investigate whether the RBBP6/YB-1 interaction can be localised to a region smaller than the 62 amino acid region at the C-terminus of YB-1.

Secondly this study will also attempt to shed light on the mechanism of ubiquitination of YB-1. Previous *in vitro* ubiquitination assays in HEK 293 cells were not able to identify which of the human E2 proteins were responsible for ubiquitination of YB-1 by RBBP6. This study will therefore use an *in vitro* reconstituted ubiquitination assay with a panel of different E2 enzymes to identify which ones co-operate with RBBP6 in ubiquitinating YB-1.

Finally, this study aims to construct mutants which abolish the homodimerisation of the RING finger domain. NMR-based structure studies show that the RING finger-like domain of RBBP6 is a homodimer in solution (Pugh *et al.*, unpublished data). Many RING finger and U-box

domains are known to be homodimers and in a number of cases homodimerisation has been shown to be essential for ubiquitination activity. In order to test whether this is true in the case of RBBP6, non-dimeric mutants first need to be generated and validated. This study aims to use NMR to investigate the oligomeric state of two different mutants of the RING finger-like domain of RBBP6.



Chapter 2: Materials and methods

2.1 General chemicals and enzymes

All the reagents used in this study were of analytical grade.

40% 37.5:1 Acrylamide:bis-acrylamide	Bio-Rad
Agarose	Lonza
Ammonium persulphate (APS)	Merck
Ampicillin	Roche
Bacteriological agar	Merck
Bovine serum albumin	Roche
Bromophenol blue	Sigma
Coomasie brilliant blue R250	Sigma
Dithiothreitol (DTT)	Roche
DNase	Roche
Ethylene diamine tetra acetic acid (EDTA)	Merck
EDTA-free protease inhibitor cocktail	Roche
Ethanol	BDH
Ethidium bromide	Sigma
Glacial acetic acid	Merck
Glucose	BDH
Glycine	BDH
Herring sperm DNA	Promega



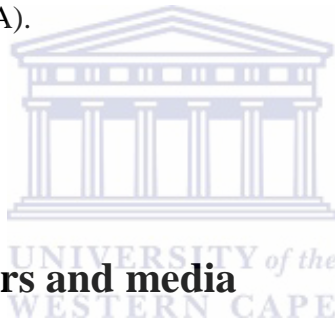
Hydrochloric acid (HCl)	Merck
Isopropyl β -D-thiogalactopyranoside (IPTG)	Roche
Kanamycin monophosphate	Roche
L-adenine hemisulphate	Sigma
Lithium acetate	Sigma
Lysozyme	Roche
Methanol	Merck
MG132 (proteasome inhibitor)	Sigma
Potassium chloride	Merck
Phenylmethylsulphonyl fluoride (PMSF)	Roche
Protein molecular weight standard	Fermentas
Reduced glutathione (GSH)	Sigma
Restriction enzymes	Fermentas
Sodium dodecyl sulphate (SDS)	Promega
Sodium azide	Roche
Sodium chloride	Merck
Sodium hydroxide	Merck
Synthetic dropout supplements (SD)	Clontech
T4 Ligase	Fermentas
TEMED (N, N, N', N' - Tetra methylethylene-diamine)	Promega
Tris (Tris[hydroxymethyl] aminoethane)	BDH
Triton X-100 (Iso-octylphenoxypolyethoxyethanol)	Roche
Tryptone	Merck



Tween 20 (Polyoxyethylene [20] sorbitan)	Merck
Yeast extract	Merck
Yeast nitrogen base	Clontech
Zinc sulphate	Merck

2.2 Synthetic peptides

Synthetic peptides used in this study (CTD-1 and CTD-2) were purchased from GenScript Corporation[®] (Piscataway, NJ, USA).



2.3 Stock solutions, buffers and media

Autoclaving of solutions was carried out at 120°C for 20 min unless otherwise stated.

4x Separating gel Buffer:

1.5M Tris-HCl, pH 8.8.

4x Stacking gel Buffer:

0.5M Tris-HCl, pH 6.8.

5x M9 salts

13.6 g Na₂HPO₄, 6.0 g KH₂PO₄, 1.0 g NaCl, 2.0 g NH₄Cl in 400 ml of Millipore water.

5X SDS Running Buffer:

25 mM Tris, 0.1% SDS and 250 mM glycine, pH 8.3.

6X DNA loading dye:

0.25% bromophenol blue, 0.25% xylene cyanol FF, 30% glycerol were mixed in distilled water.

10X Phosphate-buffered saline (PBS):

80 g NaCl, 2 g KCl, 14.4 g Na₂HPO₄, 2.4 g KH₂PO₄, was dissolved by stirring in 800 mls of deionised water. The solution was adjusted to pH 7.4 with HCl and filled up to 1 litre with distilled water. The solution was sterilised by autoclaving at 120°C for 20 min.

Ammonium persulphate:

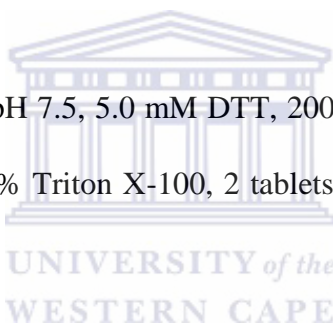
A 10% stock solution was prepared in deionised water.

Ampicillin:

A 100mg/ml stock solution was prepared in distilled water.

Cell lysis Buffer:

150 mM NaCl, 50 mM Tris-HCl, pH 7.5, 5.0 mM DTT, 200 µg/ml lysozyme, 35 µg/ml DNase, 1.0 mM PMSF, 5.0 mM EDTA, 2% Triton X-100, 2 tablets or EDTA-free cocktail of protease inhibitors.



Cleavage Buffer 1:

0.1M borate buffer, pH 8.5 fortified with 0.5 M NaCl.

Cleavage Buffer 2:

0.1M acetate buffer, pH 4.5 fortified with 0.5 M NaCl.

Chloramphenicol:

A 100 mg/ml stock solution was prepared in absolute ethanol.

Co-IP Buffer

12.5 µl of aprotinin (2mg/ml stock solution), 50 µl DTT from a 100 mM stock solution, 50 µl of 50 mM PMSF solution, 5 µl of tween-20. The volume was made up to 5 ml with 1X PBS.

Coomassie staining solution:

0.25 g coomassie brilliant blue R250, 45 % methanol and 5 % acetic acid dissolved in water.

Destaining solution:

30 % methanol and 10 % acetic acid in water.

DTT:

A 1M stock solution was prepared in 0.01 M sodium acetate, pH 5.2 and sterilised by filtration.

EDTA:

A stock solution of 0.5 M, pH 8.0 was prepared in distilled water.

Elution Buffer (GSH):

15 mM GSH, 50 mM Tris-HCl pH 8.0.

IPTG (Isopropyl β -D-thiogalactopyranoside):

A 1 M stock solution was prepared in deionised water and sterilised by filtration.

Luria bertani media (LB media):

10 g/l Tryptone, 5.0 g/l yeast extract, 5.0 g/l NaCl and 2 g/l glucose. Solution was sterilised by autoclaving.

LB agar plates:

31 g/l nutrient agar, 2 g/l glucose, 5 g/l NaCl, 5 g/l yeast extract, 10 g/l tryptone was dissolved in 1.0 litre of water and sterilised by autoclaving. The medium was allowed to cool and 100 μ g/ml of ampicillin was added and then poured into sterile plates in a biolaminar flow (Labotec, South Africa).

Lysozyme:

50 mg/ml of lysozyme solution was prepared in deionized water.

¹⁵N-labelled minimal media:

20 % Glucose, 1 M CaCl₂, 1 M MgSO₄, 400 ml of 5x M9 salts in 2 Litres of distilled water and sterilised by autoclaving.

NMR Buffer:

100 mM phosphate buffer fortified with 50 mM NaCl, 0.02 % NaN₃, 5 mM DTT, 100 μM ZnSO₄.

PreScission™ 3C protease cleavage Buffer:

50 mM Tris-HCl, pH 7.0, 150 mM NaCl, 5.0 mM DTT, 1.0 mM EDTA.

TBST Buffer

150 mM NaCl, 20 mM tris-HCl pH 8.0, 0.1 % tween-20 in double distilled water.

Tfb1 Buffer:

30 mM potassium acetate, 50 mM MnCl₂, 0.1 M KCl, 6.7 mM CaCl₂, and 15 % (v/v) glycerol.

Tfb 2 Buffer:

9 mM MOPS, 10 mM KCl, 50 mM CaCl₂, and 15 % (v/v) glycerol.

TYM Broth:

20 g/l tryptone, 5 g/l yeast extract, 3.5 g/l NaCl, 2 g/l MgCl₂.

Yeast single amino acid drop-out media agar:

2 % (w/v) glucose, 2 % (w/v) nutrient agar, 0.67 % (w/v) yeast nitrogen base, 0.067 % (w/v) single drop-out (SDO) amino acid supplement, 1 mM NaOH dissolved in double distilled water and sterilised by autoclaving at 120°C for 20 minutes before plating.

Yeast single drop-out liquid media:

2 % (w/v) glucose, 20 g/l nutrient agar, 0.67 % (w/v) yeast nitrogen base, 0.067 % (w/v) single drop-out (SDO) amino acid supplement, 1 mM NaOH dissolved in double distilled water and sterilised by autoclaving at 120°C for 20 minutes.

Yeast double drop-out media agar:

2 % (w/v) glucose, 2 % (w/v) nutrient agar, 0.67 % (w/v) yeast nitrogen base, 0.067 % (w/v) synthetic double drop-out (DDO) amino acid supplement (-L-W), 1 mM NaOH dissolved in double distilled water and sterilised by autoclaving at 120°C for 20 minutes before plating.

Yeast double drop-out liquid media:

2 % (w/v) glucose, 2 % (w/v) nutrient agar, 0.67 % (w/v) yeast nitrogen base, 0.067 % (w/v) synthetic double drop-out (DDO) amino acid supplement (-L-W), 1 mM NaOH dissolved in double distilled water and sterilised by autoclaving.

Yeast triple drop-out agar media:

2 % (w/v) glucose, 0.67 % (w/v) yeast nitrogen base, 0.067 % (w/v) synthetic triple drop-out (TDO) amino acid supplement (-L-W-H), 2 % bacterial agar, 1 mM NaOH dissolved in double distilled water and sterilised by autoclaving.

YPDA liquid media:

2 % (w/v) Difco peptone, 2 % (w/v) yeast extract, 2 % (w/v) glucose, 0.003 % L-adenine hemisulphate, dissolved in double distilled water and sterilised by autoclaving.

2.4 Commercial antibodies

Rabbit anti-HA MAb antibody (sc-805) and mouse anti-cMyc MAb antibody (sc-40) were obtained from Santa Cruz Biotechnology Inc. (Santa Cruz, CA, USA).

2.3 Plasmid vectors

2.3.1 pACT2 AD vector

The pACT2 AD vector (Clontech, Mountain View, CA, USA) shown in Fig. 2.1 is a shuttle vector that replicates autonomously in both *E.coli* and *S. cerevisiae* and contains the *bla* gene, which confers ampicillin resistance in *E. coli*. pACT2 AD (also commonly referred to as pACT2) also contains a *LEU2* nutritional gene that allows yeast auxotrophs to grow on limiting synthetic media. In Y2H assay it is used for the cloning of cDNA of prey proteins. It generates a fusion of the GAL4 AD, an HA immunoaffinity tag and a protein of interest cloned into the MCS in the correct orientation and reading frame. In yeast host cells, expression of the hybrid protein is driven by the ADH1 promoter (P) and is terminated at the ADH1 transcription termination signal (T) (shown in Fig. 2.1). The protein is targeted into the yeast nucleus by the nuclear localization sequence from the SV40 T-antigen which has been cloned into the 5'-end of the GAL4 AD sequence.

2.3.2 pGBKT7-R

The pGBKT7 vector (shown in Fig. 2.2) expresses proteins fused to the GAL4 DNA-binding domain (DNA-BD). In yeast, expression of the fusion proteins is driven by the ADH1 promoter (P_{ADH1}); transcription is terminated by the T7 and ADH1 transcription termination signals (T_{T7} and T_{ADH1}). pGBKT7 also contains the T7 promoter, a c-Myc epitope tag and a multiple cloning site. pGBKT7 replicates autonomously in both *E. coli* and *S. cerevisiae* from the pUC and 2 μ ori, respectively. The vector carries the kanamycin resistance gene for selection in *E. coli* and the TRP1 nutritional marker for selection in yeast.

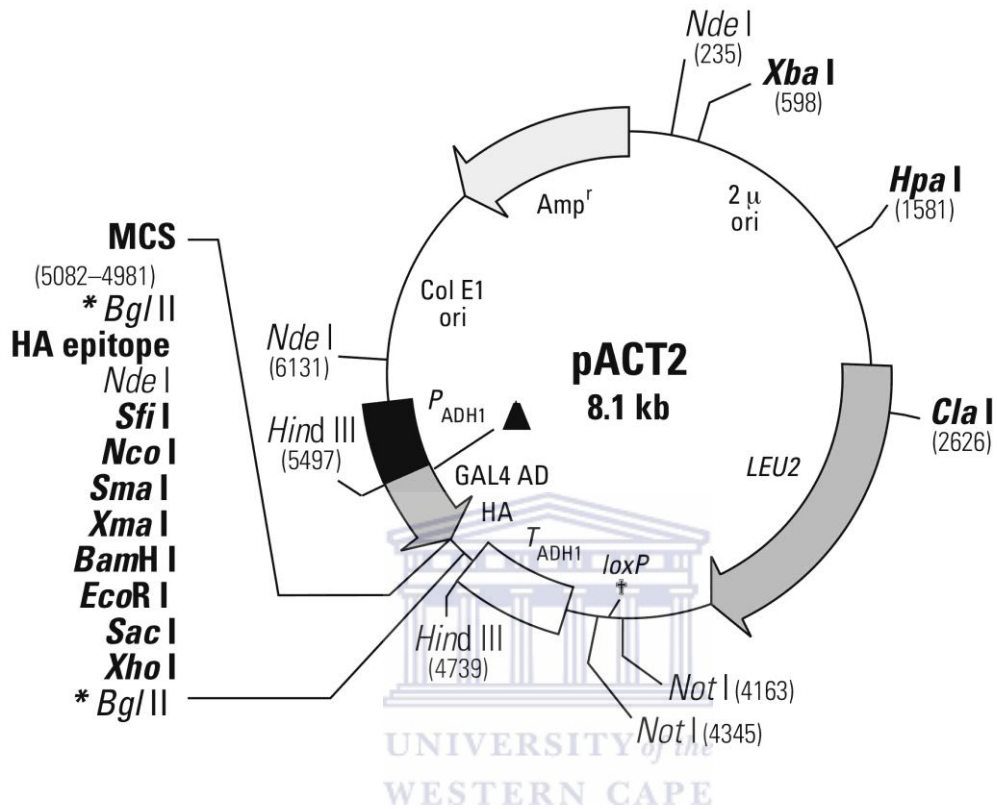


Fig. 2.1 The restriction map of pACT2 AD vector (Clontech) for cloning cDNA of prey proteins used in the yeast two-hybrid. The figure shows the restriction map and multiple cloning site (MCS) of pACT2 AD vector. The GAL4 activating domain (GAL4 AD) and the HA epitope tag are immediately upstream of the MCS.

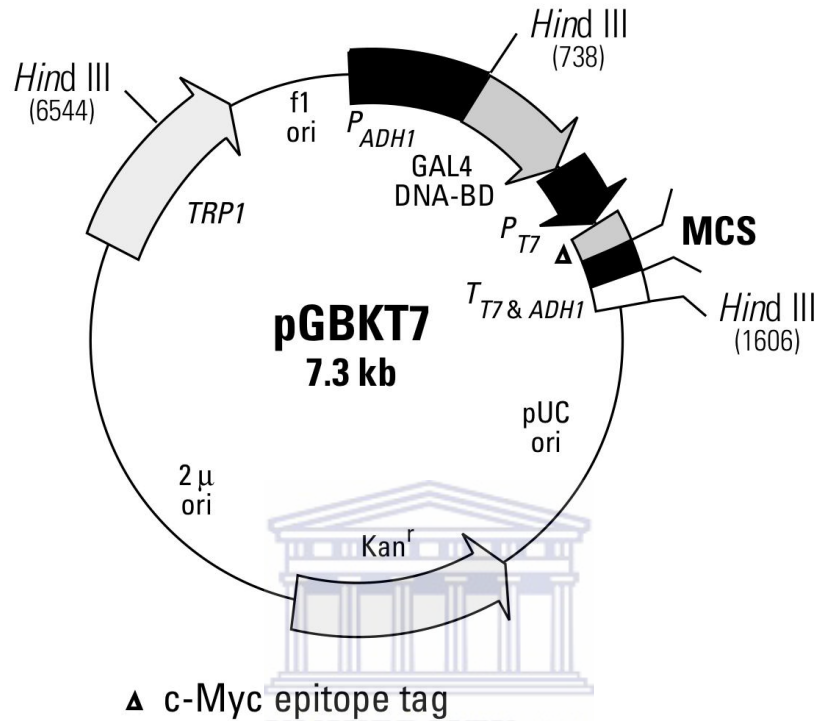


Fig. 2.2 Restriction map and main features of pGBKT7 vector (Clontech). The figure shows the restriction map and multiple cloning site (MCS) of the pGBKT7 vector. The immunoaffinity tag c-Myc is immediately upstream of the MCS. pGBKT7 vector also contains the cDNA of the GAL4 DNA-binding domain (GAL4 DNA-BD) and the kanamycin resistance gene.

2.3.3 pGEX-6P-2

pGEX-6P-2 (GE Healthcare, Waukesha, WI, USA) (Fig. 2.3) is a bacterial protein expression vector that expresses GST fused proteins. It has a multiple cloning incorporating six restriction sites, facilitating the unidirectional cloning of cDNA inserts. pGEX-6P-2 encodes the recognition sequence for the PreScission™ Protease in the linker region between the GST domain and the MCS which allows for removal of the GST from the fusion protein by enzymatic cleavage. The cleavage of fusion proteins by the PreScission™ Protease occurs between the Gln and Gly residues of the recognition sequence Glu-Val-Leu-Phe-Gln-Gly-Pro. The vector pGEX-6P-2 also incorporates an IPTG inducible *tac* promoter for high-level expression.



2.4 Bacterial cultures

2.4.1 Bacterial strain chromosomal genotype

***E. coli* MC1061** (Casadaban *et al.*, 1980):

F⁻, *araD139*, (*ara leu*) 7697, Δ *lacx74*, *galU*⁻, *galK*⁻, *hsm*⁺, *strA*.

***E. coli* BL21 Star™ pLysS (DE3)** (Studier *et al.*, 1986):

F⁻, *omp T hsdS_B(r_B⁻m_B⁻) gal dcm rne131* (DE3) (Stratagene, La Jolla, CA, USA).

***E. Coli* strain DH5 α** (Taylor *et al.*, 1993):

fhuA2 Δ (*argF-lacZ*)U169 *phoA glnV44* Φ 80 Δ (*lacZ*)M15 *gyrA96 recA1 relA1 endA1 thi-1 hsdR17*.

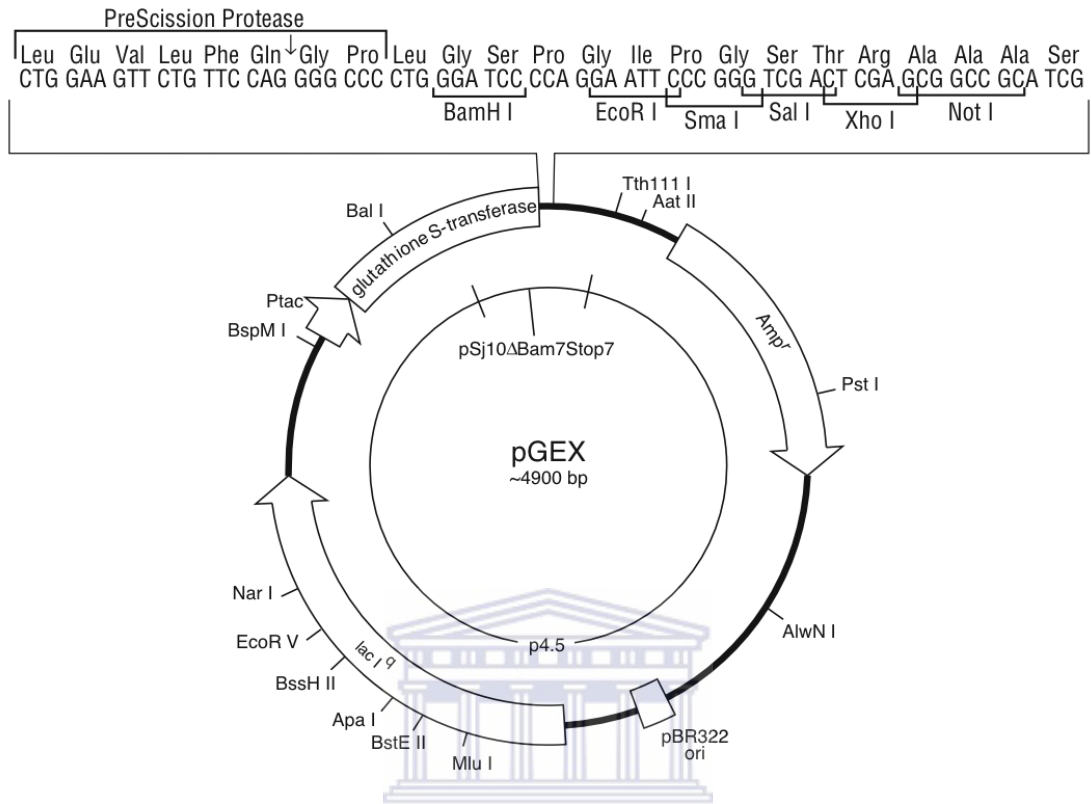


Fig. 2.3 Reading frame and main features of pGEX-6P-2. Protein coding sequences cloned in frame into the MCS of pGEX-6P-2 are fused to the C-terminus of Glutathione S-transferase (GST) gene. The vector has a PreScission™ 3C Protease recognition sequence immediately downstream of the GST-coding sequence. It also contains an ampicillin resistance gene and a bacterial origin of replication.

E. coli MC1061 and DH5 α cells were used for propagation of plasmid DNA, and *E. coli* BL21 StarTM pLysS (DE3) cells were used for the heterologous expression of recombinant proteins. The bacterial cultures were grown at 37 °C in LB medium and LB agar plates with or without ampicillin. The ampicillin was used at a final concentration of 100 μ g/ml.

2.4.2 Preparation of competent cells for transformation

A single *E. coli* colony was taken from a freshly streaked agar plate and transferred to 10 ml of TYM broth and grown at 37 °C in a shaking incubator to an OD₅₅₀ of 0.2. The culture was then scaled up to 500 ml of TYM broth and grown at 37 °C in a shaking incubator to an OD₅₅₀ of 0.2. The culture was cooled by gently swirling on ice and the bacteria were sedimented by centrifugation at 5000 *g* for 10 min at 4 °C. The bacterial pellet was then re-suspended in 250 ml of transformation buffer 1 (Tfb1) on ice and left for 30 min with intermittent swirling. The mixture was centrifuged at 5000 *g* for 10 min at 4 °C and the resultant pellet was re-suspended in 50 ml of transformation buffer 2 (Tbf2) on ice. 300 μ l aliquots of the mixture were transferred into 1.5 ml eppendorf tubes and quick frozen in liquid nitrogen. The snap-frozen aliquots were then stored at -80 °C until they were needed for transformation.

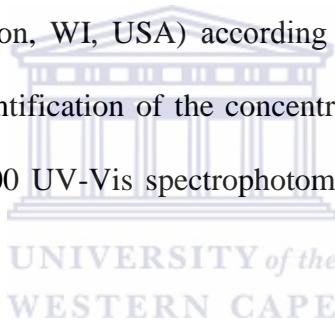
2.4.3 Bacterial transformation with plasmid DNA

Competent cells stored at -80 °C were thawed on ice and 100 μ l of competent cells were added to plasmid DNA in a 1.5 ml eppendorf tube. This mixture was then incubated on ice for 30 min. An identical tube containing cells but no plasmid DNA was set up as a control. After the 30 min incubation period the bacteria were transformed by heat shock at 37 °C for 5 min on HB/01

digital heating blocks (Omeg Scientific, Somerset West, South Africa) and immediately placed back on ice. The transformation reaction was left on ice for 5 min to allow the cells to recover. To each of the tubes, 900 μ l of pre-warmed LB without ampicillin was added and incubated at 37 °C in a shaking incubator for 90 min. 100 μ l of each transformation was plated on an LB agar plate with 100 μ g/ml ampicillin and then incubated at 37 °C for 16 hours.

2.4.4 Extraction of plasmid DNA

Plasmid DNA from transformed *E. coli* cells was extracted using the Wizard[®] Plus SV Miniprep Kit (Promega Corporation, Madison, WI, USA) according to the manufacturer's instructions. The assessment of purity and quantification of the concentration of Plasmid DNA was carried out using the NanoDrop[®] ND-1000 UV-Vis spectrophotometer (NanoDrop Technologies Inc., Wilmington, DE, USA).



2.5 Manipulation of plasmid DNA

2.5.1 Primer design

The designing of primers for the amplification of target genes was done manually, based on the human coding sequences. The forward primers incorporated a *Bam*HI restriction site and the reverse primers a *Xho* I restriction site. A stop codon was included in all reverse primers.

2.5.2 Amplification of DNA by PCR

The polymerase chain reaction (PCR) was used for the amplification of gene segments from their respective cDNA sequences. All PCR reactions were done using the GeneAmp[®] PCR system (Applied Biosystems Inc., Foster City, CA, USA). EconoTaq[™] DNA polymerase (Lucigen[®] Corporation, Middleton, WI, USA) was used for the amplification of DNA unless otherwise stated.

2.5.3 Analysis of DNA

The assessment of the purity and yield of (i) PCR products and (ii) plasmid DNA extractions was carried out using agarose gel electrophoresis. 10 µl of the DNA sample was mixed with 5 µl of 2X DNA loading dye. The mixture was then loaded into 0.8 - 1 % agarose slab gels containing 1 µg/ml of ethidium bromide. The agarose gel was then placed in a tank containing 1X TAE buffer and an electric field of 100 V was applied until the dye front reached the end of the gel. The DNA bands were visualized using a gel documentation system equipped with a long wave UV transilluminator (BioRad Laboratories Inc., Hercules, CA, USA).

2.5.4 Purification of DNA

PCR products were cleaned up using the Illustra[™] GFX[™] PCR DNA and Gel band purification Kit (GE Healthcare, Buckinghamshire, UK) according to the manufacturer's instructions.

Table 2.1 PCR reaction set up for the amplification of DNA fragments

Reaction components (Final concentrations)	Control Reaction Vol. (μl)	Experimental reaction Vol. (μl)
1X Taq polymerase reaction buffer	10	10
Forward primer and Reverse primer (0.4 μM each)	1 (each)	1 (each)
dNTPs (0.4 mM each)	2	2
Millipore water	11	11
Econo Taq™ DNA polymerase (0.5 *Units/μl)	1	1
Template DNA (2 ng/μl)	-	1
Total Volume	25	25

*One unit is defined as the amount of the Econo Taq™ polymerase that catalyses the incorporation of 10 nmol of dNTP into acid insoluble material in 30 minutes at 70 °C.

2.5.5 Restriction enzyme digestion

PCR amplified products and destination vectors were digested with FastDigest™ restriction enzymes *Bam HI* and *Xho I* (Fermentas International Inc. Ontario, Canada) unless otherwise mentioned. 30 μ l of either PCR amplified product or the destination vector and 2 μ l each of *Bam HI* and *Xho I* were added to 5 μ l of 10X restriction enzyme digestion buffer. The reaction volume was made up to 50 μ l per reaction with double distilled water after which the reaction tubes were incubated at 37 °C for 30 min on a HB/01 Digital heating block (Omeg Scientific,

Somerset West, South Africa). The digested DNA was then purified as described in section 5.4 so as to remove the restriction digestion buffer and prevent it from interfering with downstream cloning processes. 2 μ l of Shrimp alkaline Phosphatase (SAP) (New England Biolabs[®] Inc., Ipswich, MA, USA) and 5 μ l of 10x SAP reaction buffer was added to the destination vector to prevent self-religation of vector DNA. SAP dephosphorylates sticky ends of restriction enzyme-digested plasmid vectors.

2.5.6 Ligation of DNA

Insertion of target DNA into destination vectors was performed using T4 DNA ligase (Fermentas International Inc. Ontario, Canada). For any given insert, three ligation reactions were set up, each with a different insert:vector ratio: 1:3, 1:5, and 3:1. In each ligation reaction, 1 μ l of T4 DNA ligase and 2 μ l of 10X ligation buffer were added together and the ligation reaction volume scaled up to 10 μ l with double distilled water. A vector-only ligation reaction was also set up which did not contain the insert so as to monitor the vector background corresponding to self-religation of the plasmid vector. The ligation reaction was pulse-spun in a benchtop centrifuge 5415D (Eppendorf International, Hamburg, Germany) before incubation at 4°C for 16 hours.

2.5.7 Screening for positive clones

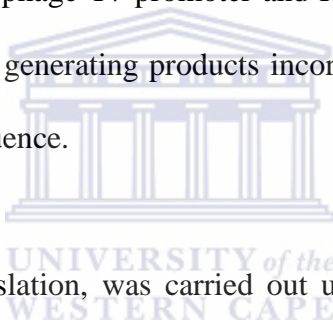
Ten colonies were picked at random from the ligation ratio with had the largest number of colonies. A small scale extraction of DNA was carried out and the presence of insert was tested by PCR using gene-specific primers. Positive colonies were sent for sequencing (Inqaba

Biotec™, Pretoria, South Africa) to further confirm the presence of desired insert. Sequence analysis was done using 4 peaks software (Mekentosj, Aalsmeer, The Netherlands).

2.6 Co-immunoprecipitation

2.6.1 *In vitro* synthesis of bait and prey proteins.

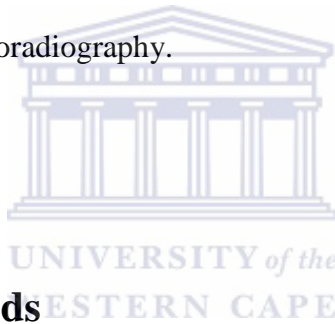
PCR-amplified cDNA sequences of bait and prey proteins were used as templates for *in vitro* synthesis of their respective proteins. Preys were amplified using pACT2 primers, generating products incorporating the bacteriophage T7 promoter and HA-epitope tag sequence. Baits were amplified using pGBKT7 primers, generating products incorporating the bait, bacteriophage T7 promoter and Myc-epitope tag sequence.



In vitro coupled transcription/translation, was carried out using the TNT® T7 Quick Coupled transcription/translation system (Promega Corporation, Madison, WI, USA), according to the manufacturer's instructions. Each translation reaction contained 7 µl of the PCR-generated DNA template, 40 µl of the TNT® T7 Quick master mix, 1 µl of PCR S30 T7 enhancer and 2 µl ³⁵S-methionine (GE Healthcare, Buckinghamshire, UK). The mixture was incubated at 30 °C for 90 minutes using a dry block heater HB2 (Hagar designs, Wilderness, South Africa). To verify the integrity of the products, the translated proteins were separated on an SDS-PAGE gel and visualized using autoradiography.

2.6.2 *In vitro* co-immunoprecipitation of bait and prey proteins

5 µl each of ³⁵S-methionine-labelled bait and prey proteins were mixed together in a 500 µl eppendorf tube and incubated for at least 1 hour at room temperature. 10 µl of agarose-conjugated Myc antibody (Santa Cruz Biotechnology Inc., Santa Cruz, CA, USA) was then added to the mixture, the volume adjusted to 250 µl with co-IP buffer. The mixture was incubated for 1 hour at 4 °C on a rotating rotor (Labnet Inc., Edison, NJ, USA) and then centrifuged for 30 sec at 10 000g on a Beckman Microfuge lite (Beckman Inc., Brea, CA, USA). The supernatant was discarded and then the pellet was washed 5 times using TBST. The washed pellet was mixed with 10 µl sample buffer and boiled for 5 min before loading on a 12.5 % SDS-PAGE gel and visualized using autoradiography.



2.7 Yeast 2-hybrid methods

2.7.1 Yeast strains used

Yeast strain AH109 phenotype (James *et al.*, 1996)

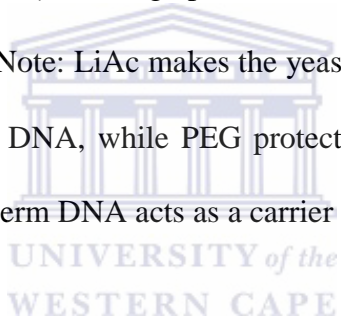
MA Ta, trp1-901, lue2-3, 112, ura3-52, his3-200, gal4D, gal80D, LYS2 : : GAL1_{UAS}-GAL1_{TATA}-HIS3, GAL2_{UAS}-GAL2_{TATA}-ADE2, URA3 : : MEL1_{UAS}-MEL1_{TATA}-lacZ.

Yeast strain Y187 phenotype (Harper *et al.*, 1993)

MA Ta, ura3-52, his3-200, ADE2-101, trp1-901, leu2-3, 112, gal4D, met, gal80D, URA3 : : GAL1_{UAS}-GAL1_{TATA}-lacZ.

2.7.2 Transformation of yeast

All strains used were *Saccharomyces cerevisiae* strains. A loopfull of yeast cells was re-suspended in 1 ml of sterile Millipore water, the mixture was and then pelleted by centrifugation for 30 sec at maximum speed using a bench-top centrifuge (Beckman Coulter, Brea, CA, USA). The supernatant was discarded and the pellet was re-suspended in 1ml of 100 mM LiAc and then incubated at 30 °C for 5 mins without shaking. 50 µl of the mixture was transferred into a 2 ml round-bottomed eppendorf tube and the cells pelleted by spinning for 20 sec at maximum speed in a bench top centrifuge and the LiAc removed using a pipette. 240 µl of 50 % poly ethylene glycol (PEG), 36 µl of 1 M LiAc, 25 µl herring-sperm DNA were then added to the pellet along with 20 µl of transforming DNA. (Note: LiAc makes the yeast cell wall more porous so that they are better able to take up plasmid DNA, while PEG protects against the harmful effect of the concentrated LiAc. The Herring Sperm DNA acts as a carrier of the plasmid DNA).



The mixture was vortexed for at least 1 min to break up the pellet and expose as many of the yeast cells as possible to the transformation mix and thereby increase the transformation efficiency. The transformation tubes were incubated in a water bath (Lasec, Cape Town, South Africa) at 42 °C for 25 min. The cells were pelleted for 30 sec in a bench top centrifuge at maximum speed and the supernatant discarded. The cells were then re-suspended in 250 µl sterile Millipore water and 150 µl of this mixture was then plated on appropriate agar plates to select for the plasmid transformed into yeast. The plates were incubated upside down in a Sanyo MIR262 ventilated incubator (Sanyo Electronic company Ltd, Ora-Gun, Japan) at 30 °C for 4 days.

2.7.3 Yeast mating

Yeast strains Y187 and AH109 are of opposite mating types, and when mated give rise to diploid yeast cells. 5 ml of pre-transformed yeast cell cultures of opposite mating types were mixed together and the volume adjusted to 50 ml by adding 2X YPDA media containing 10 µg/ml kanamycin. The mating culture was then incubated at 30 °C for 24 hours with shaking at 30 g in a YIH DER model LM-510R shaking incubator (SCILAB instrument Co. Ltd, Taipei, Taiwan), after which 200 µl of the culture was plated onto 150 mm TDO plates. The TDO plates were incubated at 30 °C for 7 days in a Sanyo MIR262 ventilated incubator (Sanyo Electronic company Ltd, Ora-Gun, Japan).



2.8 Recombinant protein expression

2.8.1 Small scale protein expression

Four freshly transformed colonies of *E. coli* BL21 pLysS (DE3) were inoculated into 10 ml LB media containing 100 µg/ml ampicillin and grown in a shaking incubator (ZHWHY-211C model, Zhicheng[®] manufacturers, Shanghai, China) for 2 hours at 37 °C. Each culture was divided into two 5 ml cultures of which one was induced with 0.5 mM IPTG and both cultures were then allowed to grow for 4 hours. Pellets from the uninduced and induced cultures were then screened for protein expression using SDS-PAGE.

2.8.2 Large scale protein expression

A 500 µl aliquot from the small-scale expression culture was inoculated into 100 ml of LB medium containing 100 µg/ml ampicillin and incubated at 37 °C overnight in a shaking incubator (ZHWHY-211C model, Zhicheng[®] manufacturers, Shanghai, China). In the morning, the overnight culture was scaled using 900 ml of fresh LB containing 100 µg/ml ampicillin was added and allowed to grow at 37 °C in a shaking incubator until an OD₅₅₀ of 0.4-0.5 was reached. IPTG was added to a final concentration of 0.5 mM, the temperature lowered to 25 °C and the culture grown for 5 hours after which the cells were harvested by centrifugation using a Beckman centrifuge J2-21 model (Beckman Coulter, Brea, CA, USA) at 10 000 *g* for 30 min. The supernatant was discarded and the cells re-suspended by gently vortexing in 30 ml of cell lysis buffer. The cells were lysed by the freeze thaw method by freezing the cell suspension at -70 °C for 5 min and subsequently thawing it at 37 °C for 5 min, with the cycle repeated 3 times. The cell suspension mixture was then centrifuged at 1000 *g* for 30 min to obtain the crude lysate. Immediate purification of the lysate was done so as to minimise degradation by bacterial proteases.

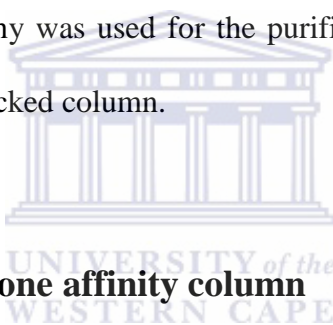
2.8.3 Expression in ¹⁵N-labelled minimal media

A 500 µl aliquot from the small scale expression culture was inoculated into 100 ml of LB medium containing 100 µg/ml ampicillin and the culture was incubated at 37 °C overnight in a shaking incubator (ZHWHY-211C model, Zhicheng[®] manufacturers, Shanghai, China). In the morning the cells were harvested by centrifugation in a Beckman centrifuge (J2-21 model, Beckman Coulter, Brea, CA, USA) at 3000 *g* for 10 min and the supernatant discarded. The

pellet was then re-suspended in 1 litre minimal media and allowed to grow at 37 °C in a shaking incubator. When an OD₅₅₀ of approximately 0.4 was reached, 100 µM ZnSO₄ was added. When OD_{550nm} reached 0.5, IPTG was added to a concentration of 0.5 mM and the incubation temperature was lowered to 25 °C and the cells grown overnight. The cells were harvested by centrifugation at 10000 g for 30 min and lysed by the freeze thaw method as described above.

2.9 Glutathione affinity chromatography

Glutathione affinity chromatography was used for the purification of GST-tagged recombinant proteins using a gravity-fed self-packed column.



2.9.1 Preparation of glutathione affinity column

Dry glutathione agarose beads (Sigma, St. Louis, MO, USA) were swelled according to the manufacturer's instructions and poured into a plastic gravity-fed column.

2.9.2 Purification of the crude lysate

The column was washed with 3 column volumes (CV) of 1 M NaCl and then equilibrated with 5 CV of 1X PBS. The crude lysate was added to the column and 1 CV of the non-bound fraction was collected as the 'flow through' from the column. The column was then washed with 6 CV of 1X PBS, with samples from the beginning and end being collected (wash and clean wash respectively) for further analysis. The bound protein was eluted from the column with 1 CV of

15 mM glutathione in 50 mM Tris-HCl, pH 8.0 and 5 fractions (1 CV each) were collected. Finally the column was washed with 2 CV of 2 M NaCl and two 1 CV fractions were collected. All of the collected fractions were analysed by SDS-PAGE.

2.9.3 Cleavage of recombinant protein

Fractions containing the fusion protein were pooled and dialysed against 2 litres of Cleavage Buffer (50 mM Tris-HCl, 150 mM NaCl, 5.0 mM DTT, 1.0 mM EDTA, pH 7.0) using a 3 500 MWCO. SnakeSkin[®] pleated dialysis tubing (Thermo Scientific, Rockford, IL, USA). After 1 hour, 50 µl of home-made PreScission[™] 3C Protease was added to the dialysis bag to separate the GST from the target protein and incubated overnight at 4°C with gentle stirring. Following cleavage, the contents of the dialysis bag were returned to the glutathione column and the target protein collected in the flow through, with GST being retained on the column. (Note: Dialysis serves the dual function of removing glutathione resulting from the first affinity step as well as changing to Cleavage Buffer).

2.9.4 Size exclusion chromatography

Following removal of most of the GST in the second glutathione affinity step, residual GST was removed by size exclusion chromatography on a Hi Prep[™] 16/60 Sephacryl[™] S-100 High Resolution column (Amersham Pharmacia Biotech Inc., Piscataway, NJ, USA). The column was equilibrated with 1 CV of NMR buffer at a flow rate of 0.75 ml/min. The sample was concentrated into 1 ml using an Amicon[®] Ultra-15 centrifugal filter device with a MWCO of 3000 Da (Millipore[®] Corporation, Billerica, MA, USA) and injected onto the column. 1 ml

fractions were collected and analysed by SDS-PAGE. Fractions containing the desired protein were pooled together and concentrated into 600 μ l for NMR analysis.

2.10 SDS-PAGE

The integrity and purity of protein fractions were analysed by SDS-PAGE as described by Laemmli (Laemmli, 1970) using a BioRad Mini-PROTEAN[®] 3 system (BioRad Laboratories, Hercules, CA, USA). 16% separating gels and 4% stacking gels were made by mixing different components as shown in the table below: the separating gel was poured into the assembled BioRad system and allowed to set, after which the stacking gel was added on top and ten well combs were used to form the wells for loading the protein samples to be analysed. Molecular weights were estimated with the aid of protein molecular weight standards (Fermantas, Hanover, MD, USA)

20 μ l aliquots of protein were mixed with 10 μ l of 2x SDS Sample Buffer, vortexed briefly and boiled at 95 °C for 5 mins. 20 μ l of the boiled mixture was loaded into the wells and separated using a potential of 100 V until the dye front reached the end of the gel. The gel was removed from the assembly and stained in a solution of Coomassie Brilliant Blue R250 for at least 1 hour, where after it was destained in destaining solution overnight. Electronic copies of SDS-PAGE gels were produced by scanning.

Table 2.2 Components used for 4% stacking gels and 16% separating gels for SDS- PAGE

Component	Volume added (ml) (4% Stacking Gel)	Volume added (16% Separating Gel)
Double distilled H₂O	6.1 ml	6.4 ml
1.5 M Tris, pH 8.8 (Separating Buffer)	-	5.25 ml
0.5 M Tris, pH 6.8 (Stacking Buffer)	2.5 ml	-
40% Acrylamide	1.5 ml	8 ml
10% SDS	100 µl	210 µl
10% APS	50 µl	120 µl
TEMED	20 µl	25 µl

2.11 Determination of protein concentration

The protein concentration was determined using the Quick Start™ Bradford Protein Assay Kit (BioRad Laboratories, Hercules, CA, USA) in the 1 ml format according to the manufacturer's instructions. Absorbance readings were taken at 595 nm using a Helios Epsilon spectrophotometer (Thermo Spectronic, Madison, WI, USA) blanked against NMR Buffer. Commercially prepared samples of bovine gamma globulin with concentration of 10, 20, 30, 40, 50, 80, 90, 100 µg/ml were used as standards. Two dilutions (1:400 and 1:800) of the protein sample were prepared and their absorbance readings taken according to the instructions on the kit. Plots of OD_{590nm} as a functions of concentration in µg/ml were generated using Microsoft Excel (Microsoft® Corporation, Redmond, WA, USA) and fitted to straight lines with y intercept = 0.

2.12 Methods in biomolecular NMR

2.12.1 Sample preparation

All NMR experiments were carried out in NMR Buffer, AT 25 °C using a Varian Inova 600 MHz spectrometer equipped with a 14.1 T 51-mm bore Oxford Magnet (Varian Inc., Palo Alto, CA, USA). 600 µl samples were pipetted into 8 inch long, 5 mm-diameter Wilmad[®] NMR tubes (Sigma-Aldrich, St. Louis, MO, USA) and 7 % (v/v) deuterium oxide (D₂O) was added to act as a lock signal. Lyophilised synthetic peptides (GenScript Corporation, Piscataway, NJ, USA) were re-suspended in double de-ionised water to give stock concentrations of 10 mM for both CTD-1 and CTD-2. 40 minute ¹H-¹⁵N-HSQC spectra were recorded using the gnhsqc pulse sequence which forms part of the BioPack suite (Varian, Palo Alto, CA, USA), with 4 transients, 128 t1-increments, 1024 points in the direct time dimension, a ¹H spectral width of 8000 Hz and a ¹⁵N spectral width of 2000 MHz. Spectra were processed using NMRDraw (Delaglio *et al.*, 1995) and displayed using NMRView (Johnson *et al.*, 1994).

2.12.2 NMR titration experiments

A series of ¹H-¹⁵N-HSQC spectra of the ¹⁵N-labelled RING finger domain were collected, one following each addition of unlabelled peptide. Peptides were added in 10 µl aliquots and the final concentration calculated taking into account the increased sample volume. ¹H-¹⁵N-HSQC spectra were overlayed so as to identify the residues that displayed significant chemical shift perturbations during the titration. Co-ordinates of the centres of resonance were extracted using NMRView and chemical shift perturbations plotted as a function of ligand concentration using pro Fit (Uetikon am See, Switzerland). Curves were fitted to the theoretical expression

$$\theta = \frac{[P] + [L] + K_D + \sqrt{([P] + [L] + K_D)^2 - 4[P][L]}}{2[P]}$$

and values extracted for K_D using an experimentally measured value for $[P]$. Here $[P]$ denotes the total protein concentration, $[L]$ the total ligand concentration and K_D the dissociation constant of the interaction.

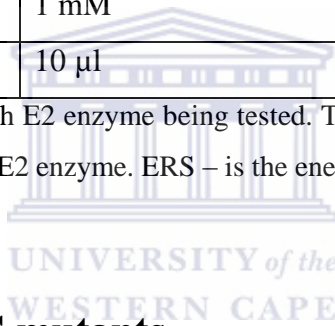
2.13 *In vitro* ubiquitination assays

Components of the ubiquitin reaction were set up as shown in Table 2.3. E1 enzyme and pre-coupled Mg-ATP solution were obtained commercially from Boston Biochem Inc. (Cambridge, MA, USA). E2 enzymes were obtained commercially from the E2 enzyme kit (Product code K-980, BostonBiochem). ^{35}S -labelled substrate (YB-1) was expressed using the TNT[®] *In vitro* transcription/translation kit (Promega Corporation, Fitchburg, WI, USA) according to the manufacturer's instructions. Bacterially expressed RING finger-like domain was used as the E3 enzyme. Proteasome inhibitor MG132 was added to block degradation of ubiquitinated proteins. The reaction was then incubated at 37 °C for 90 min using a rotating rotor at 10 g (Labnet Inc., Edison, NJ, USA) and ubiquitinated forms of ^{35}S -YB-1 were detected using SDS-PAGE followed by autoradiography.

Table 2.3 Components of the ubiquitination assay

Component	Experimental Reaction	Control Reaction
50 mM HEPES buffer pH 8.0	15 μ l	15 μ l
E1	200 nM	200 nM
E2	1 μ M	-
E3 (RING finger)	1 μ M	1 μ M
Substrate (YB-1)	1 μ M	1 μ M
MG132 (protease inhibitor)	10 μ M	10 μ M
Ubiquitin aldehyde	5 μ M	5 μ M
Ubiquitin	1 mM	1 mM
Mg-ATP solution (ERS)	10 μ l	10 μ l

A separate reaction was set up for each E2 enzyme being tested. The control reaction had all of the same components with the exception of the E2 enzyme. ERS – is the energy regeneration solution.



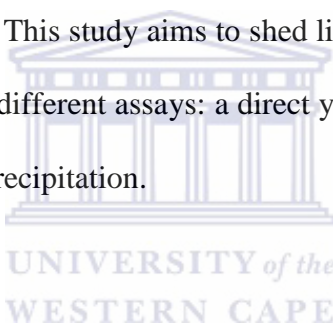
2.14 Generation of RING mutants

Expression constructs encoding for mutated RING finger-like domain were generated by GenScript Corporation, Piscataway, NJ, USA) using wild type constructs supplied by the researcher. Mutant constructs were generated in pCMV plasmids and sub-cloned into pGEX-6P-2 for bacterial expression of the protein.

Chapter 3: Investigation of the interaction between the RING finger of RBBP6 and YB-1

3.1 Introduction

YB-1 was previously identified as an interaction partner of RBBP6 in a yeast 2-hybrid screen using the RING finger-like domain of RBBP6 as bait (Chibi *et al.*, 2008). Based on the cDNA sequence of the Y2H prey vector, the RBBP6/YB-1 interaction was found to be localised within the last 62 amino acid residues of the C-terminal domain of YB-1, residues 262 - 324 (here designated as the YB-1_{Y2H} region). This study aims to shed light on the RBBP6/YB-1 interaction at the amino acid level using three different assays: a direct yeast 2-hybrid assay, NMR chemical shift perturbation and co-immunoprecipitation.



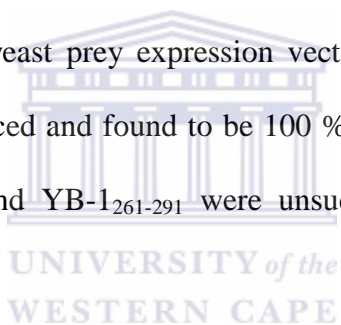
3.2 Analysis of the interaction between YB-1 and the RING finger domain of RBBP6 using a Yeast 2-hybrid assay

A panel of peptides derived from the YB-1_{Y2H} region were designed with the aim of testing their interaction with the RING finger domain of RBBP6 using a direct yeast 2-hybrid approach. The peptides were designated as YB-1₂₆₁₋₂₉₁, YB-1₂₇₇₋₃₀₆, and YB-1₂₉₂₋₃₂₄ respectively. Another fragment devoid of the last 62 amino acids at the C-terminus was also designed and this was designated as YB-1_{Δ62}. The point of including YB-1_{Δ62} in the Y2H assay was to investigate if RBBP6 also interacts with regions of YB-1 outside the region identified by the original yeast 2-hybrid screen.

3.2.1 Generation of YB-1 derived fragments

cDNA fragments corresponding to YB-1₂₆₁₋₂₉₁, YB-1₂₇₇₋₃₀₆, and YB-1₂₉₂₋₃₂₄ were PCR amplified from the prey plasmid recovered by Chibi and co-workers in the previous yeast 2-hybrid screen. The primers used for this amplification are shown in Table 3.1. Primers were designed based on the nucleotide sequence of human YB-1 (GenBank accession number AAH98435). YB-1_{Δ62} was amplified from a full length cDNA construct kindly donated by Dr. Moredreck Chibi, CNRS, University of Paris.

The amplifications of YB-1₂₇₇₋₃₀₆ and YB-1₂₉₂₋₃₂₄ were successfully carried out (see Fig.3.2) and these were then cloned into the yeast prey expression vector pACT2 as described in section 2.5.6. The constructs were sequenced and found to be 100 % correct (see Appendix II and III). The amplifications of YB-1_{Δ62} and YB-1₂₆₁₋₂₉₁ were unsuccessful because of faulty primer design.



3.2.2 Direct yeast 2-hybrid assay

The pGBKT7-RING plasmid encoding the RING finger-like domain of RBBP6 was a kind gift from Dr. Moredreck Chibi. The bait and prey expression plasmids were transformed into yeast strains of opposite mating types as described in section 2.7.2. pGBKT7-RING (bait) was transformed into AH109 and preys pACT2-YB-1₂₇₇₋₃₀₆, pACT2-YB-1₂₉₂₋₃₂₄, pACT2-YB-1_{Y2H} and empty pACT2 were transformed into the yeast strain Y187. Empty pACT2 vector was used as a negative control while pACT2-YB-1_{Y2H} was used as a positive control. Bait and prey-transformed strains were mated as described in Section 2.7.3 and the resultant diploid colonies

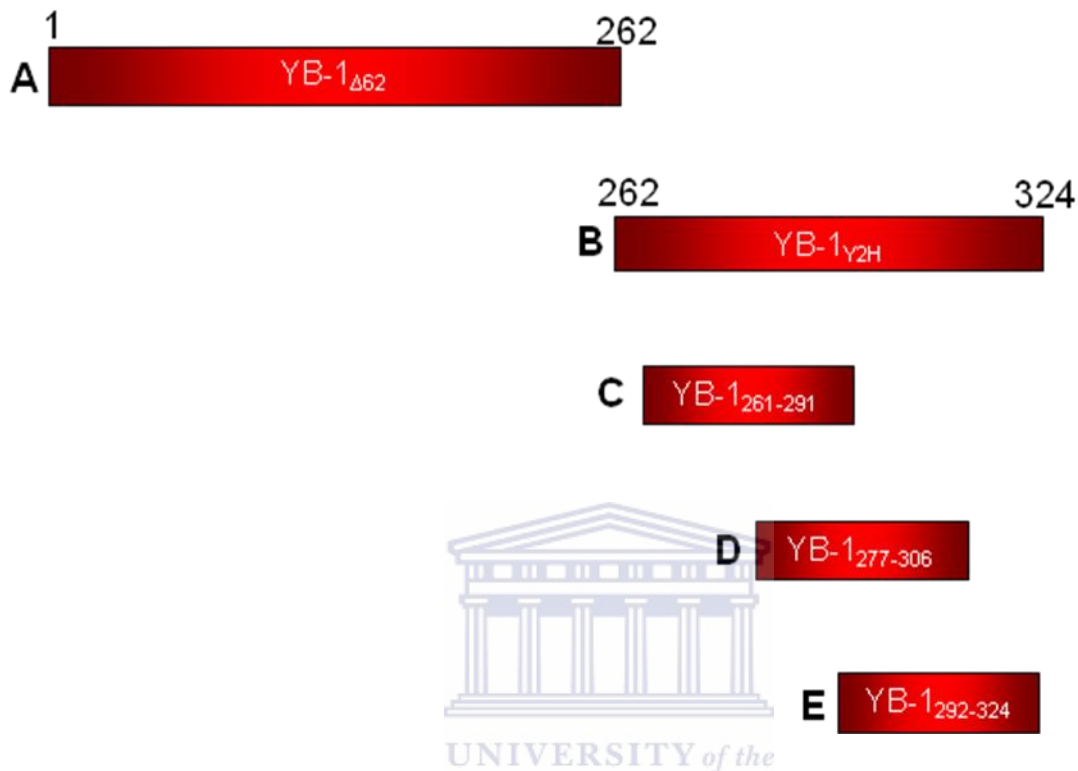


Fig. 3.1 An illustration of the designed fragment peptides tested for interaction with the RING finger domain of RBBP6. The figure shows the amino acid boundaries of the fragment peptides. The fragments are not drawn to scale. The fragment devoid of the last 62 C-terminal amino acid residues of YB-1 (YB-1_{Δ62}) is shown in (A). The last 62 amino acid region of the C-terminal domain of YB-1 is represented by YB-1_{Y2H} (B). (C), (D), and (E) show the amino acid boundaries of YB-1₂₆₁₋₂₉₁, YB-1₂₇₇₋₃₀₆, and YB-1₂₉₂₋₃₂₄ whose interaction with the RING finger domain of RBBP6 was being tested for.

Table 3.1 Primers used for the amplification of YB-1-derived fragments

Primer name	Primer sequences
YB-1 _{Δ62} Forward	5' -GAGACGGATCCAAATGAGCAGCGAGGCCGAGA-3'
YB-1 _{Δ62} Reverse	5' -TTATCCCTCGAGTTATTCTTCATTGCCGTCCTCTCT-3'
YB-1 ₂₆₁₋₂₉₁ Forward	5' -GGCAAGGATCCAAGAAGATAAAGAAAATCAAGGAG-3'
YB-1 ₂₆₁₋₂₉₁ Reverse	5' -AGGGTCCTCGAGTTAGCGTCTGCGTCGGTAATTG-3'
YB-1 ₂₇₇₋₃₀₆ Forward	5' -AGTGTGGATCCCTCAACGTCGGTACCGC-3'
YB-1 ₂₇₇₋₃₀₆ Reverse	5' -ATTGTCCTCGAGTTAGGCTGCTTTTGTCTCTTTGC-3'
YB-1 ₂₉₂₋₃₂₄ Forward	5' -CCTGAGGATCCAGAAAACCCTAAACCACAA-3'
YB-1 ₂₉₂₋₃₂₄ Reverse	5' -GTCTCCTCGAGTTACTCAGCCCCGCCCTG-3'

The nucleotide sequence shown in black font represents the sequence of the primer that is complimentary to the DNA template used in the PCR reaction. The green colour represents the nucleotide overhang tag that facilitates restriction enzyme digestion while the red and blue colours correspond to the restriction enzyme recognition site and the stop codon respectively.

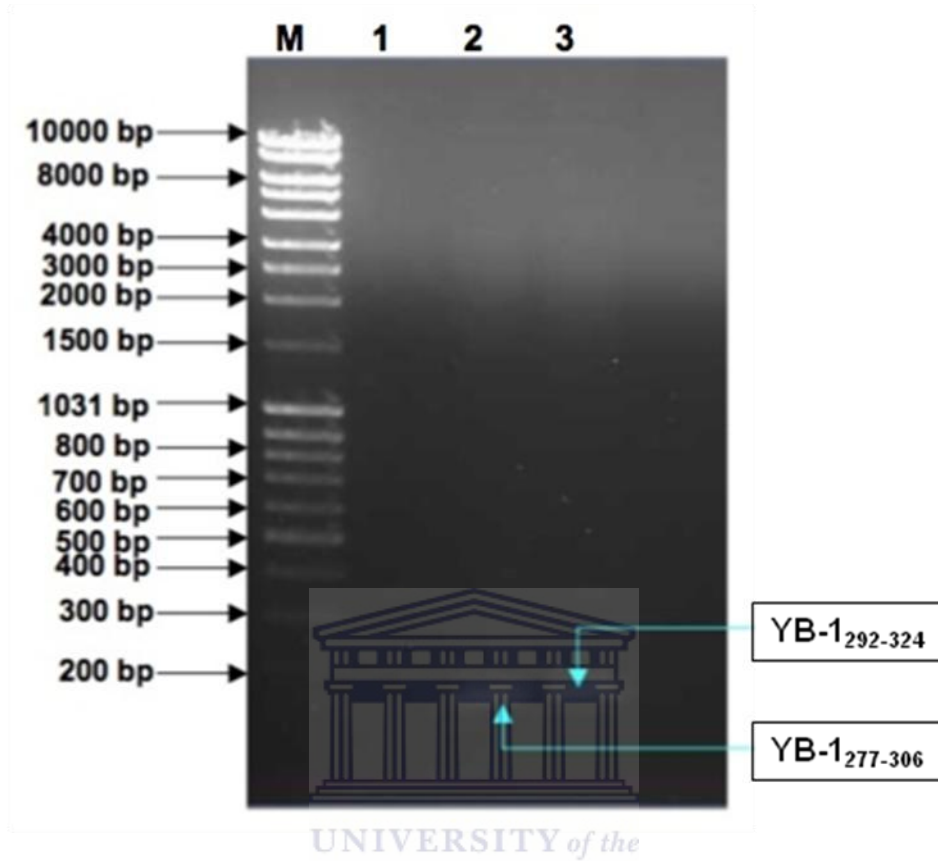
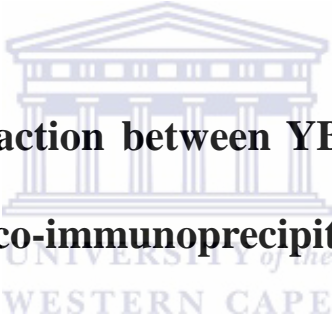


Fig. 3.2 A 1 % agarose gel image showing PCR amplification of YB-1₂₇₇₋₃₀₆ and YB-1₂₉₂₋₃₂₄. Lanes 2 and 3 correspond to the amplicons of YB-1₂₇₇₋₃₀₆ and YB-1₂₉₂₋₃₂₄ respectively. Lane 1 shows the negative control of the PCR reaction that had no DNA template in it and lane M corresponds to the DNA molecular weight marker. The expected size of both YB-1₂₇₇₋₃₀₆ and YB-1₂₉₂₋₃₂₄ is approximately 90 bp long.

were first grown on double drop-out plates and then transferred into media of higher stringency lacking 3 amino acids (triple drop-out - TDO).

Diploid yeast cells containing *bona fide* interacting bait and prey proteins are expected to grow in TDO media. Fig. 3.3 shows that diploid cells containing YB-1_{Y2H} were able to grow well on TDO plates as expected. Cells containing YB-1₂₉₂₋₃₂₄ grew moderately well whereas YB-1₂₇₇₋₃₀₆ grew poorly on TDO plates. We conclude that YB-1₂₇₇₋₃₀₆ interacts with the RING finger domain, and that YB-1₂₉₂₋₃₂₄ interacts poorly, if at all.



3.3 Analysis of the interaction between YB-1 and the RING finger domain of RBBP6 using co-immunoprecipitation assays

The YB-1-derived fragments YB-1₂₇₇₋₃₀₆ and YB-1₂₉₂₋₃₂₄ were tested for their interaction with the RING finger domain of RBBP6 using co-immunoprecipitation (co-IP) assays. ³⁵S-labelled proteins expressed as fusions with immunoaffinity tags were expressed using an *in vitro* transcription/translation kit (Promega, Corporation, Fitchburg, WI, USA).

3.3.1 Expression of proteins for use in the co-IP assay

pACT2-YB-1₂₇₇₋₃₀₆ and pACT2-YB-1₂₉₂₋₃₂₄ were used as templates to PCR-amplify cDNA for the *in vitro* expression of HA-YB-1₂₇₇₋₃₀₆ and HA-YB-1₂₉₂₋₃₂₄ respectively. pGBKT7-RING was used to produce cDNA for the expression of cMyc-RING. The primers used in the PCR reactions are shown in Table 3.2. In addition to the epitope tags, the amplified sequences incorporate

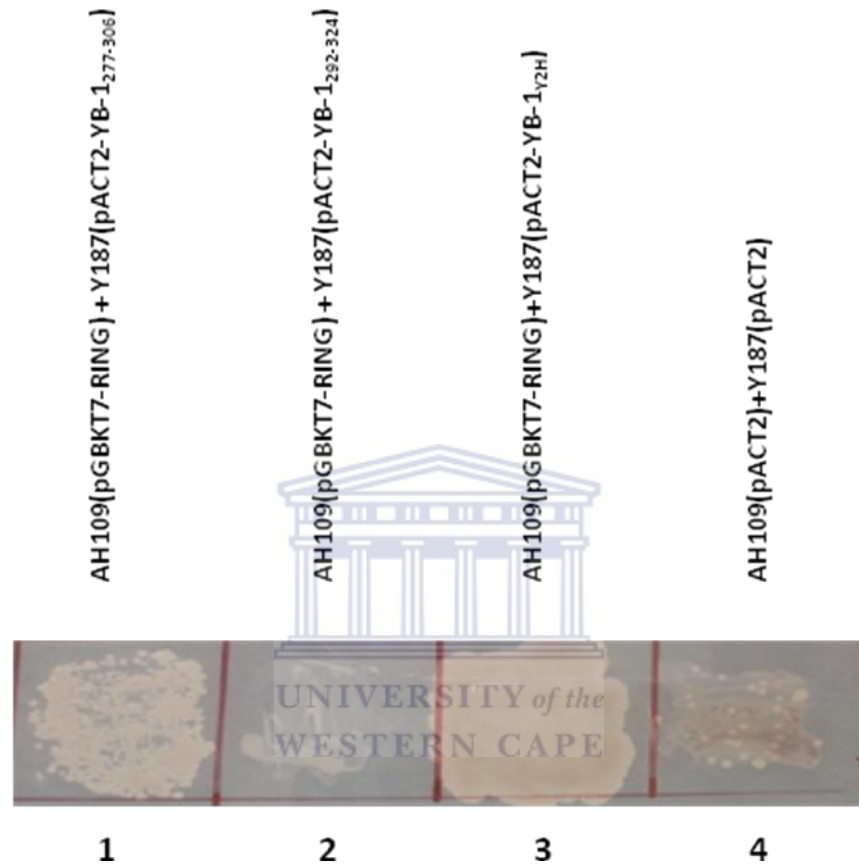


Fig. 3.3 A yeast 2-hybrid assay showing that YB-1₂₇₇₋₃₀₆ and YB-1₂₉₂₋₃₂₄ interact with RING finger *in vivo*. Yeast diploid colonies containing prey plasmids pACT2-YB-1₂₇₇₋₃₀₆ and pACT2-YB-1₂₉₂₋₃₂₄ (panels 1 and 2) were able to grow on TDO medium in the presence of pGBKT7-RING. This means that RING interacts with YB-1₂₇₇₋₃₀₆ and YB-1₂₉₂₋₃₂₄. Diploid colonies with pACT2-YB-1_{Y2H} and pGBKT7-RING (panel 3) acted as a positive control of the yeast 2-hybrid experiment while those containing empty pACT2 served as negative control. The brown colouration in panel 4 is a sign of dying yeast cells that are unable to survive in TDO media. Empty pACT2 is unable to code for bait and prey proteins therefore diploid cells containing empty pACT2 fail to survive in TDO media. Diploid yeast cells are able to grow in TDO if they contain interacting bait and prey proteins.

bacteriophage T7 promoters from the host vectors for use in the *in vitro* expression system. Amplification of HA-YB-1₂₉₂₋₃₂₄, HA-YB-1_{Y2H}, and Myc-RING was successful (see Fig. 3.4) but the generation of HA-YB-1₂₇₇₋₃₀₆ was unsuccessful. The corresponding protein fragments were produced in a cell-free system as described in Section 2.6.1. Fig. 3.5 shows that HA-YB-1₂₉₂₋₃₂₄ (lane 1), HA-YB-1_{Y2H} (lane 2) and Myc-RING (Lane 4) were successfully expressed.

Table 3.2 Primers for the PCR amplification of bait and prey inserts

Primer name	Primer sequence and primer annealing temperature (°C)
pGBKT7 Forward	5'-AATAAAATTGTAATACGACTCACTATAGGGCGAGCCGCCACCATGGAGGAGC AGAAGCTGATGTCA-3' 65°C
pGBKT7 Reverse	5'-TCACTTTAAAATTTGTATACAC-3' 44°C
pACT2 Forward	5'-AATAAAATTGTAATACGACTCACTATAGGGCGAGCCGCCACCATGTACCCA TACGACGTTCCAGAT-3' 61°C
pACT2 Reverse	5'-GGGGTTTTTCAGTATCTACGAT-3' 52°C

3.3.2 RING finger co-immunoprecipitates YB-1₂₉₂₋₃₂₄ *in vitro*

Radio-labelled HA-YB-1_{Y2H} or HA-YB-1₂₉₂₋₃₂₄ were mixed with Myc-tagged RING in a co-IP experiment and the results analysed using autoradiography (see Fig. 3.5). Anti Myc was able to precipitate HA-YB-1₂₉₂₋₃₂₄ in the presence but not in the absence of Myc-RING (see lane 5, Fig. 3.5). Myc-RING was also able to precipitate HA-YB-1_{Y2H} (lane 6) as expected from the previous Y2H screen.

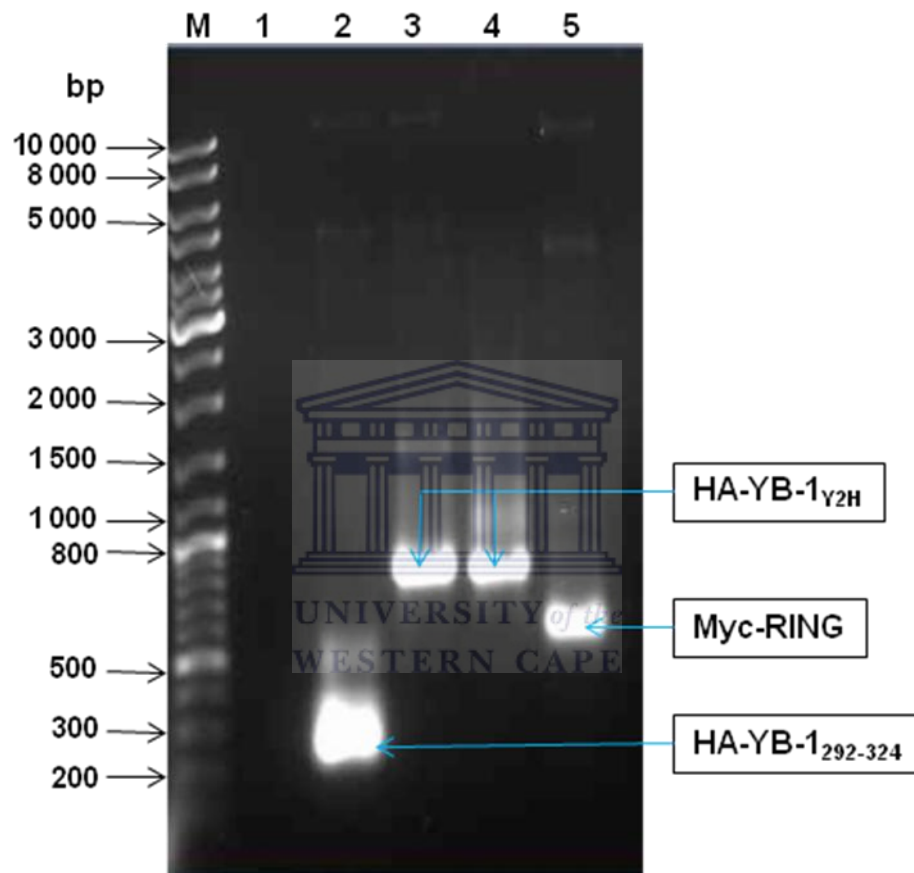


Fig. 3.4 A 1% agarose gel showing the amplification of cDNA of proteins to be subjected for co-IP analysis. The amplicons of the cDNA of test proteins were amplified by PCR as fusions of cDNA of immunoaffinity tags. Lane 1 shows the negative control of the PCR reaction that had no template DNA in it. Lane 2 shows the cDNA of HA-YB-1₂₉₂₋₃₂₄, while lanes 3 and 4 contain the cDNA of HA-YB-1_{Y2H}. Lane 5 shows the cDNA of Myc-RING. The DNA molecular weight marker is shown in lane M.

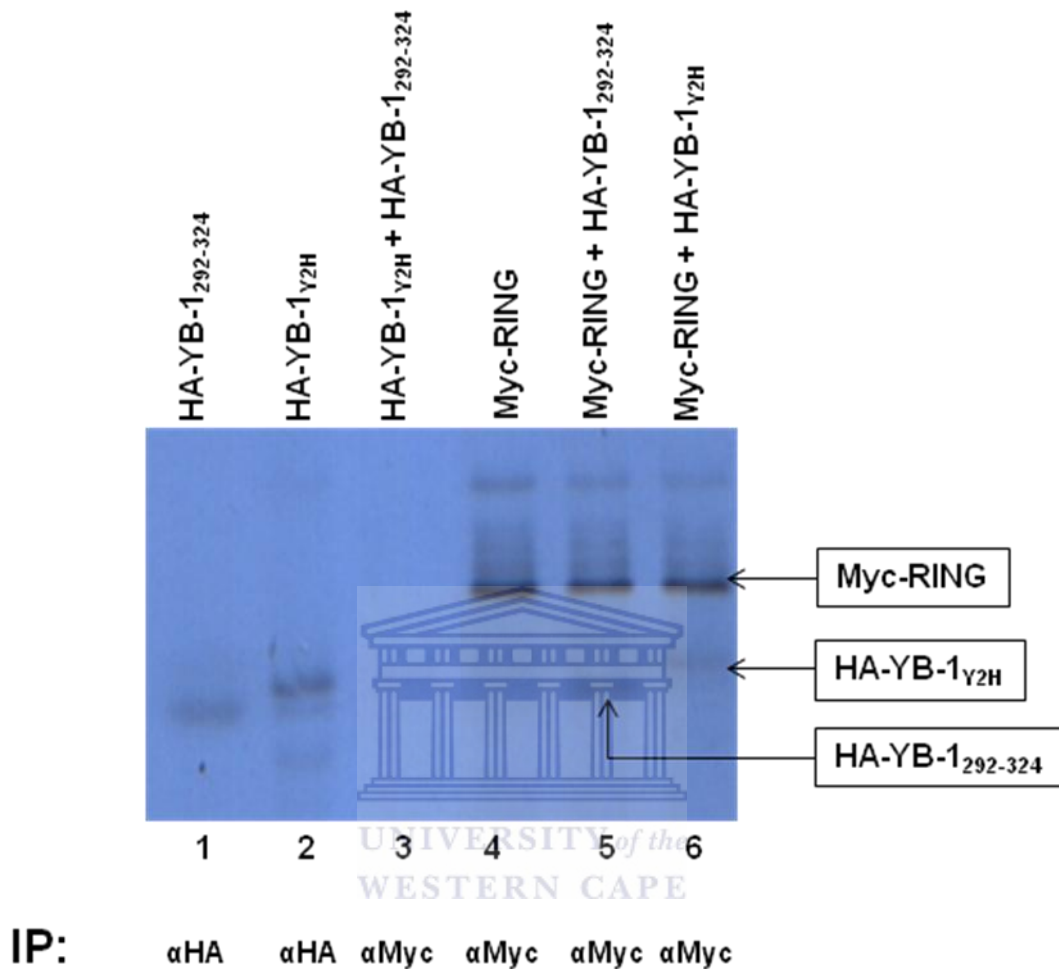


Fig. 3.5 An autoradiograph showing the immunoprecipitation of *in vitro* generated ³⁵S-labelled proteins. The antibodies used to precipitate the proteins are shown in each respective lane. Lanes 1 and 2 respectively correspond to individual immunoprecipitates of HA-YB-1₂₉₂₋₃₂₄ and HA-YB-1_{Y2H} precipitated with anti-HA (αHA) antibody. Lane 4 corresponds to co-immunoprecipitation of Myc-RING with anti-Myc antibody. Lanes 5 shows Myc-RING and HA-YB-1₂₉₂₋₃₂₄ which were co-immunoprecipitated with anti-Myc antibody. This indicates that RING and YB-1₂₉₂₋₃₂₄ interact together *in vitro*. Co-immunoprecipitation of RING and YB-1_{Y2H} is shown in lane 6 which acts as a positive control for the co-IP assay. Lane 3 corresponds to the negative control of the assay in which HA-YB-1₂₉₂₋₃₂₄ and HA-YB-1_{Y2H} were not precipitated by anti-Myc (αMyc) antibody itself.

Although the quantities of YB-1 peptides precipitated by Myc-RING are small, lanes 1 and 2 suggest that the total amount of the peptides present in the reactions was not large, and so the results do not necessarily imply that the interactions are weak.

3.4 Analysis of the interaction between YB-1 and the RING finger domain of RBBP6 using NMR spectroscopy

Synthetic peptides CTD-1 and CTD-2 derived from YB-1_{Y2H} were tested for their interaction with bacterially expressed ¹⁵N-labelled RING finger domain using NMR chemical shift perturbation analysis. The amino acid sequences and percentage purities of these synthetic peptides are shown in Table 3.3. The amino acid boundaries of these synthetic peptides relative to YB-1_{Y2H} are shown in Fig. 3.6. CTD-1 and CTD-2 were designed to correspond as closely as possible (given the constant of solubility) to peptides YB-1₂₆₂₋₂₉₁ and YB-1₂₇₇₋₃₀₆ used in the yeast 2-hybrid and co-IP studies.

Table 3.3 Synthetic peptides and their amino acid composition

Peptide	Amino acid composition	% Purity
CTD-1	EDKENQGDETQGQQPPQRRYRRNFNYRRRR	99.2
CTD-2	PENPKPQDGKETKAADPPAENS SAPEAEQGGAE	98.5

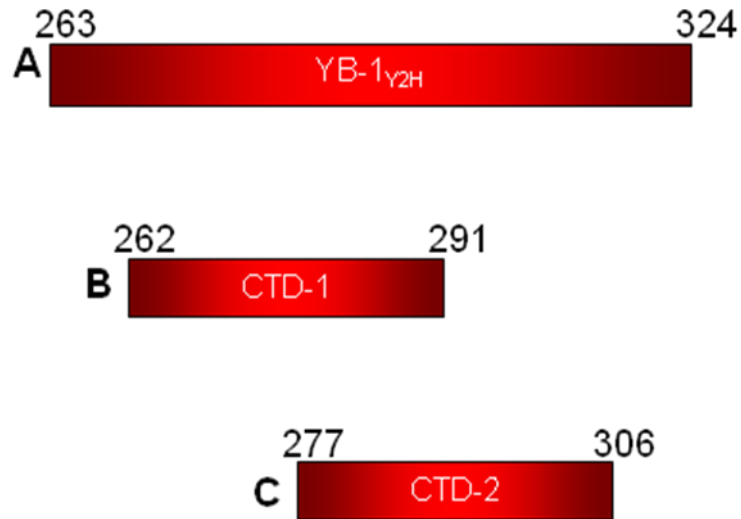
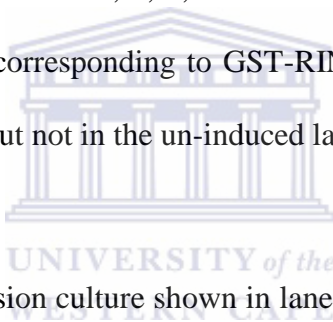


Fig. 3.6 An illustration of the synthetic peptides tested for interaction with the RING finger domain of RBBP6 using ^1H - ^{15}N -HSQC NMR. The figure shows the amino acid boundaries of the fragment peptides relative to YB-1_{Y2H}. CTD-1 and CTD-2 were tested for interaction with ^{15}N -labelled RING. **A** Shows the YB-1_{Y2H} fragment and its amino acid boundaries. **B** and **C** show the amino acid boundaries for the synthetic peptides CTD-1 and CTD-2 respectively.

3.4.1 Expression and purification of the RING finger domain of RBBP6 for use in NMR

The RING finger domain was expressed as a GST fusion protein using the pGEX-6P-2 vector system (GE Healthcare, Waukesha, WI, USA). The pGEX-6P-2-RING expression construct was cloned and kindly provided by Takalani Mulaudzi (Department of Biotechnology, UWC). *E. coli* BL21 (DE3) pLysS cells were transformed with pGEX-6P-2-RING as described in Section 2.4.3 and screened for the recombinant protein expression as described in Section 2.8.1. Fig 3.7 shows the result of small-scale expression assays for 4 different colonies. The uninduced lysates are shown in lanes 1, 3, 5, and 7 while lanes 2, 4, 6, and 8 show the induced lysates. A prominent band of approximately 36.8 kDa, corresponding to GST-RING (GST - 26.6 kDa, RING - 10.2 kDa), is seen in the induced lanes but not in the un-induced lanes.



500 μ l from the small-scale expression culture shown in lanes 7 and 8 of Fig. 3.7 was inoculated into 100 ml of 15 N-labelled minimal media as described in Section 2.8.3. GST-RING was purified away from *E. Coli*'s native proteins using glutathione-affinity chromatography as described in Section 2.9.2. Fig. 3.8A shows that high levels of expression were obtained. The GST-RING fusion protein was cleaved using 3C protease (Fig. 3.8B lane 2) and GST and uncleaved fusion protein (lanes 6-9) were removed by a second glutathione-affinity step, while free RING finger domain was collected in the flow through (Fig. 3.8B lanes 3 and 4). Flow-through fractions were pooled together in preparation for downstream purification steps. Residual GST and other contaminating proteins were removed from RING by size exclusion chromatography (Fig 3.9A) as described in Section 2.9.4.

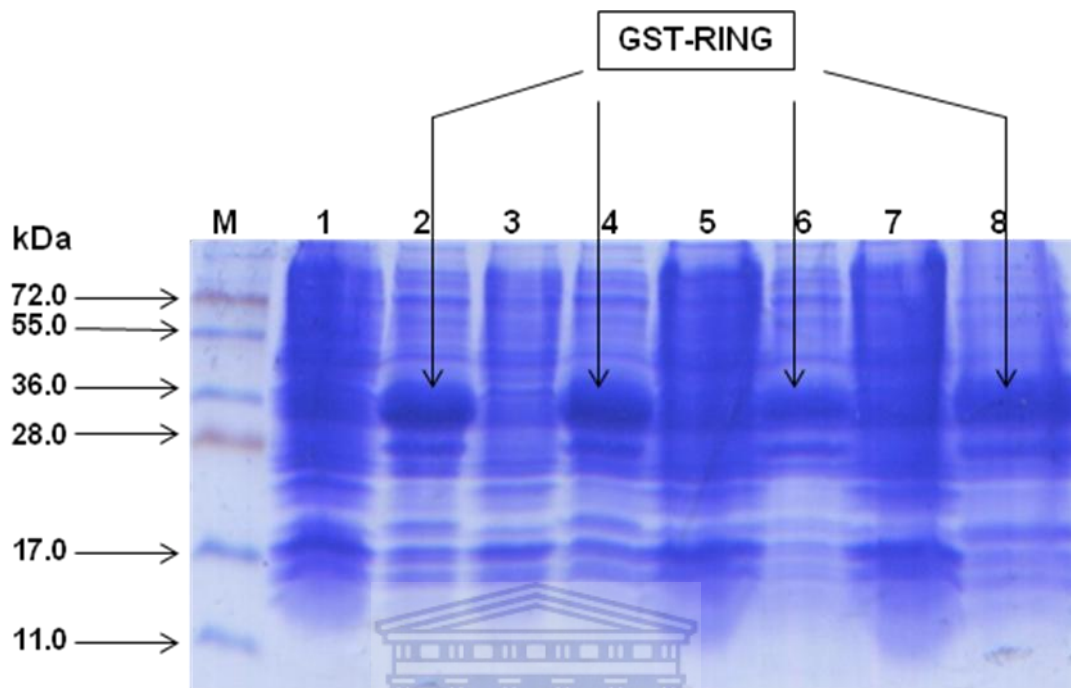


Fig. 3.7 SDS-PAGE analysis of the small-scale expression of GST-RING in a 16 % acrylamide gel. Lanes 1, 3, 5, and 7 show uninduced protein expression. Lanes 2, 4, 6 and 8 show the induced protein expression. Lane M contains a protein molecular weight marker. The induced expression is characterised by the presence of a prominent band at ~36.8 kDa which is absent in the uninduced lanes.

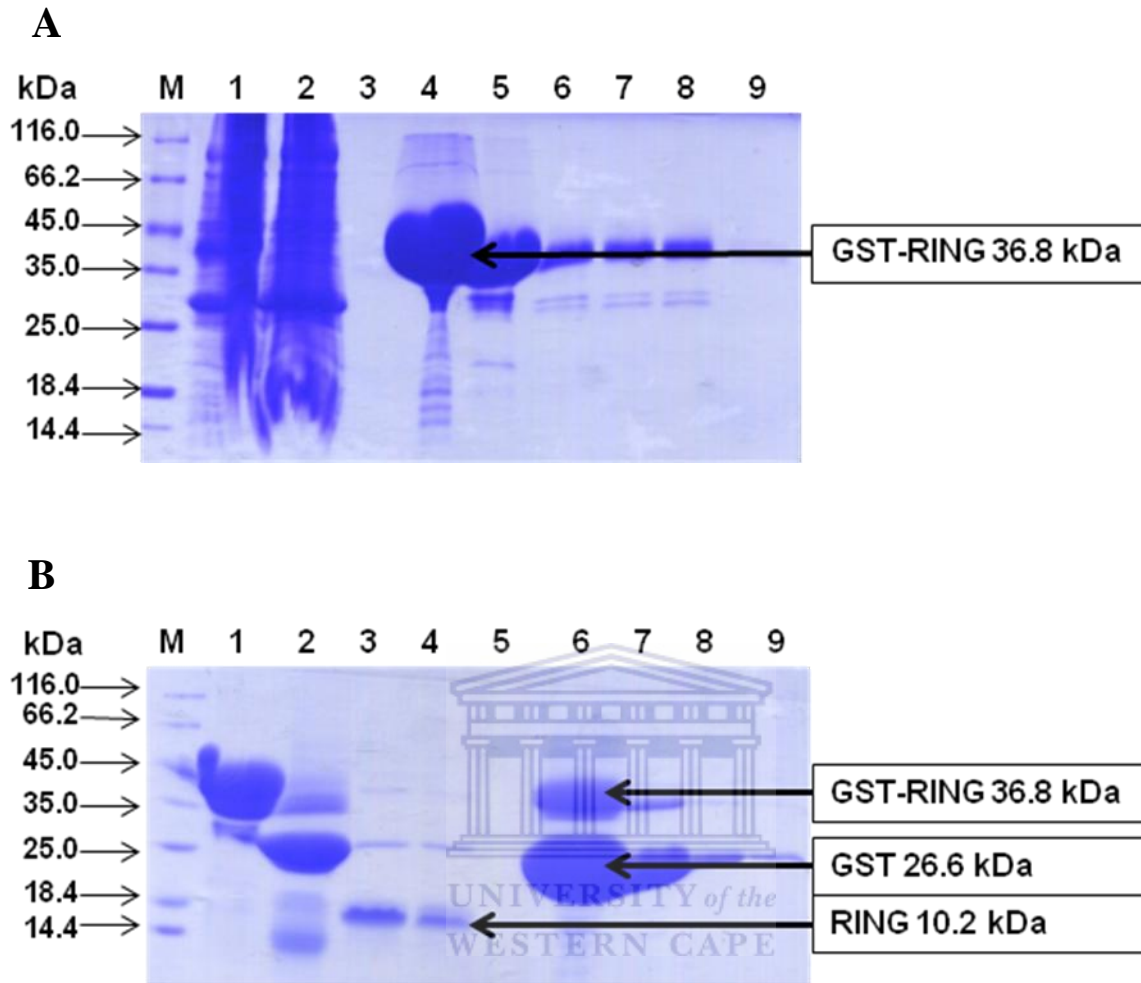


Fig. 3.8 Large-scale expression, affinity purification and cleavage of GST-RING using PreScission™ 3C Protease. (A) Expression of GST-RING in minimal media. Lane 1 shows the crude lysate whilst lane 2 shows the flow through, lane 3 shows the column wash, lanes 4-8 each correspond to the fractions eluted from the GST column. Lane 9 shows the fraction eluted during the NaCl wash. Lane M shows the protein molecular weight marker. (B) Lane 1 shows the uncleaved fusion protein, lane 2 shows the cleaved protein and lanes 3 and 4 both show the flow through, containing predominantly the isolated RING finger domain. Lane 5 corresponds to the column-wash, while lanes 6 and 7 show what was eluted with 10 mM glutathione. Lane M shows the protein molecular weight marker. The isolated DWNN domain has previously been reported to migrate at an anomalously large apparent molecular weight (M.A. Kappo, PhD thesis, UWC 2009)

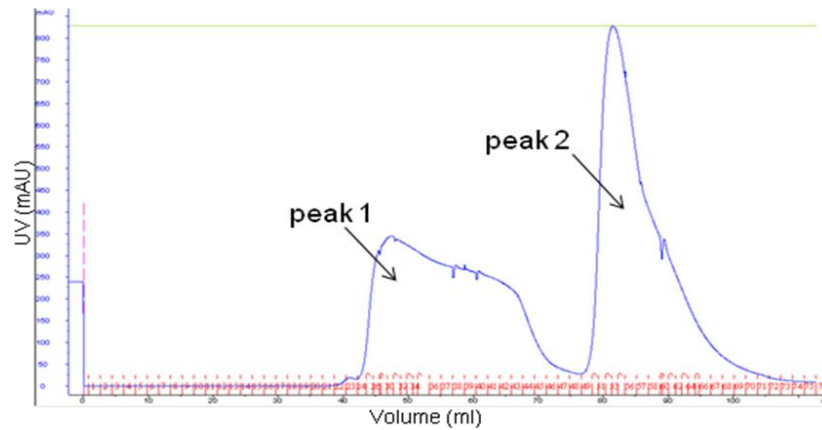
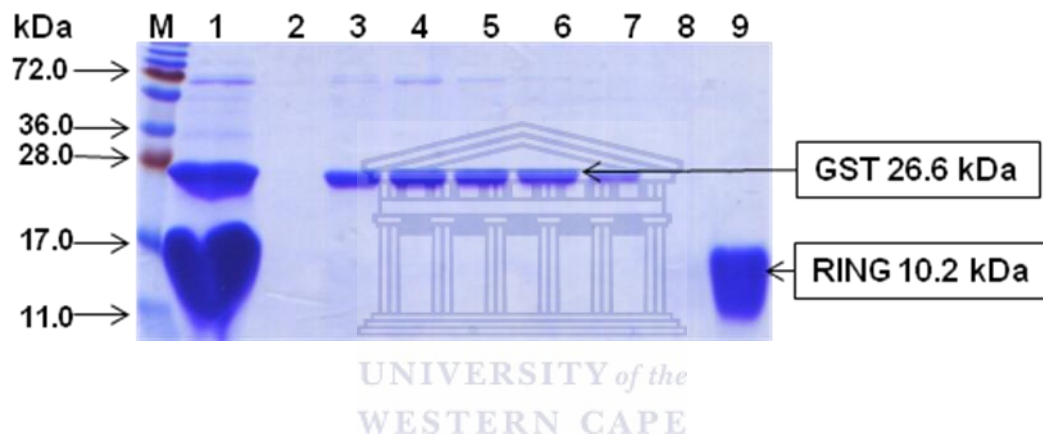
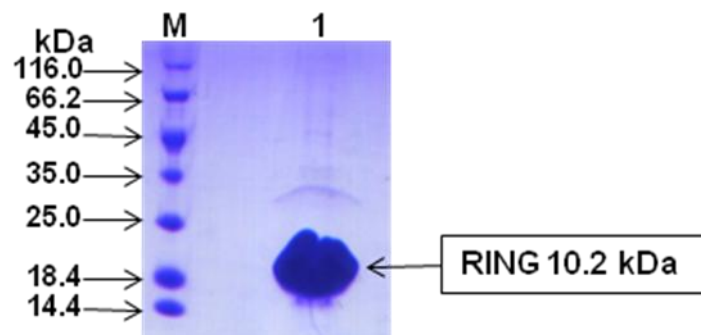
A**B****C**

Fig. 3.9 Purification of RING finger domain by size exclusion chromatography. (A) Peak 1 and 2 correspond to GST and RING finger domain respectively. (B) SDS-PAGE analysis of the fractions from the FPLC. Lane 1 corresponds to the unpurified protein sample before purification, lane 3 corresponds to the fraction at the top of Peak 1. Lanes 2, 4, 5, 6, and 7 correspond to some of the fractions eluted under peak 1. Lane 8 corresponds to the fraction at the beginning of Peak 2 while lane 9 corresponds to the fraction at the top of Peak 2. (C) SDS PAGE gel of purified RING finger domain after gel filtration. Lane M in all the gels corresponds to the protein molecular weight marker.

Since the GST(MW 26.6 kDa) has a higher molecular weight than that of the RING finger domain (10.2 kDa), it eluted earlier than the RING finger domain, as expected, and a clear separation between GST (peak 1) and RING (Peak 2) was achieved as shown in Fig 3.9A. Fractions were collected and their contents assessed by SDS-PAGE analysis as shown in Fig. 3.9B. Fractions containing pure RING finger were pooled and concentrated into 600 μ l for NMR analysis. Fig 3.9C shows that the final sample of RING finger domain was highly pure.

Note: the RING finger-like domain migrates on SDS-PAGE gels at an apparent molecular weight of 18 kDa rather than the expected 10.2 kDa. This has been noted previously and is a feature of this protein.



3.4.2 Determination of protein concentration

The concentration of the expressed sample was determined by the Bradford method as described in Section 2.11. The absorbance readings of standard protein concentrations (Table 3.4) were used to construct the standard curve shown in Fig. 3.14. All the absorbance readings were taken at 595 nm. The equation $y = 0.0043x - 0.008$ was used to determine the concentration of the RING finger domain protein preparations.

At 1:800 dilution of the RING finger domain the absorbance was found to be 0.201 (Table 3.4) which, using the standard curve, corresponds to 48.6 μ g/ml, which is equivalent to an original concentration of 38.9 mg/ml. At 1:400 dilution of the RING finger domain, the absorbance was found to be 0.3675 (Table 3.4), which is equivalent to an original concentration of 34.9 mg/ml. Since the molecular weight of RING finger domain is 10.2296 kDa the molar concentrations of

Table 3.4 Absorbance values for the gamma globulin standards and RING

Concentration ($\mu\text{g/ml}$)	Absorbance at 595 nm
Gamma globulin Standards	
10	0.0135
20	0.070
30	0.1385
40	0.1785
50	0.212
80	0.3615
90	0.376
100	0.401
Sample dilutions	
1:400	0.3675
1:800	0.201

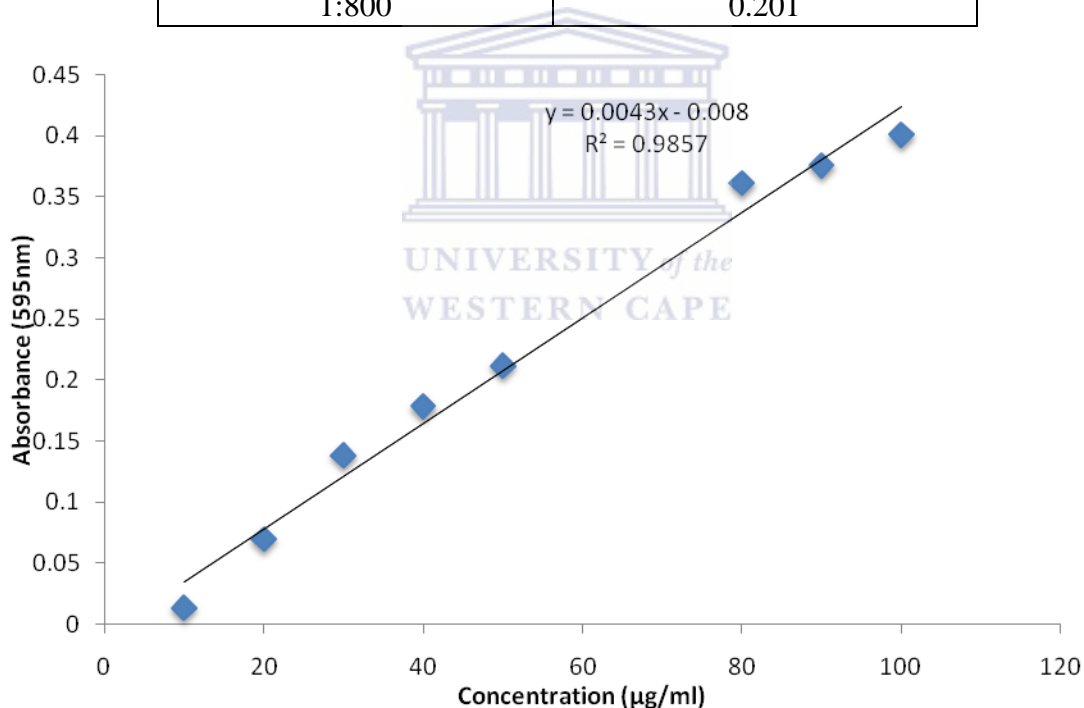
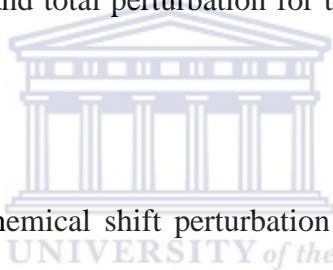


Fig. 3.10 Gamma globulin standard curve for the determination of the protein concentration of the RING finger domain. A_{595} values of the standard protein (gamma globulin) plotted against different concentrations of gamma globulin. The unknown concentration of RING was determined using the A_{595} values at different dilutions. The equation of the standard curve was used to calculate the concentration of RING finger domain.

the RING finger domain protein preparations translate to 3.8 mM and 3.4 mM respectively. Averaging the two values gives the concentration as 3.6 mM.

3.4.4 RING interacts with YB-1 through part of its C-terminal helix.

NMR chemical shift perturbations were used to map the YB-1 binding site onto the RING finger domain. Fig. 3.11 shows that CTD-1 induced small but concentration-dependent shifts on the ^1H - ^{15}N -HSQC spectrum of ^{15}N -labelled RING finger domain. Perturbations were plotted as a function of concentration (Fig. 3.12) and fitted to the expected theoretical expression given in Section 2.12.2. The values of K_D and total perturbation for the most affected residues are given in Table 3.5.



The values of K_D and the total chemical shift perturbation for the most affected residues are shown in Table 3.5. Most of them fall in the region 324-330, which lie along an extended surface on the face of the homodimer adjacent to the C-terminal helix (see Fig. 3.14). Structural analysis and ^{15}N -relaxation studies (Pugh *et al.*, unpublished data) show that this surface is rigid and structured, and is therefore a potential interaction surface for YB-1. Fig.3.13 shows that CTD-2 produced perturbations that are broadly consistent with those produced by CTD-1, but of a smaller magnitude, which suggests a weaker interaction between CTD-2 and the RING finger-like domain of RBBP6.

Table 3.5 K_D values and total chemical shifts

Residue	Total chemical shift change (ppm)	K_D (μ M)
Asn ³²⁴	0.065	176
Glu ³²⁵	0.056	487
Thr ³²⁶	0.145	263
Gly ³²⁷	0.047	256
Tyr ³²⁸	0.087	334
Thr ³²⁹	0.078	117
Lys ³³⁰	0.054	455

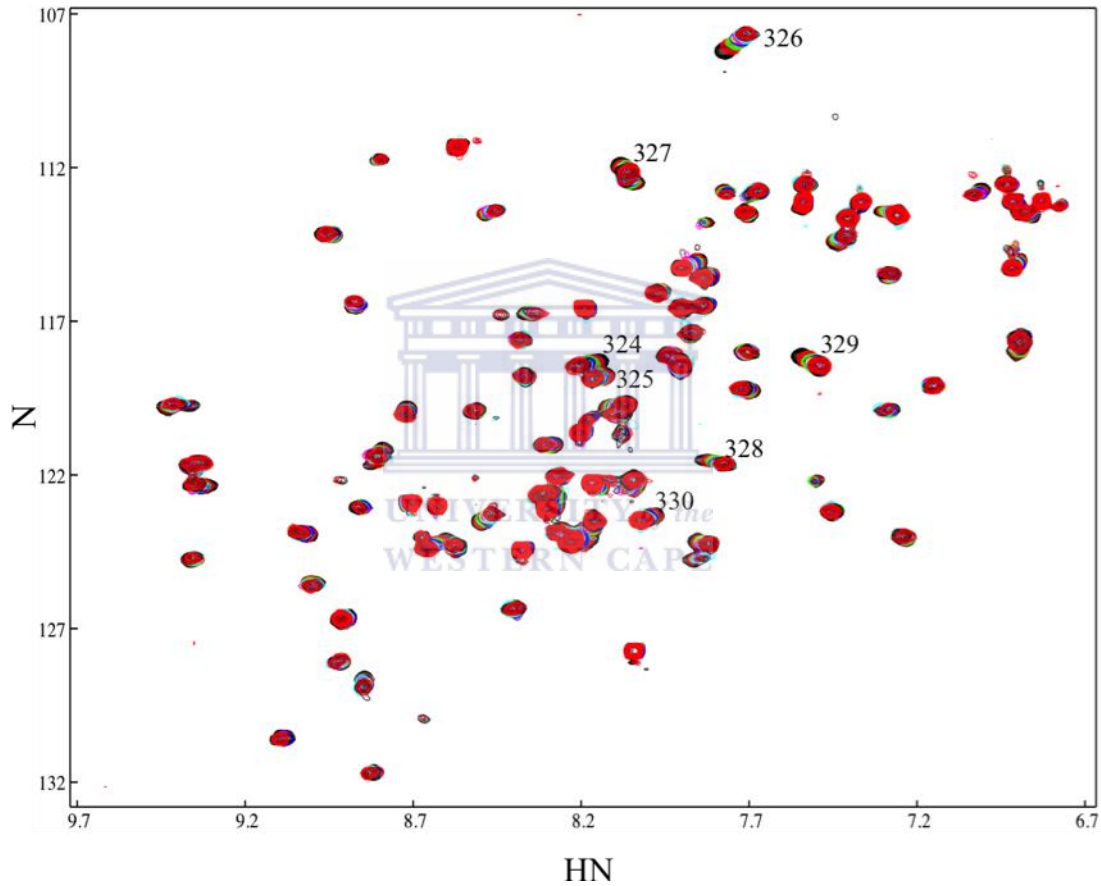


Fig. 3.11 Overlay of ^1H - ^{15}N -HSQC spectra of ^{15}N -labeled RING with increasing concentration of unlabelled CTD-1 peptide. Chemical shift perturbations are characteristic of an interaction between substrate and ligand. The RING residues Asn³²⁴, Glu³²⁵, Thr³²⁶, Gly³²⁷, Tyr³²⁸, Thr³²⁹, and Lys³³⁰ are perturbed the most owing to binding to the CTD 1 peptide. Backbone assignment of resonances was carried out by Pugh *et al.*, unpublished data.

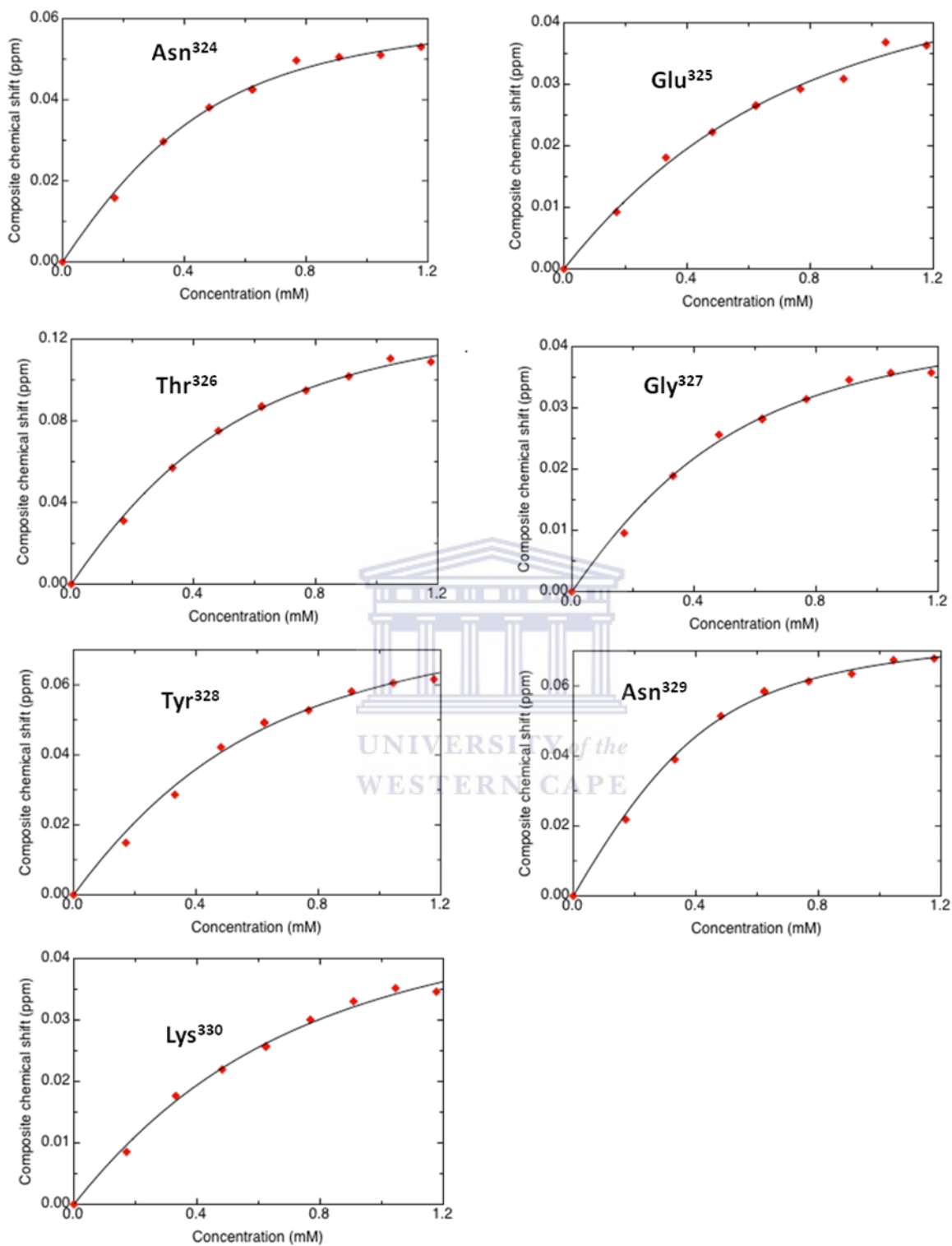


Fig. 3.12 Composite chemical shifts of residues of the RING finger domain of RBBP6 that displayed significant perturbations on titration with CTD-1.

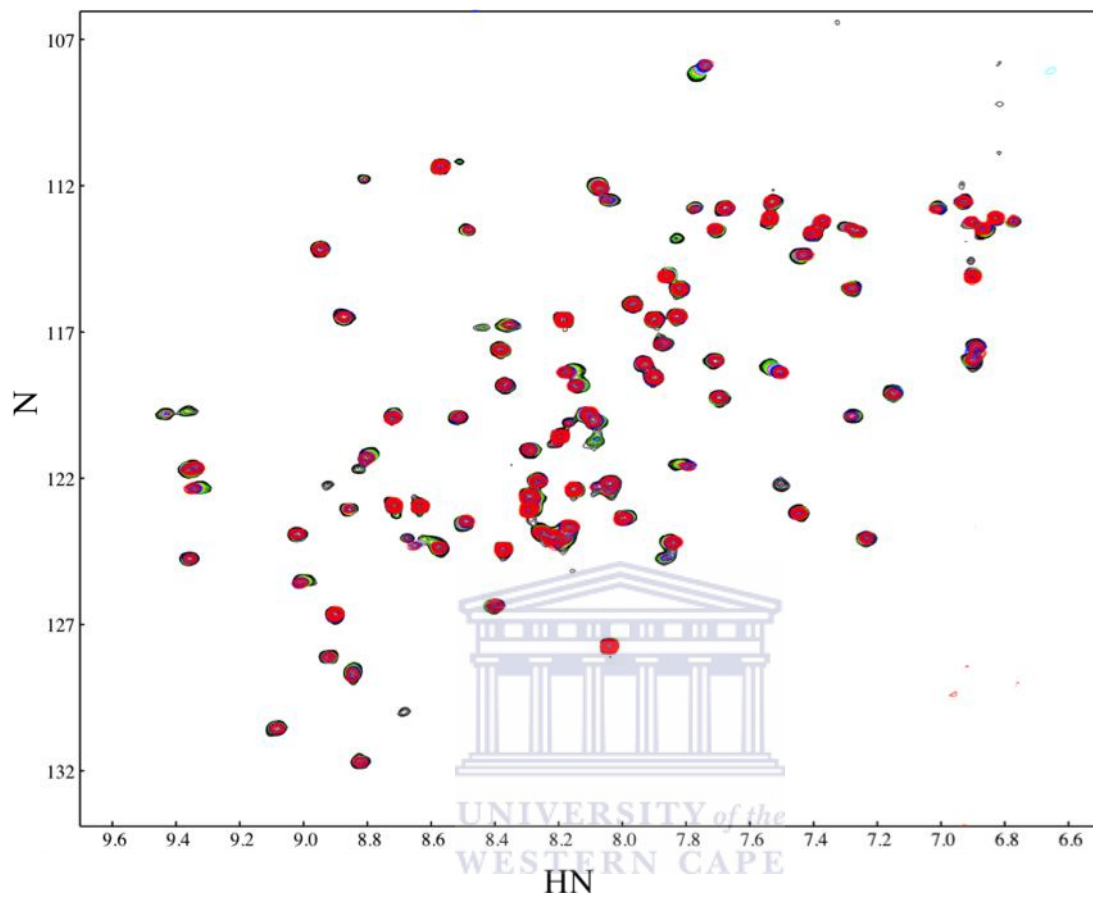


Fig. 3.13 Overlay of ^1H - ^{15}N -HSQC spectra of ^{15}N -labeled RING with increasing concentration of CTD-2 peptide.

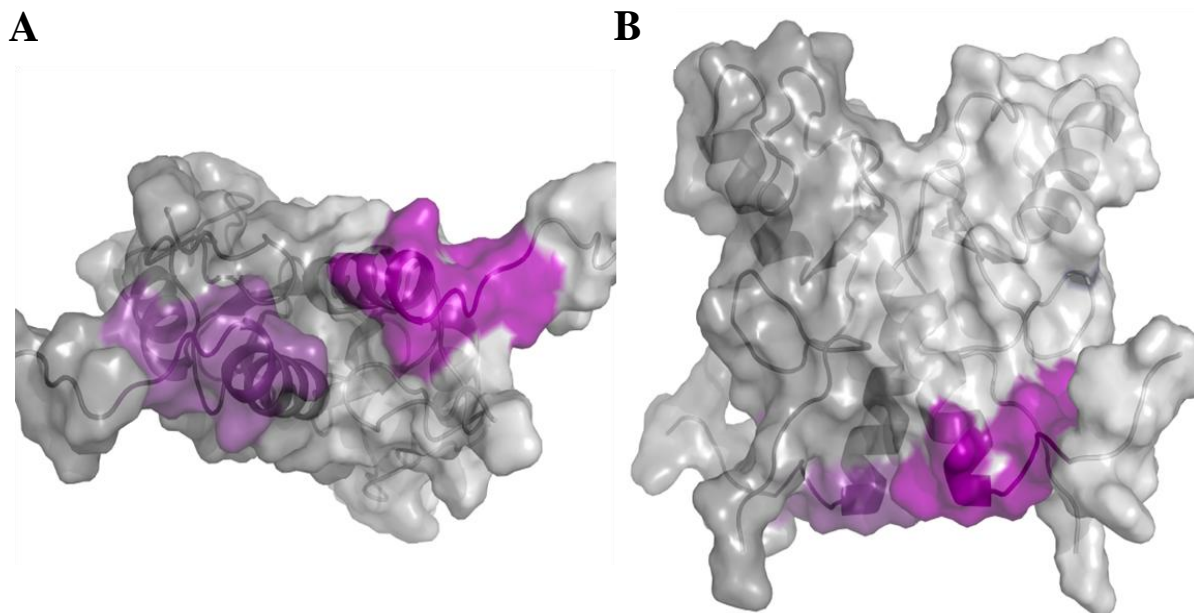


Fig. 3.14 Surface representation of the homodimer of the RING finger-like domain of RBBP6 showing the YB-1 binding site. The localisation of the residues (Asn³²⁴, Glu³²⁵, Thr³²⁶, Gly³²⁷, Tyr³²⁸, Thr³²⁹, and Lys³³⁰) interacting with CTD-1 are shown in purple. These residues lie along an extended surface on the face of the homodimer adjacent to the C-terminal helix. The end view of the molecule is shown in **A**) while the side view of the same molecule is shown in **B**). In both views the YB-1 binding site is shown in dark purple in one monomer and in light purple in the other monomer.

Chapter 4: Functional investigations

4.1 Identification of cognate RBBP6 E2s using an *in vitro* ubiquitination assay

RBBP6 was previously shown to act as an E3 ubiquitin ligase in the ubiquitination of YB-1 in HEK 293 cells (Chibi *et al.*, 2008). Human cells contain 35 different E2 enzymes, any of which could be involved in ubiquitinating YB-1. Establishment of a fully *in vitro* assay for investigating RBBP6-mediated ubiquitination of YB-1 requires that active E2s be identified so that they can be expressed in bacteria for use in *in vitro* assays. In order to identify the E2 involved, a preliminary small scale screen of 3 different E2s was carried out. The E2s selected were UbcH5c, UbcH7 and Ubc13. UbcH5c was chosen for screening because it is the most promiscuous of the E2s, meaning that it is active in many ubiquitin reactions in conjunction with many different E3s. UbcH7 is a known cognate E2 of c-Cbl, a RING finger containing E3-ligase (Zheng *et al.*, 2000). Ubc13 shares the S-P-A motif also found in UbcH5c, which has been proposed as a determinant of E2s active with the CHIP family of E3 ligases (Xu *et al.*, 2008). Since the RING finger domain of RBBP6 is highly similar to the U-box domain of CHIP (Pugh *et al.*, unpublished data), Ubc13 may also be expected to be active in conjunction with RBBP6. UbcH7 does not contain the S-P-A motif and therefore may be expected not to have activity in conjunction with RBBP6.

4.1.1 UbcH5c and UbcH7 facilitate YB-1 ubiquitination *in vitro*

Human E2s UbcH5c, UbcH7 and Ubc13 were tested for activity in the ubiquitination of YB-1 *in vitro* as described in Section 2.13. *In vitro* translated/transcribed YB-1 was used as a substrate, incorporating ³⁵S-methionine to facilitate detection by autoradiography. The RING finger domain which was used as the E3 in this assay was produced by *in vitro* transcription/translation but without radioactive labelling. Fig. 4.1 shows that addition of UbcH5c produces a ladder of higher molecular weight bands above YB-1 that is suggestive of ubiquitination. Contrary to expectation, UbcH7 also appears to produce ubiquitination, whereas Ubc13 does not.

4.2 Investigation of the effect of mutagenesis on the homodimeric state of the RING finger



Previous structural studies indicate that the RING finger domain of RBBP6 is a homodimer in solution (Pugh *et al.*, unpublished data). Homodimerisation of some RING finger domains and other U-boxes has been shown to affect the ubiquitination activity of this class of E3s (Deshaies *et al.*, 2009; Zhang *et al.*, 2005; Poyurovsky *et al.*, 2007; Zhang *et al.*, 2005), although the reason for this still remains elusive. In order to be able to probe the effect of the homodimer on ubiquitination, we sought to design mutants which abrogate the dimerisation. This was done by introducing single amino acid substitutions at the RING dimer interface.

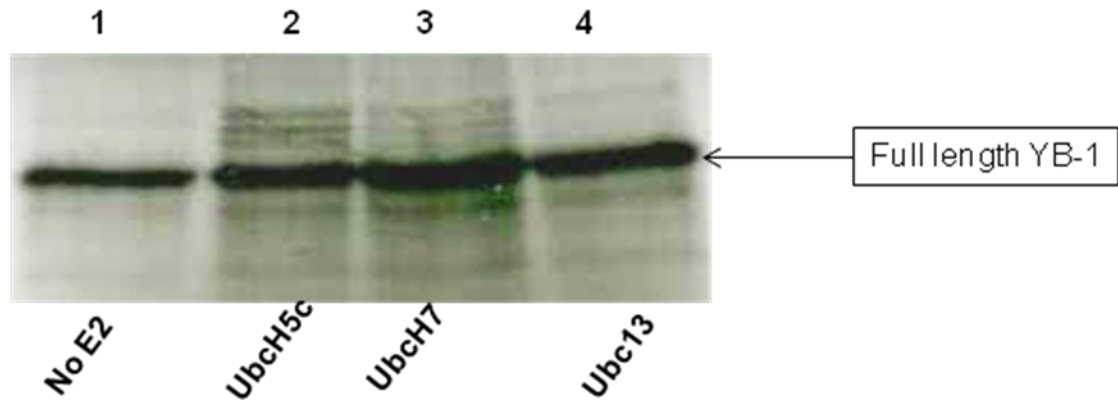
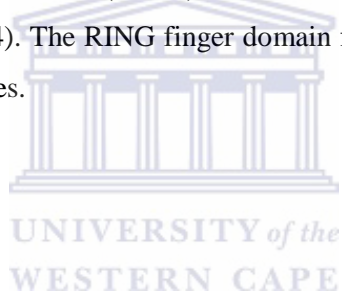


Fig. 4.1 An autoradiograph showing the ubiquitination of YB-1 in the presence of different E2s. UbcH5c produces higher molecular weight bands above YB-1 (lane 2) consistent with ubiquitinated species that are not present when it is absent (lane 1). Similar but fainter bands are seen in the case of UbcH7 (lane 3) but not Ubc13 (lane 4). The RING finger domain from RBBP6 (E3), E1, ubiquitin, 35S-YB-1 and ATP were present in all lanes.



In homologous structures such as CHIP, an asparagine corresponding to N312 of RBBP6 is located close to the dimer interface and forms hydrogen bonds with its counterpart in the other monomer. Replacement of this residue with an aspartic acid (N312D) should produce a -/- electrostatic repulsion, thereby possibly breaking the dimer. The structure also suggests that lysine 313 makes a salt bridge with D255 or E256 in the opposite monomer. Substituting lysine 313 with a glutamate residue (K313E) should replace the salt bridge with -/- repulsion, thereby breaking the dimer. Mutations corresponding to N312D and K313E were therefore introduced into the pGEX-RING expression construct and verified by sequencing (Appendix IV and V). ¹⁵N-labelled mutants were then produced in bacteria in the same manner as for wild type RING.

Previous NMR investigations have revealed concentration-dependant chemical shift perturbation resonances in the ¹H-¹⁵N-HSQC spectra corresponding to residues involved in the dimerisation interface (M.A. Kappo, PhD thesis, UWC 2009). This data suggests that there could be an exchange between the monomer and the dimer which happens at a rate faster than the timescale for NMR observations, resulting in a population-average between the spectra of the fully monomeric and fully dimeric species respectively. The result is a single resonance located at the population-weighted average of the two spectra. ¹⁵N-relaxation studies confirmed that the low concentration limit corresponds to the monomer, and the high concentration limit to the dimer, as expected (Atkinson, A., unpublished data).

The findings of this study show that the ¹H-¹⁵N-HSQC spectra of both RING^{N312D} and RING^{K313E} mutants approximate the low concentration limit of the dilution series more closely than that of the high concentration limit, suggesting that both mutants were monomeric. This is

particularly clear in the case of RING^{K313E}, in which the mutated residue lies near the edge of the dimerisation interface and therefore is not likely to have much effect other than disruption of the dimer. Fig. 4.3A shows that the green resonances which correspond to RING^{K313E}, lie close to the low concentration limits of a number of residues which shift significantly on dilution.

RING^{N312D} on the other hand, lies at the centre of the dimerisation interface and the mutation may be imputed to have effects on the ¹H-¹⁵N-HSQC spectrum over and above disruption of the dimer. The monomeric nature of both RING^{N312D} and RING^{K313E} was confirmed by ¹⁵N-relaxation experiments (Atkinson, A., unpublished data).

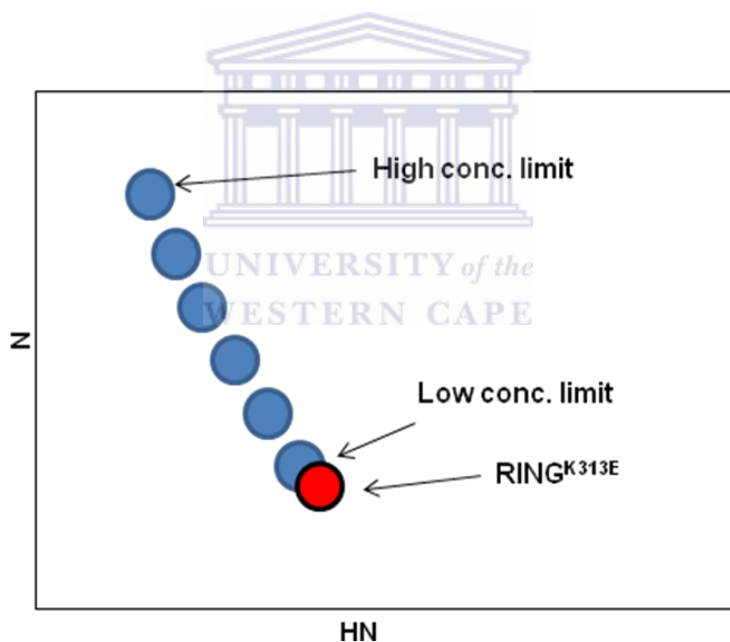


Fig. 4.2 A schematic illustration of the effect of concentration on resonances from the ¹H-¹⁵N-HSQC spectrum of the RING finger domain of RBBP6. Since the monomer and dimer are in fast exchange, the position of the peak reflects the fraction of molecules in the dimeric state, which changes as a function of concentration limit, which is unattainable since it corresponds to zero concentration, corresponds to pure monomer; the high concentration limit, which is also unattainable since it corresponds to infinite concentration, corresponds to pure dimer. The RING^{K313E} mutant approximates the low concentration limit

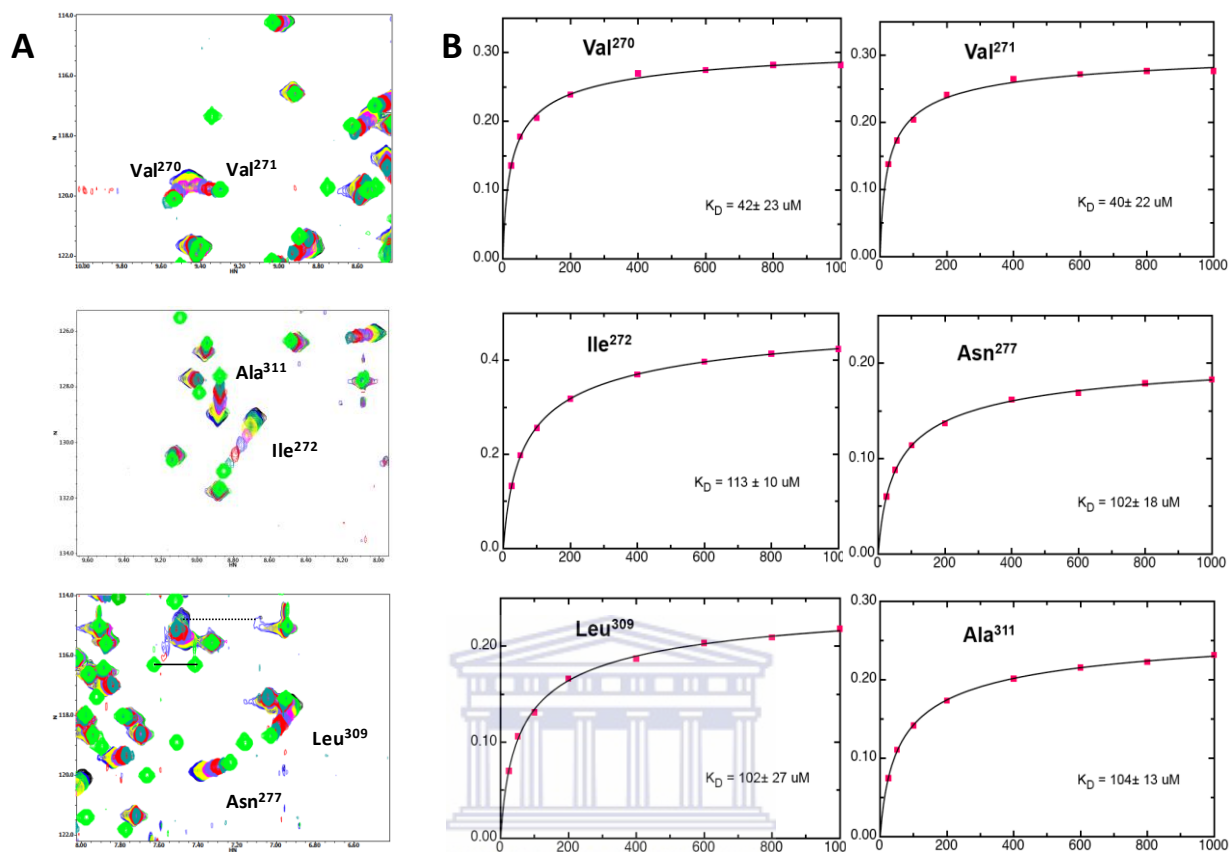
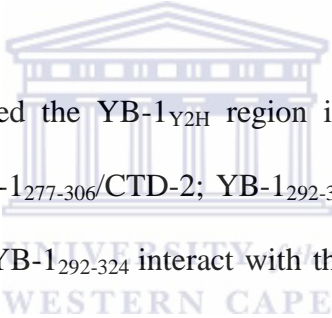


Fig.4.3 NMR analysis of the residue resonances of the RING^{K313E} mutant on an ^1H - ^{15}N -HSQC spectra. A) shows an ^1H - ^{15}N -HSQC overlay of the wild type RING dilution series with that of RING^{K313E}. The green resonances correspond to residues of RING^{K313E} and these lie close to the low concentration limits of a number of residues which shift significantly on dilution. The chemical shifts and the K_D values of the residues that exhibited significant perturbations are shown in (B).

Chapter 5: Discussion and Conclusions

5.1 *In vitro* investigation of the RBBP6/YB-1 interaction

This study investigates the structural basis underlying the interaction between the RING finger domain of RBBP6 and YB-1. Preliminary yeast 2-hybrid studies concluded that the RBBP6/YB-1 interaction is localised within the C-terminal 62 amino acid region of YB-1 (Chibi *et al.*, 2008). That conclusion was based on the cDNA sequence of the yeast 2-hybrid prey isolated in the screen. The results of this study, although preliminary, suggest that the entire YB-1_{Y2H} region may play a role in the interaction of RBBP6 with YB-1.



All three interaction assays divided the YB-1_{Y2H} region into approximately the same three fragments: YB-1₂₆₁₋₂₉₁/CTD-1; YB-1₂₇₇₋₃₀₆/CTD-2; YB-1₂₉₂₋₃₂₄. The direct yeast 2-hybrid assay showed that both YB-1₂₇₇₋₃₀₆ and YB-1₂₉₂₋₃₂₄ interact with the RING finger domain of RBBP6, although the interaction with YB-1₂₉₂₋₃₂₄ appeared to be much weaker than that with YB-1₂₇₇₋₃₀₆. The assay could not be performed for YB-1₂₆₁₋₂₉₁ because the attempt to make the Y2H construct was unsuccessful. The immunoprecipitation assay showed that YB-1₂₉₂₋₃₂₄ is immunoprecipitated by RING. The assay could not be performed for YB-1₂₇₇₋₃₀₆ because the attempt to generate this fragment *in vitro* was unsuccessful and for YB-1₂₆₁₋₂₉₁ for the reason given above. The NMR chemical shift perturbation assay showed that both CTD-1 and CTD-2 interact with the RING finger domain of RBBP6 although the interaction with CTD-2 appeared to be weaker than that with CTD-1 (Fig. 3.11 and Fig. 3.13). Taken together, the results provide evidence that the interaction of YB-1₂₆₁₋₂₉₁/CTD-1 is stronger than that of YB-1₂₇₇₋₃₀₆/CTD-2 which is stronger

than that of YB-1₂₉₂₋₃₂₄/CTD-3. However the conclusion is preliminary and would need further experimental investigation.

5.2 Ubiquitination of YB-1

The *in vitro* ubiquitination assay provides evidence that both UbcH5c and UbcH7 have E2 activity against YB-1 in cooperation with RBBP6, but that Ubc13 does not (Fig. 4.1). Because of the promiscuity of UbcH5c it is perhaps not surprising that it supports RBBP6-mediated ubiquitination of YB-1. UbcH5c and Ubc13 both contain the S-P-A motif, which has been proposed to determine specificity for CHIP E3s (Xu *et al.*, 2008). Since the RING finger domain of RBBP6 most closely resembles the U-box from CHIP (Pugh *et al.*, unpublished data) we may therefore expect Ubc13 to also support RBBP6-mediated ubiquitination. Surprisingly it does not, but UbcH7, which does not contain the S-P-A motif, does.



The observation that RBBP6 can interact with more than one E2 in YB-1 ubiquitination epitomizes functional redundancy within E2 enzyme family. Apart from RBBP6, there are some RING-containing E3s which have been shown to interact with more than one E2 enzyme. For example the breast cancer-associated E3, BRCA1 is known to interact with ten E2 enzymes (Christensen *et al.*, 2009). The rationale behind the functional redundancy exhibited by E2 enzymes is not clear. This is a surprising observation given that the E2 enzyme family has undergone evolutionary expansion (Markson *et al.*, 2009).

The method described in this study for the screening of E2s is quite robust and is not time consuming, implying that a set of E2s that interact with a given E3 enzyme can be defined within

a reasonable space of time. Also some E2 enzymes which evade detection by other methods are easily detected using this method. For example, biomolecular NMR failed to detect the interaction between UbcH5 and the RING finger domain of RBBP6 (Pugh and Klevitt unpublished data). However, it is noteworthy that the ubiquitination data shown in Fig. 4.1 is not fully convincing and hence additional studies will be required to fully substantiate the results. Additional studies may include a fully reconstituted assay using bacterially expressed YB-1 and HA-tagged ubiquitin, so that poly-ubiquitin chains can be detected by western-blotting with anti-HA antibody.

5.3 Implications of the RBBP6/YB-1 interaction for human health

The findings of this study confirm that RBBP6 interacts with YB-1 at the same region as Heterogeneous Nuclear Ribonucleoprotein K (hnRNP K) and p53 (Fig. 5.1) (Sorokin *et al.*, 2007; Lasham *et al.*, 2003; Zhang *et al.*, 2005). Since RBBP6 is known to interact with p53, this may suggest that p53, YB-1 and RBBP6 are involved in a complex. The same applies to hnRNP K, which, like RBBP6, is involved in mRNA splicing.

The RBBP6/YB-1 interaction has significant clinical implications as it presents a novel approach in the development of therapeutic strategies against cancer. The observation that RBBP6 ubiquitinates YB-1, thereby marking it for destruction by the cell, implies that RBBP6 may repress YB-1-mediated cellular functions. The structural architecture of the RBBP6/YB-1 interaction could therefore be used as a guide in the design of drugs to suppress levels of YB-1. Conceivably, the interaction between the RING finger domain of RBBP6 and YB-1 could be manipulated to produce a drug that mimics the RING finger in the manner in which it binds to

YB-1. Such a drug may keep YB-1-mediated phenotypes at bay. Taken together, this implies that the RING finger domain of RBBP6 could be a disease-modifying and ‘druggable’ target.

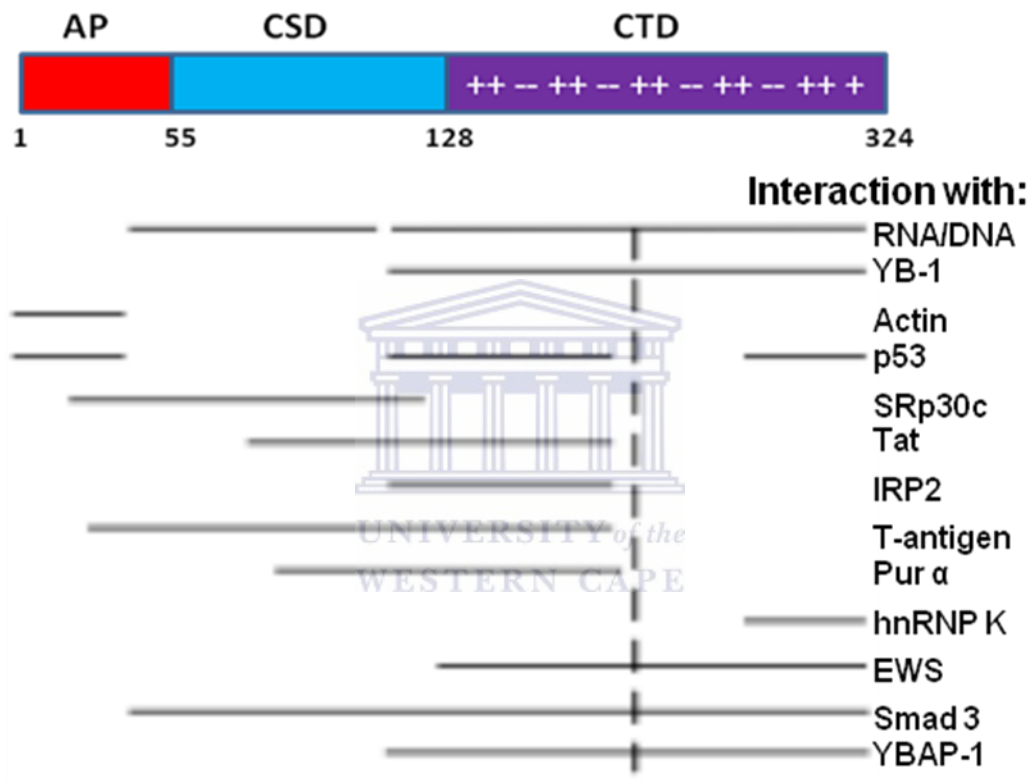


Fig. 5.1 An illustration of some of the proteins that interact with YB-1. The diagram shows the proteins known to interact with different regions of YB-1. Adapted from Sorokin *et. al* 2007.

5.4 Prospective studies

Since the screening of E2s done in this study was done from a limited set of E2s, it is also possible that UbcH5 and UbcH7 are not the only E2s that interact with RBBP6. This therefore, provides the impetus for defining the whole set of RBBP6's cognate E2s. To accomplish this task a larger screen of E2s should be carried out. Since the findings of this study support the speculation that the RING finger domain of RBBP6 could be 'druggable' target, it is imperative to carry out NMR studies that investigate the druggability of this domain.



References

Abhari,B.A. & Davoodi,J. (2010). BIR2 domain of XIAP plays a marginal role in inhibition of executioner caspases. **Int. J. Biol. Macromol.** 46, 337-341.

Angers,S., Salahpour,A. & Bouvier,M. (2002). Dimerization: an emerging concept for G protein-coupled receptor ontogeny and function. **Annu. Rev. Pharmacol. Toxicol.** 42, 409-435.

Arai,R., Yoshikawa,S., Murayama,K., Imai,Y. *et al.* (2006). Structure of human ubiquitin-conjugating enzyme E2 G2 (UBE2G2/UBC7). **Acta Crystallogr. Sect. F. Struct. Biol. Cryst. Commun.** 62, 330-334.

Baboshina,O.V., Crinelli,R., Siepmann,T.J. & Haas,A.L. (2001). N-end rule specificity within the ubiquitin/proteasome pathway is not an affinity effect. **J. Biol. Chem.** 276, 39428-39437.

Bader,A.G. & Vogt,P.K. (2005). Inhibition of protein synthesis by Y box-binding protein 1 blocks oncogenic cell transformation. **Mol. Cell Biol.** 25, 2095-2106.

Basaki,Y., Hosoi,F., Oda,Y., Fotovati,A. *et al.* (2007). Akt-dependent nuclear localization of Y-box-binding protein 1 in acquisition of malignant characteristics by human ovarian cancer cells. **Oncogene** 26, 2736-2746.

Beaudenon,S. & Huibregtse,J.M. (2008). HPV E6, E6AP and cervical cancer. **BMC. Biochem.** 9 *Suppl 1*, S4.

Berggard,T., Linse,S. & James,P. (2007). Methods for the detection and analysis of protein-protein interactions. **Proteomics**. 7, 2833-2842.

Berquin,I.M., Pang,B., Dziubinski,M.L., Scott,L.M. *et al.* (2005). Y-box-binding protein 1 confers EGF independence to human mammary epithelial cells. **Oncogene** 24, 3177-3186.

Casadaban,M.J., Chou,J. & Cohen,S.N. (1980). In vitro gene fusions that join an enzymatically active beta-galactosidase segment to amino-terminal fragments of exogenous proteins: Escherichia coli plasmid vectors for the detection and cloning of translational initiation signals. **J. Bacteriol.** 143, 971-980.

Causier,B. (2004). Studying the interactome with the yeast two-hybrid system and mass spectrometry. **Mass Spectrom. Rev.** 23, 350-367.

Causier,B. & Davies,B. (2002). Analysing protein-protein interactions with the yeast two-hybrid system. **Plant Mol. Biol.** 50, 855-870.

Chernov,K.G., Mechulam,A., Popova,N.V., Pastre,D. *et al.* (2008). YB-1 promotes microtubule assembly in vitro through interaction with tubulin and microtubules. **BMC. Biochem.** 9, 23.

Chibi,M., Meyer,M., Skepu,A., DJ,G.R. *et al.* (2008). RBBP6 interacts with multifunctional protein YB-1 through its RING finger domain, leading to ubiquitination and proteosomal degradation of YB-1. **J. Mol. Biol.** 384, 908-916.

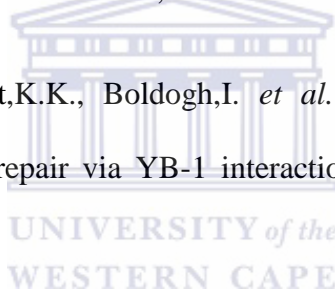
Choi,C.H. (2005). ABC transporters as multidrug resistance mechanisms and the development of chemosensitizers for their reversal. **Cancer Cell Int.** 5, 30.

Christensen,D.E. & Klevit,R.E. (2009). Dynamic interactions of proteins in complex networks: identifying the complete set of interacting E2s for functional investigation of E3-dependent protein ubiquitination. **FEBS J.** 276, 5381-5389.

Cohen,S.B., Ma,W., Valova,V.A., Algie,M. *et al.* (2010). Genotoxic stress-induced nuclear localization of oncoprotein YB-1 in the absence of proteolytic processing. **Oncogene** 29, 403-410.

Dahl,E., En-Nia,A., Wiesmann,F., Krings,R. *et al.* (2009). Nuclear detection of Y-box protein-1 (YB-1) closely associates with progesterone receptor negativity and is a strong adverse survival factor in human breast cancer. **BMC. Cancer** 9, 410.

Das,S., Chattopadhyay,R., Bhakat,K.K., Boldogh,I. *et al.* (2007). Stimulation of NEIL2-mediated oxidized base excision repair via YB-1 interaction during oxidative stress. **J. Biol. Chem.** 282, 28474-28484.



de Souza-Pinto,N.C., Mason,P.A., Hashiguchi,K., Weissman,L. *et al.* (2009). Novel DNA mismatch-repair activity involving YB-1 in human mitochondria. **DNA Repair (Amst)** 8, 704-719.

Delaglio,F., Grzesiek,S., Vuister,G.W., Zhu,G. *et al.* (1995). NMRPipe: a multidimensional spectral processing system based on UNIX pipes. **J. Biomol. NMR** 6, 277-293.

Deshaies,R.J. & Joazeiro,C.A. (2009). RING domain E3 ubiquitin ligases. **Annu. Rev. Biochem.** 78, 399-434.

Didier,D.K., Schiffenbauer,J., Woulfe,S.L., Zacheis,M. *et al.* (1988). Characterization of the cDNA encoding a protein binding to the major histocompatibility complex class II Y box. **Proc. Natl. Acad. Sci. U. S. A** 85, 7322-7326.

Edwin,F., Anderson,K. & Patel,T.B. (2010). HECT domain-containing E3 ubiquitin ligase Nedd4 interacts with and ubiquitinates Sprouty2. **J. Biol. Chem.** 285, 255-264.

En-Nia,A., Yilmaz,E., Klinge,U., Lovett,D.H. *et al.* (2005). Transcription factor YB-1 mediates DNA polymerase alpha gene expression. **J. Biol. Chem.** 280, 7702-7711.

Evdokimova,V., Ovchinnikov,L.P. & Sorensen,P.H. (2006a). Y-box binding protein 1: providing a new angle on translational regulation. **Cell Cycle** 5, 1143-1147.

Evdokimova,V., Ruzanov,P., Anglesio,M.S., Sorokin,A.V. *et al.* (2006b). Akt-mediated YB-1 phosphorylation activates translation of silent mRNA species. **Mol. Cell Biol.** 26, 277-292.

Evdokimova,V., Tognon,C., Ng,T., Ruzanov,P. *et al.* (2009). Translational activation of snail1 and other developmentally regulated transcription factors by YB-1 promotes an epithelial-mesenchymal transition. **Cancer Cell** 15, 402-415.

Fields,S. & Song,O. (1989). A novel genetic system to detect protein-protein interactions. **Nature** 340, 245-246.

Frye,B.C., Halfter,S., Djudjaj,S., Muehlenberg,P. *et al.* (2009). Y-box protein-1 is actively secreted through a non-classical pathway and acts as an extracellular mitogen. **EMBO Rep.** 10, 783-789.

Fujii,T., Kawahara,A., Basaki,Y., Hattori,S. *et al.* (2008). Expression of HER2 and estrogen receptor alpha depends upon nuclear localization of Y-box binding protein-1 in human breast cancers. **Cancer Res.** 68, 1504-1512.

Fujita,T., Ito,K., Izumi,H., Kimura,M. *et al.* (2005). Increased nuclear localization of transcription factor Y-box binding protein 1 accompanied by up-regulation of P-glycoprotein in breast cancer pretreated with paclitaxel. **Clin. Cancer Res.** 11, 8837-8844.

Gao,S. & Scott,R.E. (2002). P2P-R protein overexpression restricts mitotic progression at prometaphase and promotes mitotic apoptosis. **J. Cell Physiol** 193, 199-207.

Gao,S. & Scott,R.E. (2003). Stable overexpression of specific segments of the P2P-R protein in human MCF-7 cells promotes camptothecin-induced apoptosis. **J. Cell Physiol** 197, 445-452.

Gaudreault,I., Guay,D. & Lebel,M. (2004). YB-1 promotes strand separation in vitro of duplex DNA containing either mispaired bases or cisplatin modifications, exhibits endonucleolytic activities and binds several DNA repair proteins. **Nucleic Acids Res.** 32, 316-327.

Gimenez-Bonafe,P., Fedoruk,M.N., Whitmore,T.G., Akbari,M. *et al.* (2004). YB-1 is upregulated during prostate cancer tumor progression and increases P-glycoprotein activity. **Prostate** 59, 337-349.

Glockzin,G., Mantwill,K., Jurchott,K., Bernshausen,A. *et al.* (2006). Characterization of the recombinant adenovirus vector AdYB-1: implications for oncolytic vector development. **J. Virol.** 80, 3904-3911.

Grossman,S.R., Deato,M.E., Brignone,C., Chan,H.M. *et al.* (2003). Polyubiquitination of p53 by a ubiquitin ligase activity of p300. **Science** 300, 342-344.

Guay,D., Evoy,A.A., Paquet,E., Garand,C. *et al.* (2008). The strand separation and nuclease activities associated with YB-1 are dispensable for cisplatin resistance but overexpression of YB-1 in MCF7 and MDA-MB-231 breast tumor cells generates several chemoresistance signatures. **Int. J. Biochem. Cell Biol.** 40, 2492-2507.

Habibi,G., Leung,S., Law,J.H., Gelmon,K. *et al.* (2008). Redefining prognostic factors for breast cancer: YB-1 is a stronger predictor of relapse and disease-specific survival than estrogen receptor or HER-2 across all tumor subtypes. **Breast Cancer Res.** 10, R86.

Haenzelmann,P., Stingle,J., Hofmann,K., Schindelin,H. *et al.* (2010). The Yeast E4 ubiquitin ligase Ufd2 interacts with the ubiquitin-like domains of Rad23 and Dsk2 via a novel and distinct ubiquitin-like binding domain. **J. Biol. Chem.**

Halgren,T.A. (2009). Identifying and characterizing binding sites and assessing druggability. **J. Chem. Inf. Model.** 49, 377-389.

Hanlon,A.D., Larkin,M.I. & Reddick,R.M. (2010). Free-solution, label-free protein-protein interactions characterized by dynamic light scattering. **Biophys. J.** 98, 297-304.

Harper,J.W., Adami,G.R., Wei,N., Keyomarsi,K. *et al.* (1993). The p21 Cdk-interacting protein Cip1 is a potent inhibitor of G1 cyclin-dependent kinases. **Cell** 75, 805-816.

Hatakeyama,S., Yada,M., Matsumoto,M., Ishida,N. *et al.* (2001). U box proteins as a new family of ubiquitin-protein ligases. **J. Biol. Chem.** 276, 33111-33120.

Homer,C., Knight,D.A., Hananeia,L., Sheard,P. *et al.* (2005). Y-box factor YB1 controls p53 apoptotic function. **Oncogene** 24, 8314-8325.

Huang,J., Tan,P.H., Li,K.B., Matsumoto,K. *et al.* (2005). Y-box binding protein, YB-1, as a marker of tumor aggressiveness and response to adjuvant chemotherapy in breast cancer. **Int. J. Oncol.** 26, 607-613.

Huang,N. & Jacobson,M.P. (2010). Binding-site assessment by virtual fragment screening. **PLoS. One.** 5, e10109.

Huang,X., Ushijima,K., Komai,K., Takemoto,Y. *et al.* (2004). Co-expression of Y box-binding protein-1 and P-glycoprotein as a prognostic marker for survival in epithelial ovarian cancer. **Gynecol. Oncol.** 93, 287-291.

Inouye,M. & Phadtare,S. (2004). Cold shock response and adaptation at near-freezing temperature in microorganisms. **Sci. STKE.** 2004, e26.

Jain,N.U., Wyckoff,T.J., Raetz,C.R. & Prestegard,J.H. (2004). Rapid analysis of large protein-protein complexes using NMR-derived orientational constraints: the 95 kDa complex of LpxA with acyl carrier protein. **J. Mol. Biol.** 343, 1379-1389.

James,P., Halladay,J. & Craig,E.A. (1996). Genomic libraries and a host strain designed for highly efficient two-hybrid selection in yeast. **Genetics** 144, 1425-1436.

Joazeiro,C.A. & Weissman,A.M. (2000). RING finger proteins: mediators of ubiquitin ligase activity. **Cell** 102, 549-552.

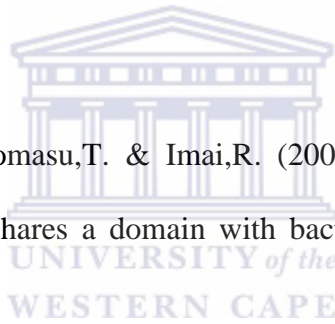
Joazeiro,C.A., Wing,S.S., Huang,H., Levenson,J.D. *et al.* (1999). The tyrosine kinase negative regulator c-Cbl as a RING-type, E2-dependent ubiquitin-protein ligase. **Science** 286, 309-312.

Johnson,B.A. & Blevins,R.A. (1994). NMR View: A computer program for the visualization and analysis of NMR data. **Journal of Biomolecular NMR** 4, 603-614.

Jurchott,K., Bergmann,S., Stein,U., Walther,W. *et al.* (2003). YB-1 as a cell cycle-regulated transcription factor facilitating cyclin A and cyclin B1 gene expression. **J. Biol. Chem.** 278, 27988-27996.

Karlson,D. & Imai,R. (2003). Conservation of the cold shock domain protein family in plants. **Plant Physiol** 131, 12-15.

Karlson,D., Nakaminami,K., Toyomasu,T. & Imai,R. (2002). A cold-regulated nucleic acid-binding protein of winter wheat shares a domain with bacterial cold shock proteins. **J. Biol. Chem.** 277, 35248-35256.



Kashihara,M., Azuma,K., Kawahara,A., Basaki,Y. *et al.* (2009). Nuclear Y-box binding protein-1, a predictive marker of prognosis, is correlated with expression of HER2/ErbB2 and HER3/ErbB3 in non-small cell lung cancer. **J. Thorac. Oncol.** 4, 1066-1074.

Kerscher,O., Felberbaum,R. & Hochstrasser,M. (2006). Modification of proteins by ubiquitin and ubiquitin-like proteins. **Annu. Rev. Cell Dev. Biol.** 22, 159-180.

Khandelwal,P., Padala,M.K., Cox,J. & Guntaka,R.V. (2009). The N-terminal domain of y-box binding protein-1 induces cell cycle arrest in g2/m phase by binding to cyclin d1. **Int. J. Cell Biol.** 2009, 243532.

Kim,J.S., Park,S.J., Kwak,K.J., Kim,Y.O. *et al.* (2007). Cold shock domain proteins and glycine-rich RNA-binding proteins from *Arabidopsis thaliana* can promote the cold adaptation process in *Escherichia coli*. **Nucleic Acids Res.** 35, 506-516.

Kloks,C.P., Spronk,C.A., Lasonder,E., Hoffmann,A. *et al.* (2002). The solution structure and DNA-binding properties of the cold-shock domain of the human Y-box protein YB-1. **J. Mol. Biol.** 316, 317-326.

Kohno,K., Izumi,H., Uchiumi,T., Ashizuka,M. *et al.* (2003). The pleiotropic functions of the Y-box-binding protein, YB-1. **Bioessays** 25, 691-698.

Kume,K., Iizumi,Y., Shimada,M., Ito,Y. *et al.* (2010). Role of N-end rule ubiquitin ligases UBR1 and UBR2 in regulating the leucine-mTOR signaling pathway. **Genes Cells** 15, 339-349.

Kuwano,M., Oda,Y., Izumi,H., Yang,S.J. *et al.* (2004). The role of nuclear Y-box binding protein 1 as a global marker in drug resistance. **Mol. Cancer Ther.** 3, 1485-1492.

Laemmli,U.K. (1970). Cleavage of structural proteins during the assembly of the head of bacteriophage T4. **Nature** 227, 680-685.

Lasham,A., Moloney,S., Hale,T., Homer,C. *et al.* (2003). The Y-box-binding protein, YB1, is a potential negative regulator of the p53 tumor suppressor. **J. Biol. Chem.** 278, 35516-35523.

Li,L., Deng,B., Xing,G., Teng,Y. *et al.* (2007). PACT is a negative regulator of p53 and essential for cell growth and embryonic development. **Proc. Natl. Acad. Sci. U. S. A** 104, 7951-7956.

Lu,Z.H., Books,J.T. & Ley,T.J. (2005). YB-1 is important for late-stage embryonic development, optimal cellular stress responses, and the prevention of premature senescence. **Mol. Cell Biol.** 25, 4625-4637.

Markson,G., Kiel,C., Hyde,R., Brown,S. *et al.* (2009). Analysis of the human E2 ubiquitin conjugating enzyme protein interaction network. **Genome Res.** 19, 1905-1911.

Matsumoto,K. & Bay,B.H. (2005). Significance of the Y-box proteins in human cancers. **J. Mol. Genet. Med.** 1, 11-17.

Matsumoto,K. & Wolffe,A.P. (1998). Gene regulation by Y-box proteins: coupling control of transcription and translation. **Trends Cell Biol.** 8, 318-323.

McCoy,M.A. & Wyss,D.F. (2002). Structures of protein-protein complexes are docked using only NMR restraints from residual dipolar coupling and chemical shift perturbations. **J. Am. Chem. Soc.** 124, 2104-2105.

Mertens,P.R., Steinmann,K., fonso-Jaume,M.A., En-Nia,A. *et al.* (2002). Combinatorial interactions of p53, activating protein-2, and YB-1 with a single enhancer element regulate gelatinase A expression in neoplastic cells. **J. Biol. Chem.** 277, 24875-24882.

Mogk,A., Schmidt,R. & Bukau,B. (2007). The N-end rule pathway for regulated proteolysis: prokaryotic and eukaryotic strategies. **Trends Cell Biol.** 17, 165-172.

Mouneimne,G. & Brugge,J.S. (2009). YB-1 translational control of epithelial-mesenchyme transition. **Cancer Cell** 15, 357-359.

Nakaminami,K., Karlson,D.T. & Imai,R. (2006). Functional conservation of cold shock domains in bacteria and higher plants. **Proc. Natl. Acad. Sci. U. S. A** *103*, 10122-10127.

Nekrasov,M.P., Ivshina,M.P., Chernov,K.G., Kovrigina,E.A. *et al.* (2003). The mRNA-binding protein YB-1 (p50) prevents association of the eukaryotic initiation factor eIF4G with mRNA and inhibits protein synthesis at the initiation stage. **J. Biol. Chem.** *278*, 13936-13943.

Peidis,P., Giannakouros,T., Burow,M.E., Williams,R.W. *et al.* (2010). Systems genetics analyses predict a transcription role for P2P-R: molecular confirmation that P2P-R is a transcriptional co-repressor. **BMC. Syst. Biol.** *4*, 14.

Phadtare,S. (2004). Recent developments in bacterial cold-shock response. **Curr. Issues Mol. Biol.** *6*, 125-136.

Piebler,J. (2005). New methodologies for measuring protein interactions in vivo and in vitro. **Curr. Opin. Struct. Biol.** *15*, 4-14.

Poyurovsky,M.V., Priest,C., Kentsis,A., Borden,K.L. *et al.* (2007). The Mdm2 RING domain C-terminus is required for supramolecular assembly and ubiquitin ligase activity. **EMBO J** *26*, 90-101.

Pugh,D.J., Ab,E., Faro,A., Lutya,P.T. *et al.* (2006). DWNN, a novel ubiquitin-like domain, implicates RBBP6 in mRNA processing and ubiquitin-like pathways. **BMC. Struct. Biol.** *6*, 1.

Rauen,T., Raffetseder,U., Frye,B.C., Djudjaj,S. *et al.* (2009). YB-1 acts as a ligand for Notch-3 receptors and modulates receptor activation. **J. Biol. Chem.** *284*, 26928-26940.

Ruzanov,P.V., Evdokimova,V.M., Korneeva,N.L., Hershey,J.W. *et al.* (1999). Interaction of the universal mRNA-binding protein, p50, with actin: a possible link between mRNA and microfilaments. **J. Cell Sci.** *112 (Pt 20)*, 3487-3496.

Saji,H., Toi,M., Saji,S., Koike,M. *et al.* (2003). Nuclear expression of YB-1 protein correlates with P-glycoprotein expression in human breast carcinoma. **Cancer Lett.** *190*, 191-197.

Sakai,Y., Saijo,M., Coelho,K., Kishino,T. *et al.* (1995). cDNA sequence and chromosomal localization of a novel human protein, RBQ-1 (RBBP6), that binds to the retinoblastoma gene product. **Genomics** *30*, 98-101.

Selivanova,O.M., Guryanov,S.G., Enin,G.A., Skabkin,M.A. *et al.* (2010). YB-1 is capable of forming extended nanofibrils. **Biochemistry (Mosc.)** *75*, 115-120.

Shi,Y., Di,G., Taylor,D., Sarkeshik,A. *et al.* (2009). Molecular architecture of the human pre-mRNA 3' processing complex. **Mol. Cell** *33*, 365-376.

Shu-Nu,C., Lin,C.H. & Lin,A. (2000). An acidic amino acid cluster regulates the nucleolar localization and ribosome assembly of human ribosomal protein L22. **FEBS Lett.** *484*, 22-28.

Simons,A., Melamed-Bessudo,C., Wolkowicz,R., Sperling,J. *et al.* (1997). PACT: cloning and characterization of a cellular p53 binding protein that interacts with Rb. **Oncogene** *14*, 145-155.

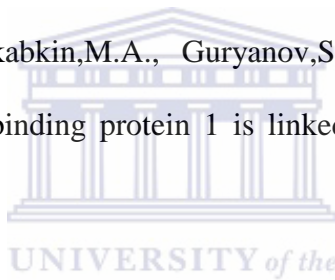
Skabkin,M.A., Evdokimova,V., Thomas,A.A. & Ovchinnikov,L.P. (2001). The major messenger ribonucleoprotein particle protein p50 (YB-1) promotes nucleic acid strand annealing. **J. Biol. Chem.** *276*, 44841-44847.

Skabkin,M.A., Kiselyova,O.I., Chernov,K.G., Sorokin,A.V. *et al.* (2004). Structural organization of mRNA complexes with major core mRNP protein YB-1. **Nucleic Acids Res.** 32, 5621-5635.

Soop,T., Nashchekin,D., Zhao,J., Sun,X. *et al.* (2003). A p50-like Y-box protein with a putative translational role becomes associated with pre-mRNA concomitant with transcription. **J. Cell Sci.** 116, 1493-1503.

Sorokin,A.V., Kim,E.R. & Ovchinnikov,L.P. (2007). Nucleocytoplasmic transport of proteins. **Biochemistry (Mosc.)** 72, 1439-1457.

Sorokin,A.V., Selyutina,A.A., Skabkin,M.A., Guryanov,S.G. *et al.* (2005). Proteasome-mediated cleavage of the Y-box-binding protein 1 is linked to DNA-damage stress response. **EMBO J.** 24, 3602-3612.



Stratford,A.L., Habibi,G., Astanehe,A., Jiang,H. *et al.* (2007). Epidermal growth factor receptor (EGFR) is transcriptionally induced by the Y-box binding protein-1 (YB-1) and can be inhibited with Iressa in basal-like breast cancer, providing a potential target for therapy. **Breast Cancer Res.** 9, R61.

Studier,F.W. & Moffatt,B.A. (1986). Use of bacteriophage T7 RNA polymerase to direct selective high-level expression of cloned genes. **J. Mol. Biol.** 189, 113-130.

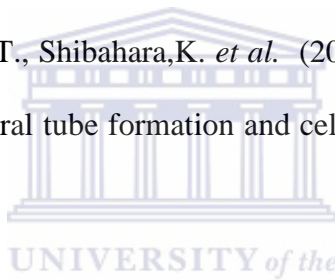
Takiya,S., Nishita,Y., Ishikawa,S., Ohno,K. *et al.* (2004). Bombyx Y-box protein BYB facilitates specific DNA interaction of various DNA binding proteins independently of the cold shock domain. **J. Biochem.** 135, 683-693.

Tasaki,T., Mulder,L.C., Iwamatsu,A., Lee,M.J. *et al.* (2005). A family of mammalian E3 ubiquitin ligases that contain the UBR box motif and recognize N-degrons. **Mol. Cell Biol.** 25, 7120-7136.

Taylor,R.G., Walker,D.C. & McInnes,R.R. (1993). E. coli host strains significantly affect the quality of small scale plasmid DNA preparations used for sequencing. **Nucleic Acids Res.** 21, 1677-1678.

Tsang,W.Y., Wang,L., Chen,Z., Sanchez,I. *et al.* (2007). SCAPER, a novel cyclin A-interacting protein that regulates cell cycle progression. **J. Cell Biol.** 178, 621-633.

Uchiumi,T., Fotovati,A., Sasaguri,T., Shibahara,K. *et al.* (2006). YB-1 is important for an early stage embryonic development: neural tube formation and cell proliferation. **J. Biol. Chem.** 281, 40440-40449.



Vaiman,A.V., Stromskaya,T.P., Rybalkina,E.Y., Sorokin,A.V. *et al.* (2006). Intracellular localization and content of YB-1 protein in multidrug resistant tumor cells. **Biochemistry (Mosc.)** 71, 146-154.

Valadao,A.F., Fantappie,M.R., LoVerde,P.T., Pena,S.D. *et al.* (2002). Y-box binding protein from *Schistosoma mansoni*: interaction with DNA and RNA. **Mol. Biochem. Parasitol.** 125, 47-57.

van Dijk,A.D., Fushman,D. & Bonvin,A.M. (2005). Various strategies of using residual dipolar couplings in NMR-driven protein docking: application to Lys48-linked di-ubiquitin and validation against ¹⁵N-relaxation data. **Proteins** 60, 367-381.

van Wijk,S.J. & Timmers,H.T. (2010). The family of ubiquitin-conjugating enzymes (E2s): deciding between life and death of proteins. **FASEB J.** *24*, 981-993.

van,D.M., van Dijk,A.D., Hsu,V., Boelens,R. *et al.* (2006). Information-driven protein-DNA docking using HADDOCK: it is a matter of flexibility. **Nucleic Acids Res.** *34*, 3317-3325.

Varshavsky,A. (2008). The N-end rule at atomic resolution. **Nat. Struct. Mol. Biol.** *15*, 1238-1240.

Vaynberg,J. & Qin,J. (2006). Weak protein-protein interactions as probed by NMR spectroscopy. **Trends Biotechnol.** *24*, 22-27.

Vo,L.T., Minet,M., Schmitter,J.M., Lacroute,F. *et al.* (2001). Mpe1, a zinc knuckle protein, is an essential component of yeast cleavage and polyadenylation factor required for the cleavage and polyadenylation of mRNA. **Mol. Cell Biol.** *21*, 8346-8356.

Wang,B., Ngoi,S., Wang,J., Chong,S.S. *et al.* (2006). The promoter region of the MDR1 gene is largely invariant, but different single nucleotide polymorphism haplotypes affect MDR1 promoter activity differently in different cell lines. **Mol. Pharmacol.** *70*, 267-276.

Worringer,K.A. & Panning,B. (2007). Zinc finger protein Zn72D promotes productive splicing of the maleless transcript. **Mol. Cell Biol.** *27*, 8760-8769.

Wu,J., Lee,C., Yokom,D., Jiang,H. *et al.* (2006). Disruption of the Y-box binding protein-1 results in suppression of the epidermal growth factor receptor and HER-2. **Cancer Res.** *66*, 4872-4879.

Wu,W.W., Sun,Y.H. & Pante,N. (2007). Nuclear import of influenza A viral ribonucleoprotein complexes is mediated by two nuclear localization sequences on viral nucleoprotein. **Virology** **J.** *4*, 49.

Xu,Z., Kohli,E., Devlin,K.I., Bold,M. *et al.* (2008). Interactions between the quality control ubiquitin ligase CHIP and ubiquitin conjugating enzymes. **BMC. Struct. Biol.** *8*, 26.

Yamashita,M., Ying,S.X., Zhang,G.M., Li,C. *et al.* (2005). Ubiquitin ligase Smurf1 controls osteoblast activity and bone homeostasis by targeting MEKK2 for degradation. **Cell** *121*, 101-113.

Yoshitake,Y., Nakatsura,T., Monji,M., Senju,S. *et al.* (2004). Proliferation potential-related protein, an ideal esophageal cancer antigen for immunotherapy, identified using complementary DNA microarray analysis. **Clin. Cancer Res.** *10*, 6437-6448.

Zenker,M., Mayerle,J., Lerch,M.M., Tagariello,A. *et al.* (2005). Deficiency of UBR1, a ubiquitin ligase of the N-end rule pathway, causes pancreatic dysfunction, malformations and mental retardation (Johanson-Blizzard syndrome). **Nat. Genet.** *37*, 1345-1350.

Zhang,M., Windheim,M., Roe,S.M., Peggie,M. *et al.* (2005). Chaperoned Ubiquitylation-- Crystal Structures of the CHIP U Box E3 Ubiquitin Ligase and a CHIP-Ubc13-Uev1a Complex. **Molecular Cell** *20*, 525-538.

Zheng,N., Wang,P., Jeffrey,P.D. & Pavletich,N.P. (2000). Structure of a c-Cbl-UbcH7 complex: RING domain function in ubiquitin-protein ligases. **Cell** *102*, 533-539.

Appendix I: Amino acid sequence of CTDYB-1

GGVPVQGSKYAADRNHYRRYPRRRGPPRNYQQNYQNSESGEKNEGSESAPEGQAQQR
RPYRRRRFPPYYMRRPYGRRPQYSNPPVQGEVMEGADNQGAGEQGRPVRQNMRYGYR
PRFRRGPPRQRQPREDGNEEDKENQGDETQGQQPPQRRYRRNFNYRRRRPENPKPQDG
KETKAADPPAENSSAPEAEQGGAE



Appendix II: Sequence analysis of YB-1₂₇₇₋₃₀₆ cloned into pACT2 AD vector.

Sequencing for pACT2-cloned inserts was done using the pACT2 forward primer.

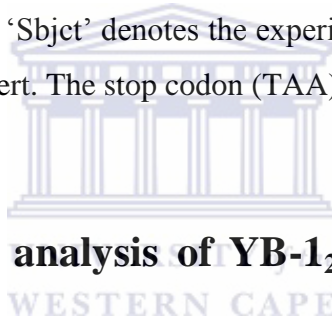
```

Score = 193 bits (104), Expect = 7e-55
Identities = 104/104 (100%), Gaps = 0/104 (0%)
Strand=Plus/Plus

Query 1  GGATCCCTCAACGTCGGTACCGCCGCAACTTCAATTACCGACGCAGACGCCAGAAAACC 60
          |||
Sbjct 1  GGATCCCTCAACGTCGGTACCGCCGCAACTTCAATTACCGACGCAGACGCCAGAAAACC 60

Query 61  CTAAACCACAAGATGGCAAAGAGACAAAAGCAGCC TAACTCGAG 104
          |||
Sbjct 61  CTAAACCACAAGATGGCAAAGAGACAAAAGCAGCC TAACTCGAG 104
  
```

Restriction sites are highlighted in red *Xho I* (CTCGAG) and *Bam HI* (GGATCC). ‘Query’ denotes the expected sequence and ‘Sbjct’ denotes the experimental sequence determined for the sequence analysis of the cloned insert. The stop codon (TAA) is highlighted in yellow.



Appendix III: Sequence analysis of YB-1₂₉₂₋₃₂₄ cloned into pACT2 AD vector.

```

Score = 209 bits (113), Expect = 8e-60
Identities = 113/113 (100%), Gaps = 0/113 (0%)
Strand=Plus/Plus

Query 1  GGATCC CAGAAAACCTAAACCACAAGATGGCAAAGAGACAAAAGCAGCCGATCCACCAG 60
          |||
Sbjct 1  GGATCC CAGAAAACCTAAACCACAAGATGGCAAAGAGACAAAAGCAGCCGATCCACCAG 60

Query 61  CTGAGAATTTCGTCCGCTCCCAGGCTGAGCAGGGCGGGGCTGAG TAACTCGAG 113
          |||
Sbjct 61  CTGAGAATTTCGTCCGCTCCCAGGCTGAGCAGGGCGGGGCTGAG TAACTCGAG 113
  
```

Restriction sites are highlighted in red *Xho I* (CTCGAG) and *Bam HI* (GGATCC). ‘Query’ denotes the expected sequence and ‘Sbjct’ denotes the experimental sequence determined for the sequence analysis of the cloned insert. The stop codon (TAA) is highlighted in yellow.

Appendix IV: Sequence analysis of RING^{N312D} cloned into pGEX-6P-

2 vector.

Score = 510 bits (276), Expect = 1e-149
Identities = 278/279 (99%), Gaps = 0/279 (0%)
Strand=Plus/Plus

```
Query 1  GGATCCGAAGATGATCCTATCCAGATGAATTGTTGTGTCATCTGCAAGGATATTATG 60
      |||
Sbjct 1  GGATCCGAAGATGATCCTATCCAGATGAATTGTTGTGTCATCTGCAAGGATATTATG 60

Query 61  ACTGATGCTGTTGTGATTCCCTGCTGTGAAACAGTTACTGTGATGAATGTATAAGAACA 120
      |||
Sbjct 61  ACTGATGCTGTTGTGATTCCCTGCTGTGAAACAGTTACTGTGATGAATGTATAAGAACA 120

Query 121  GCACCTCTGGAATCAGATGAGCACACATGTCCGACGTGTCATCAAATGATGTTTCTCCT 180
      |||
Sbjct 121  GCACCTCTGGAATCAGATGAGCACACATGTCCGACGTGTCATCAAATGATGTTTCTCCT 180

Query 181  GATGCTTTAATTGCCAATAAATTTTACGACAGGCTGTAATAACTTCAAAAATGAAACT 240
      |||
Sbjct 181  GATGCTTTAATTGCCGATAAATTTTACGACAGGCTGTAATAACTTCAAAAATGAAACT 240

Query 241  GGCTATACAAAAGACTACGAAAACAGTGATAA 279
      |||
Sbjct 241  GGCTATACAAAAGACTACGAAAACAGTGATAACTCCAG 279
```

The query represents the wildtype sequence and the subject (Sbjct) represents the mutant sequence. The mutated codon is shown in green. AAT codon in the wildtype codes for Asparagine, N and the substitution mutation GAT in the mutant codes for Aspartic acid, D. Restriction sites are highlighted in red *Xho I* (CTCGAG) and *Bam HI* (GGATCC). ‘Query’ denotes the expected sequence and ‘Sbjct’ denotes the experimental sequence determined for the sequence analysis of the cloned insert. The stop codons (TAA and TGA) are highlighted in yellow.

Appendix V: Sequence analysis of RING^{K313E} cloned into pGEX-6P-

2 vector.

Score = 505 bits (273), Expect = 6e-148
Identities = 277/279 (99%), Gaps = 0/279 (0%)
Strand=Plus/Plus

```
Query 1  GGATCCGAAGATGATCCTATCCAGATGAATTGTTGTGTCTCATCTGCAAGGATATTATG 60
          |||
Sbjct 1  GGATCCGAAGATGATCCTATCCAGATGAATTGTTGTGTCTCATCTGCAAGGATATTATG 60

Query 61  ACTGATGCTGTTGTGATTCCCTGCTGTGGAAACAGTTACTGTGATGAATGTATAAGAACA 120
          |||
Sbjct 61  ACTGATGCTGTTGTGATTCCCTGCTGTGGAAACAGTTACTGTGATGAATGTATAAGAACA 120

Query 121  GCACCTCTGGAATCAGATGAGCACACATGTCCGACGTGTTCATCAAATGATGTTTCTCCT 180
          |||
Sbjct 121  GCACCTCTGGAATCAGATGAGCACACATGTCCGACGTGTTCATCAAATGATGTTTCTCCT 180

Query 181  GATGCTTTAATTGCCAATAAAATTTTACGACAGGCTGTAATAACTTCAAAAATGAAACT 240
          |||
Sbjct 181  GATGCTTTAATTGCCAATGAAATTTTACGACAGGCGTAAATAACTTCAAAAATGAAACT 240

Query 241  GGCTATACAAAAGACTACGAAAACAGTGATAACTCCAG 279
          |||
Sbjct 241  GGCTATACAAAAGACTACGAAAACAGTGATAACTCCAG 279
```

The query represents the wildtype sequence and the subject (Sbjct) represents the mutant sequence. The mutated codon is shown in green. AAA codon in the wildtype codes for Lysine, K and the substitution mutation GAA in the mutant codes for Glutamic acid, D. Restriction sites are highlighted in red *Xho I* (CTCGAG) and *Bam HI* (GGATCC). ‘Query’ denotes the expected sequence and ‘Sbjct’ denotes the experimental sequence determined for the sequence analysis of the cloned insert. The stop codons (TAA and TGA) are highlighted in yellow.